The effects of friction reducing polymers on the operation of journal bearings

Hampson, L. G.

THE EFFECTS OF FRICTION REDUCING POLYMERS ON THE OPERATION OF JOURNAL BEARINGS

L.G. HAMPSON, B.Sc.

A thesis submitted for the degree of Ph.D. at

Durham University

The Department of Engineering Science

Durham University

March 1972

ACKNOWLEDGEMENTS

I wish to thank Dr. H. Naylor, of Thornton Research Centre, for his advice and encouragement throughout the project. Discussions with Sir Derman Christopherson, Professor G.R. Higginson and Professor H. Marsh were particularly valuable.

The work was sponsored by Shell International Petroleum Ltd.

CONTENTS

ABSTRACT 1

NOTATION 2

INTRODUCTION 4

TURBULENCE IN JOURNAL BEARINGS 9
1. LARGE RELATIVE CLEARANCE: TRANSITION EFFECTS 9
A. THE CONCENTRIC CASE
B. THE ECCENTRIC CASE

2. TURBULENT JOURNAL BEARING CHARACTERISTICS 13

3. PREVIOUS INVESTIGATIONS 16
A. WILCOCK
B. SMITH AND FULLER
C. HUGGINS

TURBULENT FRICTION REDUCTION BY HIGH MOLECULAR WEIGHT POLYMERS 25
1. PREVIOUS INVESTIGATIONS 25
2. THE MECHANISM OF FRICTION REDUCTION 39
3. THE PRACTICAL USE OF FRICTION REDUCING POLYMERS 41

THE EXPERIMENTAL RIG 43
1. THE DRIVE SYSTEM 43
2. THE SHAFT AND SLAVE BEARINGS 47
3. THE LOADING SYSTEM 48
4. SPEED MEASUREMENT 50
5. TORQUE MEASUREMENT 50
6. LUBRICANT TEMPERATURE MEASUREMENT 51
7. LUBRICANT FLOWRATE AND FEED PRESSURE MEASUREMENT 51
8. TEST LUBRICANT SUPPLY SYSTEM 51
9. LOCATION OF THE TEST BEARING 52
10. ECCENTRICITY MEASUREMENT 52
11. TEST BEARING HOUSING AND DRAINAGE 53

THE DEVELOPMENT OF THE TEST BEARING 54
1. ORIGINAL INTENTIONS 54
2. THE CONCENTRIC BEARING 56
3. FILM EXTENT VARIATION: THE TRANSPARENT BEARING 57
4. FINAL DESIGN OF THE TEST BEARING 61

EXPERIMENTAL RESULTS AND DISCUSSION 63
1. THE EFFECT OF LUBRICANT FLOWRATE ON BEARING FRICTION 63
2. THE EFFECT OF LOAD ON BEARING FRICTION 65
3. FRICTION RESULTS WITH WATER LUBRICATION 69
A. THE TORQUE DUE TO THE LOADING SYSTEM 69
B. THE TORQUE DUE TO THE ANGULAR MOMENTUM OF THE LUBRICANT 69
C. COMPARISON WITH PREVIOUS INVESTIGATIONS 73

4. THE EFFECTS OF A POLYMER ADDITIVE ON BEARING PERFORMANCE 76
A. FRICTION 76
B. WHIRL STABILITY 80
C. PRESSURE DISTRIBUTION 85
D. POLYMER DEGRADATION 85
E. LUBRICANT FLOWRATE 89

CONCLUSIONS 92

FUTURE WORK 94

APPENDICES 95
1. FILM EXTENT IN JOURNAL BEARINGS
A. BASIC THEORY
B. THE MINIMUM ENERGY PRINCIPLE
C. NO SIDE LEAKAGE CASE
D. SIDE LEAKAGE CASE
E. DISCUSSION
F. COMPUTER PROGRAMME AND RESULTS
2. TABULATED TEST RESULTS 124
3. POLYMER SOLUTION PREPARATION 137
4. TEST PROCEDURE 138

REFERENCES 140

ABSTRACT

As rotating machines become larger, an increasing number of plain journal bearings operate in the turbulent regime. The addition of small amounts of high molecular weight polymers to the lubricant offers an attractive method of counteracting the increased power loss. This effect has previously been investigated for turbulent flow in pipes.

Experiments are described on the operation of a four-inch diameter bearing lubricated with a very dilute, aqueous solution of poly(ethylene oxide).

It is shown that the film extent in large clearance bearings is very dependent on the operating parameters. A numerical analysis based on the Reynolds equation indicates that a minimum dissipation principle can be used to explain the delay in the formation of a full width film.

The transition to turbulence occurred at a Reynolds number of 2000. There was little evidence of Taylor vortices. The bearing friction was significantly affected by the angular momentum of the leakage flow.

Very low concentrations of polymer were found to be effective in reducing the friction. Typically, 0.005% by weight causing a reduction of 45% at a Reynolds number of 3500. The bearing was also significantly stabilised against whirling, although the pressure distribution was unchanged.

The polymer became ineffective after approximately twenty passes through the bearing. The degradation caused by shearing will probably be the factor limiting commercial exploitation of friction reduction in turbulent bearings.

NOTATION

c	mean radial clearance
d	pipe diameter
D	bearing diameter
e	eccentricity
F	friction force
h	film thickness
k	surface roughness factor
L	axial bearing width
$\dot{m}$	mass flow rate of lubricant
M	$= ph^{3/2}$
N	shaft speed (revs/s)
p	pressure
P	mean bearing pressure = W/LD
Q	volume flowrate
R	bearing radius
T	friction torque
u	velocity in pipe flow; velocity in direction rotation
U	surface velocity
V	mean velocity in pipe flow
W	bearing load
x	distance round bearing in direction of rotation
y	distance across bearing normal to direction of motion distance from pipe wall
z	distance from bearing surface through film thickness

α angle in γ-space after min. film thickness for film breakdown

α' angle after min. film thickness for film breakdown

β angle after max. film thickness for film formation

γ angle round bearing from max. film thickness according to Sommerfeld transformation

ϵ eccentricity ratio = e/c

η lubricant viscosity

θ angle round bearing from max. film thickness in direction of rotation

θ_1 angle at start of film

θ_2 angle at breakdown of film = $\pi + \alpha'$

ν lubricant kinematic viscosity = η/ρ

ρ lubricant density

τ shear stress; τ_w wall shear stress

ϕ lubricant outlet temperature

ψ attitude angle, between line of centres and load direction

ω shaft speed (radians/s)

$f = 2\tau_w/V^2\rho$ friction factor pipe flow

$F^* = Fc/\eta ULR$

$FC = FR/Wc$

$h^* = h/c$

$M^* = p^* h^{*3/2}$

$p^* = pc^2/6UR\eta$

$Q^* = 2Q/UcL$

Re = Reynolds number = Uc/ν bearings

= Vd/ν pipe flow

S = Sommerfeld number = $Pc^2/NR^2\eta$

$T^* = T/N^2D^4L\rho$

$W^* = Wc^2/6UR^2L\eta$

$y^* = y/L$

INTRODUCTION

'To the machine designer, all bearings are necessary evils contributing nothing to the product of the machine; and any virtues they have are only of a negative order. Their merits consist in absorbing as little power as possible, wearing out as slowly as possible, occupying as little space as possible and costing as little as possible'.

Michell

A bearing is used to separate surfaces, so preventing the transmission of undesirable forces. In rolling-contact bearings, the surfaces are mechanically separated and the lubricant only improves the operation. Plain bearings must be lubricated because the fluid film is intrinsically involved with the mechanism of separation.

Hydrostatic plain bearings can operate without relative motion of the surfaces; fluid is supplied at high pressure to force the surfaces apart.

Hydrodynamic plain bearings are self acting. High pressures are produced internally as a consequence of relative motion of the surfaces, which must bound a converging wedge of fluid. The most common geometry, the journal bearing, can be basically considered as a circular shaft passing through a slightly larger hole. Radial loads force the shaft into an eccentric position, so forming a wedge of fluid. There will not be any wear as long as the hydrodynamic pressures are high enough to prevent contact. During stopping and starting, or when overloaded, the film thickness can be reduced to the same order as the surface roughness. Only then does the choice of lubricant and bearing material become important.

As long as full hydrodynamic operation is maintained the frictional forces are very small, being caused by the shearing of the fluid. A well designed bearing can carry high loads before any contact occurs. The friction is normally proportional to the speed but is almost independent of the load

carried. At high loads the friction coefficient can be as low as 0.0005.

Hydrodynamic bearings are most suitable for surface velocities above 1 m/s. Almost any fluid can be used although a mineral oil, being an excellent boundary lubricant, is most common. However air, water and liquid sodium have all been used; special precautions such as hydrostatic separation might be necessary at low speeds. The design of liquid lubricated hydrodynamic bearings is not critical and Michells ideal can be approached.

Both rolling contact and hydrodynamic bearings have a long history of application, but the latter was the first type to be rigorously analysed. Attention was restricted to the frictional properties of material and lubricants until it was discovered that very low frictions were sometimes achieved, and that this could be associated with high internal pressures.

In 1886, Reynolds* produced an extensive analysis of the hydrodynamic phenomenon which provided the basis for all the work that followed. He formed a differential equation and produced analytical solutions for certain restricted cases. Although the equation was originally developed from first principles, it can be derived as a particular case of the Navier-Stokes equations. The Reynolds boundary conditions are still generally accepted although they have been disputed.

The basic Reynolds equation assumes: incompressible Newtonian fluid; negligible curvatures; laminar flow; constant viscosity and pressure through the film; negligible body forces; negligible fluid inertia, and steady conditions. These restrictions are often realistic but the effects of dynamic loading, turbulent flow and non-Newtonian lubricants have also been studied since the original work.

During laminar flow there is no large scale mixing between the layers of

---

* References are given in alphabetical order at the end of the thesis.

fluid and the surface drag is proportional to the mean flow velocity. Viscous forces predominate and any oscillations are quickly damped out. At higher flow velocities, inertia forces become relatively greater and at a critical point are comparable with the viscous forces. Oscillations are then amplified, the flow becomes unstable and intermixing occurs.

In well established turbulent flow, the inertia forces predominate and the velocities in the core of the flow fluctuate randomly. The frictional drag is proportional to the square of the mean velocity. Near to the wall there is a thin layer unaffected by the turbulence called the laminar sublayer. Its thickness depends on the surface roughness and the relative importance of inertia forces. A non-dimensional group, the Reynolds number, indicates the relative importance of the two forces and so can be used to predict the onset and extent of turbulence.

At high values of the Reynolds number the mean velocity is high throughout the turbulent core because of vigorous intermixing and the laminar boundary layer is accordingly very thin.

The viscous shear stress for a Newtonian fluid is given by

$$\tau_{visc} = \eta \frac{du}{dy}$$

This is the only force involved in laminar flow. The velocity has to fall very rapidly across the laminar sublayer in turbulent flow and so the shear stress at the wall is high.

The turbulent shear stress has an additional component τ_T due to large scale momentum exchanges, whereas the viscous stress can be considered due to momentum exchanges on a molecular scale.

τ_T is due to the flux of x-momentum from the middle of the flow towards the boundary walls. Its magnitude is given by $\rho(\overline{u'v'})$, where $\overline{u'v'}$ is the

mean of the product of the two fluctuating velocity components; the flow velocity in the x direction being $u = u' + \bar{u}$. This stress is non zero for the usual situation where u' and v' vary randomly.

A hydrodynamic journal bearing is one of the few flow situations that is normally laminar. However as rotating machines become larger, an increasing number of bearings operate in the turbulent regime. This situation is becoming prevalent in modern high output turbo-alternators which use oil-lubricated bearings up to 0.6m in diameter. Some nuclear power plants use liquid sodium as a lubricant, this has a low viscosity and so the bearings are often turbulent.

The total power loss in the bearings of a large power plant has been estimated as 0.5% of the total output. The amount due to turbulent operation can be as much as 2.5 MW; it is evidently important to know as much as possible about the design of turbulent bearings and to reduce unnecessary losses. The increase in friction accompanying turbulence might be more acceptable if the bearing load capacity increased proportionally. However on this basis turbulence in bearings has proved to cause a reduction in efficiency.

One of the most interesting recent discoveries in the fluid mechanics field is the reduction in the turbulent drag that can be caused by small additions of high molecular weight polymers to a fluid. Typically, a 0.005% concentration can cause a reduction of 50%. The phenomenon has been extensively investigated in pipe flow experiments and has been exploited in several applications. However, the gradual reduction in effectiveness as the polymer solution is sheared greatly limits its use.

The object of the project described in this report was to investigate the possibility of reducing the losses in turbulent journal bearings by the addition of a polymer to the lubricant. Reviews of turbulent bearing behaviour and polymer friction reduction are presented. Various problems encountered

through testing a large scale effect on small scale apparatus are described. Finally the effects of a high molecular weight polymer on the friction, whirl stability and lubricant flow rate are discussed.

TURBULENCE IN JOURNAL BEARINGS

1. LARGE RELATIVE CLEARANCE: TRANSITION EFFECTS

A. The concentric case

Taylor (1923, 1936) investigated experimentally and theoretically the stability of fluid between two cylinders, one of which was rotating. The relative clearances (0.06 to 0.34) were much greater than those for loaded journal bearings. The work is relevant because it provides information about the transition region, between laminar and turbulent flow, which is extended by using very large clearances. Taylor's mathematical analysis of fluid stability is the only example closely agreeing with experimental results.

Taylor predicted the onset and form of an instability in his experimental apparatus, which consisted of two long cylinders constrained to be concentric. A high length to gap ratio ensured that end effects were small. Dye was injected from the wall of the inner cylinder and the flow observed through the transparent outer cylinder.

With the inner cylinder rotating, the flow was completely concentric at low speeds but broke down into a secondary flow of toroidal vortices as the speed reached a critical value. These Taylor vortices, as they are now called, are shown in Fig.1. They constitute a steady secondary laminar flow and are not to be confused with turbulence.

The onset of the instability was shown to occur at a critical value of a non-dimensional group known as the Taylor number, Ta.

$$Ta = \frac{(2\pi N)^2 Rc^3}{\nu^2} \quad \text{for } C \ll R$$

A generally accepted value of the critical Taylor number is 1708.

At even higher speeds, the secondary flow became less stable and finally broke down into turbulence at a Reynolds number of 2000. The Reynolds number

is defined by:

$$Re = \frac{2\pi RNc}{\nu}$$

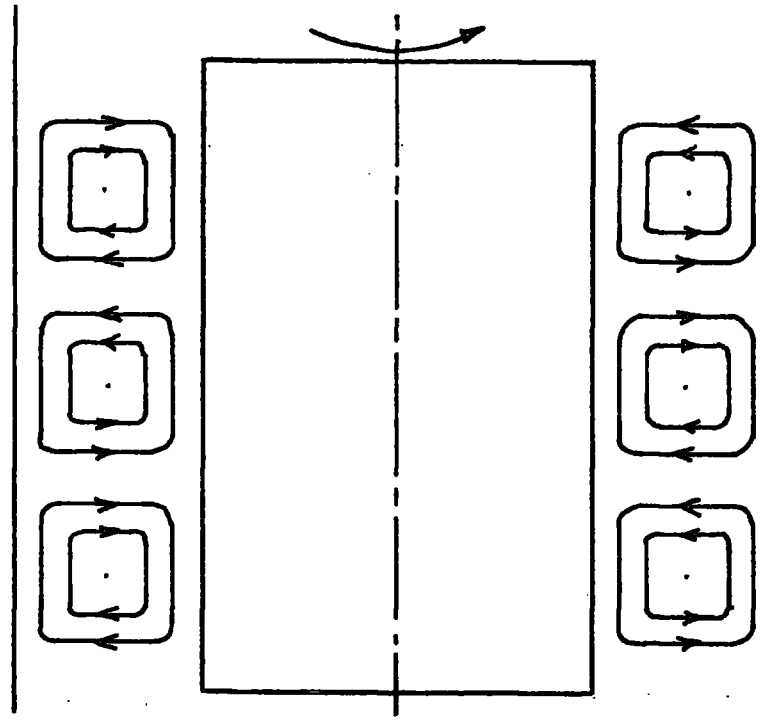

Fig.1. TAYLOR VORTICES

With the outer cylinder rotating, the flow was completely stable until it again broke down into turbulence at a Reynolds number of about 2000. A flow system is stabilised if the product (velocity x radius) increases with the radius.

Taylor performed a second series of experiments which showed that the frictional torque increased as laminar flow broke down. Considering Torque α $(\text{speed})^n$, he found that for laminar flow n = 1 as expected. During transition n increased, reaching a maximum of about 1.8 when turbulence was fully established. The observed changes in the flow were directly associated with the changes in gradient.

Relating Taylor's information to journal bearings i.e. inner cylinder rotating, vortices will only appear if the critical Taylor number is reached

before the onset of turbulence. That is:

$$41.1 \quad \frac{R}{c} < 2000 \quad \text{or} \quad \frac{c}{R} > \frac{1}{2500}$$

Journal bearings typically have a clearance ratio of about 1/1000 and so vortices should form at Re = 1300 and breakdown into turbulence at Re = 2000. This assumes the shaft and the bearing to be concentric.

B. The eccentric case

Castle and Mobbs (1967, 1970) have investigated the effect of eccentricity on the formation of Taylor vortices. This is obviously more relevant to journal bearing operation. Their apparatus was similar to that of Taylor but enabled the inner cylinder to be displaced. The clearance ratio was a compromise between bearing practice and that required for observation of vortices over a reasonable speed range.

The main findings were:

... The transition from laminar to turbulent flow took place in several discrete steps representing different forms of instability. For example the vortices did not extend completely across the wide gap region when first formed; but they suddenly jumped across at a higher speed.

... Eccentric operation increased the critical Taylor number, typically by a factor of 3 for an eccentricity ratio of 0.7.

... The onset of the second instability when the vortices filled the clearance was associated with a sudden increase in the torque gradient.

These results are in agreement with those of Cole (1957) who also found that axial flow can have a pronounced effect on the transition, increasing the critical Taylor number.

If Taylor vortices appeared in journal bearings they would be closely followed by turbulence. The factors adversely affecting the formation of stable secondary flow are as follows:

1. eccentricity
2. axial flow
3. small clearance ratio
4. turbulence near lubricant supply grooving
5. an incomplete film.

Cole has observed vortices in a 180° bearing but they were very irregular. Some sort of circulation might possibly occur in the full film region of a complete journal bearing.

2. JOURNAL BEARING CHARACTERISTICS

A simple dimensional analysis is possible for the journal bearing. For laminar flow, the viscous forces predominate and the important variables are: L, R, N, F, W, c, η. A relationship can be produced using the Pi theorem.

$$\left(\frac{F}{W}\right) = \phi\left\{ S, \frac{L}{R}, \frac{c}{R} \right\}$$

Where S is the Sommerfeld number, defined by

$$S = \frac{W}{2LRN\eta}\left(\frac{c^2}{R^2}\right)$$

The eccentricity ratio is closely dependent on the value of S which indicates the degree of loading. According to this simple analysis, the friction coefficient for a particular bearing will depend only on the Sommerfeld number.

When a bearing becomes turbulent, the inertia forces are important and fluid density must be considered. The modified non-dimensional relationship is:

$$\left(\frac{F}{W}\right) = \phi'\left\{ S, Re, \frac{L}{R}, \frac{c}{R} \right\}$$

Where Re is the Reynolds number as defined by Taylor

$$Re = \frac{2\pi NRc}{\nu}$$

For turbulent operation, the friction characteristics of a bearing cannot be shown on a simple plot of two parameters because both Re and S must be considered. At constant S, the friction coefficient is constant for laminar flow but will become dependent on Re after the transition, either to turbulence at Re = 2000 or to Taylor vortices.

Friction measurements are often most conveniently taken for constant loads. This method is satisfactory for laminar bearings but constant Sommerfeld number is more useful for turbulent bearings. Cross-plotting between results

at different loads can sometimes be used to compare results at constant S values. If the eccentricity ratio can be accurately measured then it can be used as an alternative method of analysis.

For a concentric and completely full laminar bearing, the friction torque is given by the simple Petroff formula (which assumes a small clearance ratio and constant viscosity):

$$T = \frac{\eta N D^3 \pi^2 L}{2c}$$

This equation can be rewritten in terms of a non-dimensional torque T^* and the Reynolds number.

$$\frac{T}{\rho N^2 D^4 L} = T^* = \frac{\pi^3}{2Re}$$

Alternatively an expression can be derived involving the Sommerfeld number.

$$\frac{F}{W} \cdot \frac{R}{c} = \frac{2\pi^2}{S}$$

A concentric bearing can not develop internal pressures and so carry a load. Because fluids can normally withstand only small negative pressures, there will be a cavitated region in the diverging part of the film. In this area the fluid breaks up into filaments which contribute nothing to the load capacity although they increase the friction.

The Petroff expression does not strictly apply to a loaded bearing, but it is found to agree closely with experimental results. The error in neglecting the eccentricity, which increases the friction, is offset by the reduced area of sheared fluid. An exact analysis is possible taking into account the eccentricity and the cavitation, but there is usually a considerable uncertainty in both the value of the running clearance and in the effective viscosity; therefore Petroff suffices.

The integrated pressure forces on the bearing and shaft act through the respective centres. This causes a difference in the frictional forces at the two surfaces; the shaft torque will be greater by an amount $We\sin\Psi$ to account for the offset.

Experimental results for journal bearings operating in both laminar and turbulent regimes are often plotted in the form T^* vs. Re. A log-log plot should show a gradient of -1 in the laminar regime tending towards zero after the transition. Either constant Sommerfeld number or constant eccentricity is the ideal test condition but constant load is often used. Apart from the difficulty of analysing the results, there are certain practical problems involved in operating at constant load. A large shaft speed range has to be covered and so the eccentricity varies greatly. A load which causes contact at low speeds is often not high enough to suppress whirl at high speeds. Whirl is a dynamic instability caused by the mass of the shaft (or the mass of the bearing if this is free) acting on the stiffness of the lubricating film; it occurs only at low eccentricity ratios.

3. PREVIOUS EXPERIMENTAL INVESTIGATIONS

The few previous experimental investigations of turbulent journal bearing behaviour show a variety of approaches in arranging for the film to have a high Reynolds number. The most realistic method is to use a large diameter bearing with a normal clearance. An increased clearance ratio, low viscosity or high shaft speed is more suitable for small scale laboratory apparatus. Unfortunately, results are often not directly comparable because of the differences between machines. In particular the behaviour at the transition point is affected. Some workers have attributed their results to the appearance of Taylor vortices, others have noticed only a transition to turbulence.

The Reynolds number usually used is based on the mean clearance and an assumed mean lubricant viscosity. The actual value of Re will vary round the film and so turbulence will develop gradually rather than suddenly encompass all of the film. The mean Re value is justifiable because the frictional torque is a summation of the shear force over the whole bearing area.

Three very different investigations are closely considered because they illustrate the behaviour of turbulent bearings and so provide a basis for the discussion of experimental results. The following table gives details of the apparatus. The mean Reynolds number, specified above, is used for all the quoted results.

DETAILS OF EXPERIMENTAL APPARATUS

WILCOCK		SMITH and FULLER	HUGGINS	
0.203	0.102	0.076	0.61	Bearing Diameter (m)
0.5	1	1	0.75	Width/Diameter
1.7, 2.5, 4.4	3.8	2.93	2 and 0.8 *	clearance ratio x 10^3
150		1.15	1200	power (kw)
333		124	60	max speed (r/s)
8570		4000	9000	max Re
10.3 for all tests		4.6	21.4	max mean pressure (bar)
white metal/steel		bronze/st. steel	white metal/steel	bearing/shaft material
OIL		WATER	OIL	Lubricant
grooves $\pm 90^{\circ}$ to load		hole opp. load	grooves $\pm 90^{\circ}$ to load	oil feed
T, N, Q, ϵ, temps. round bearing		T, N, Q, ϵ pressures round bearing. In and Out temp.	T, N, Q, ϵ. In and Out temp.	parameters measured
outlet temp.		(In + Out)/2	Outlet temp.	Mean temp. for viscosity
Bearing loaded through hydrostatic		Bearing loaded through hydrostatic	shaft loaded through pads	Loading method
Direct		Direct	Heat Balance	Friction measurement

* Elliptical bearing.

A. Wilcock (1950)

The first investigation into the characteristics of loaded journal bearings operating in the turbulent regime was carried out by Wilcock in the United States. His most interesting results are shown on Fig.2 in the form of a log-log plot of T^* vs. Re.

As expected, Wilcock found that the torque was directly proportional to the Reynolds number at low speeds. Most of his results were taken with the bearings supplied at both the leading and trailing inlet grooves. These showed a definite transition at about the speed predicted by Taylor for vortex formation. One set of results, unfortunately from a different bearing, were taken with only the leading groove supplied. This showed a transition at nearly twice the Taylor critical value although at less than the Reynolds number for full turbulence.

In both cases the gradient of the curve changed from -1 to nearly zero when turbulence was fully established. However, the transition is more gradual than that observed by Castle and Mobbs (1967) and Wilcock's suggestion that it represents the appearance of vortices is questionable. An irregular secondary flow might account for the behaviour but the transition would be expected at a Reynolds number greater than that predicted by Taylor for concentric flow.

The increased transitional Re value when only the leading groove is supplied is consistent with a shortening of the film. This would decrease the real Re and perhaps further stabilise the film against vortex formation. It must be concluded, in the light of Castle's and Mobbs' work, that the friction measurements are more realistically explained by the gradual growth of turbulence.

The transition from laminar flow was also indicated by increased film temperatures, by a lowering of the flowrate and by a decrease in the eccentricity ratio. These parameters did not show the transition as distinctly as the increase in torque.

Wilcock also plotted his results as friction coefficient vs. Sommerfeld number. Fig.3 shows that the friction coefficient was increased by turbulence.

Both methods used in the presentation of the results ignore the significance of one of the important factors and so neither are suitable for general comparisons.

B. Smith and Fuller (1956)

The apparatus used for this work was very similar to that of the present project, however the results are different.

Smith and Fuller investigated both the frictional losses in a small water lubricated bearing and the change in load capacity accompanying turbulence.

The friction results for an unloaded bearing are shown in Fig.2. The bearing was lightly loaded at high speeds to suppress whirl and the results were extrapolated to zero load. This procedure is fundamentally more acceptable than that used by Wilcock but the information gained has little application to a practical situation. The paper does not state if the bearing weight and the effect of the supply pressure were accounted for.

The experimental points follow the Petroff line very closely until almost exactly the predicted Re for concentric Taylor vortices. After a well defined transition region the results can be represented by:

$$T^* = 0.605\ Re^{-0.43}$$

Lubrication with water offers several experimental advantages over mineral oils because of the reduced viscosity and much smaller change with temperature. Power losses and film temperatures are reduced, and the calculated mean viscosity more accurately represents the true situation. However the results of Smith and Fuller are surprising because of the well defined transition, which suggests that Taylor vortices can be formed in a

bearing at low loads. No details of the lubricant supply are given but considering the position of the feed hole, the large clearance and the early transition, a high pressure was probably used to almost fill the bearing. The large axial flow would be expected to stabilise the bearing.

Fig.4 shows the effect of eccentricity on the bearing friction. For a laminar film the friction increases slightly at high eccentricity ratios but falls slightly when the bearing is turbulent. This interesting effect is probably a consequence of the lowering of the mean Reynolds number causing more of the film to become laminar.

Measurements round the bearing showed that the pressure profile was of a similar shape for both laminar and turbulent operation. The actual loads carried at certain eccentricity ratios were compared with laminar theory. The values closely agreed before transition but the experimental load for a turbulent film was higher than predicted. However the increase in load capacity was not as great as the increase in friction. On this basis a turbulent lubrication film is less efficient than a laminar film. This result corresponds to the trend towards higher friction coefficients shown on Fig.3 for other investigations.

Considering the increases in the transitional Reynolds number observed since this work it would be interesting to have details of the lubricant flowrate and feed pressure. The significance of the results could then be evaluated.

C. Huggins (1966)

This work is interesting because it involves tests on a large turbo-generator bearing.

The rig was designed around a fixed bearing because this arrangement is dynamically more realistic than the fixed shaft usually chosen for

experimental apparatus. However this method excludes direct friction measurement and Huggins resorted to a heat balance calculation, which is obviously not as satisfactory and throws a certain amount of doubt onto the results.

As can be seen in Fig.2, there is a change in the T^*/Re gradient at about Re = 2000. There does not appear to be a Taylor vortex condition. One interesting aspect of this plot is that the pre-transition results lie on a line of slope -0.56 not -1 as expected. This effect is also noticeable in the Sommerfeld plot shown on Fig.3.

A lot of results were manipulated so that the variation of the friction coefficient with Reynolds number could be shown at constant Sommerfeld number. Fig.5 shows that inertia forces are important even before the transition, causing a dependency on Re. Huggins felt restrained from using the term laminar for the pre-transition region calling it quasi-laminar. The oil grooving was particularly generous in this case; it is probable that the flow in these areas became turbulent at very low speeds. The sudden transition would then occur when the remainder of the film became turbulent.

It is difficult to draw any satisfactory conclusions about the fundamental behaviour of turbulent bearings from this work but it indicates the effects encountered in a practical situation.

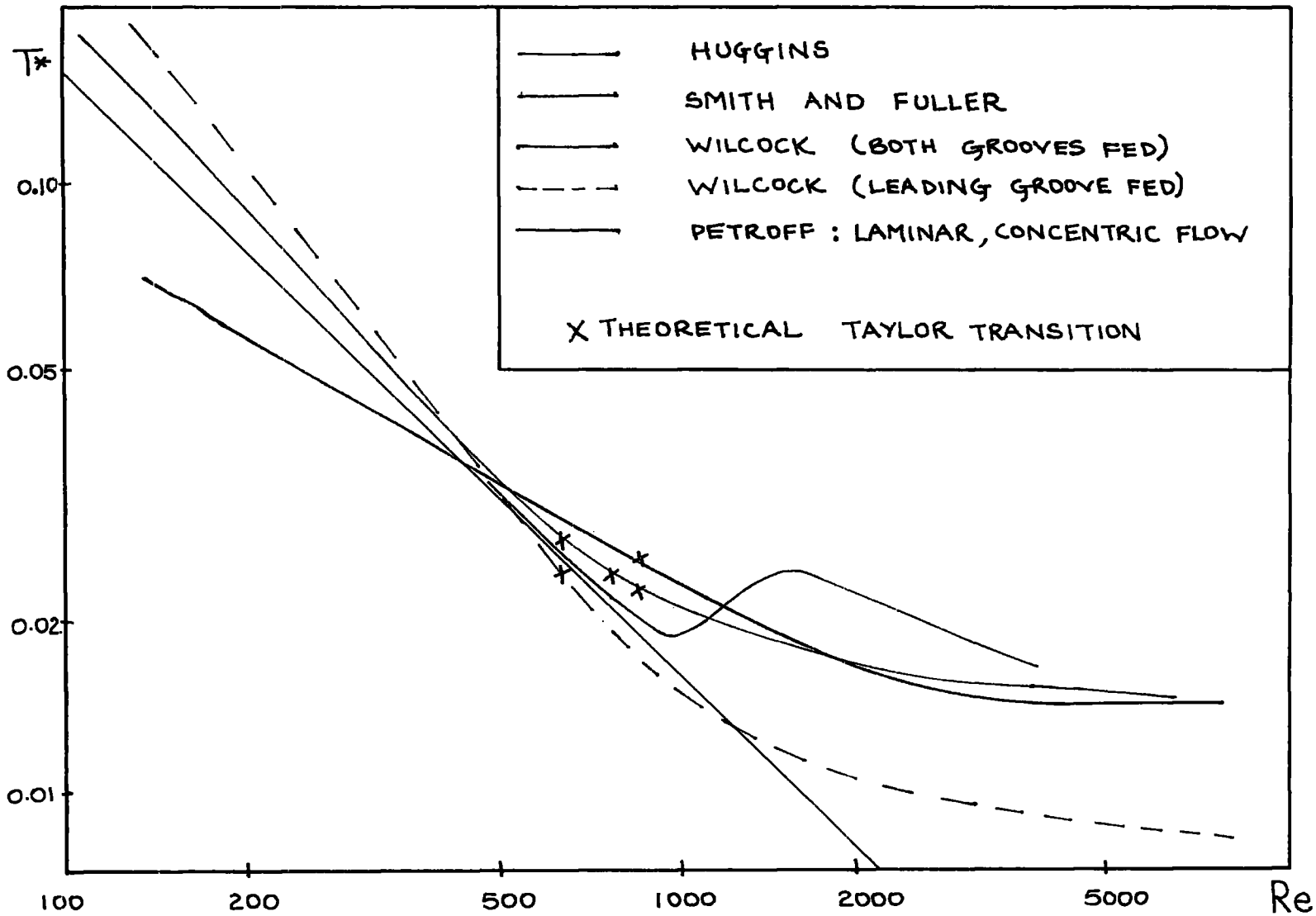

FIG. 2 NON-D TORQUE VS. REYNOLDS NO.

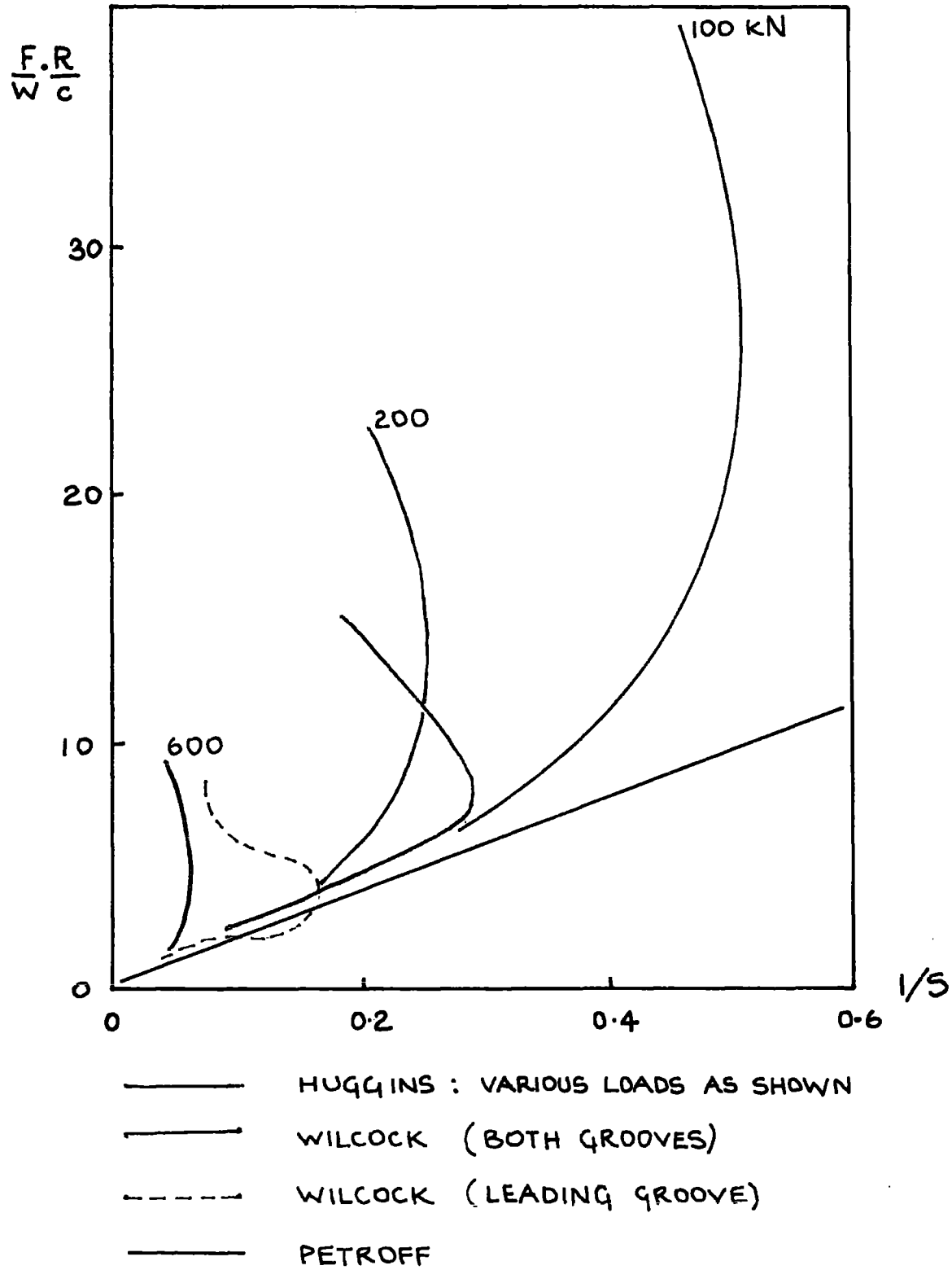

FIG. 3 FRICTION COEFFICIENT vs SOMMERFELD RECIPROCAL

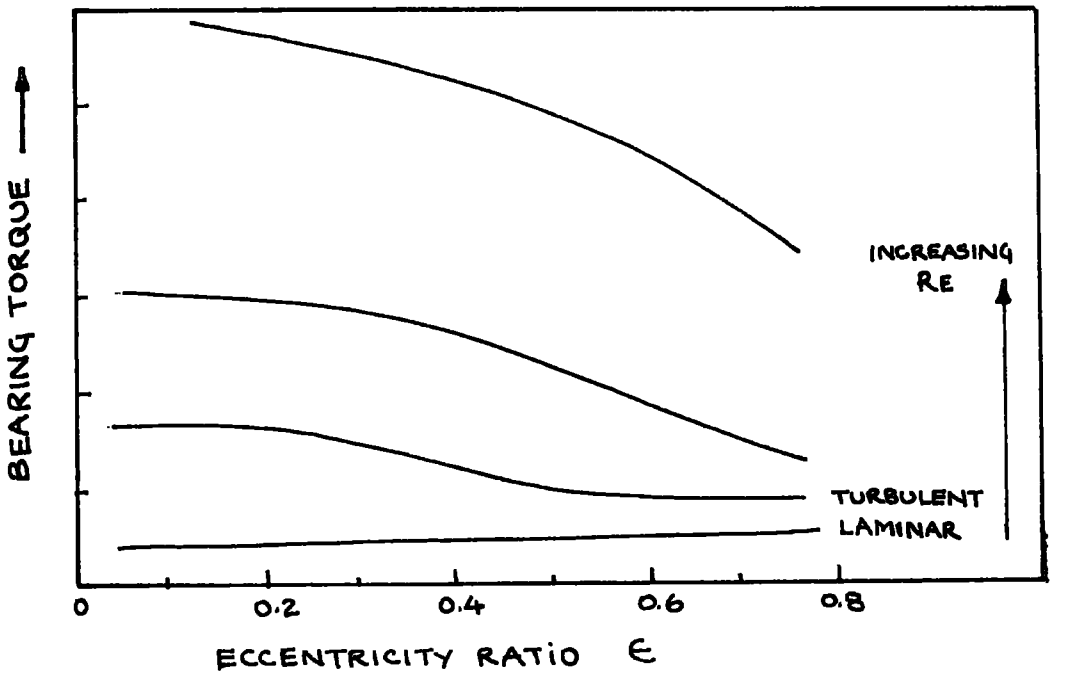

FIG.4 SMITH AND FULLER : EXPERIMENTAL RESULTS

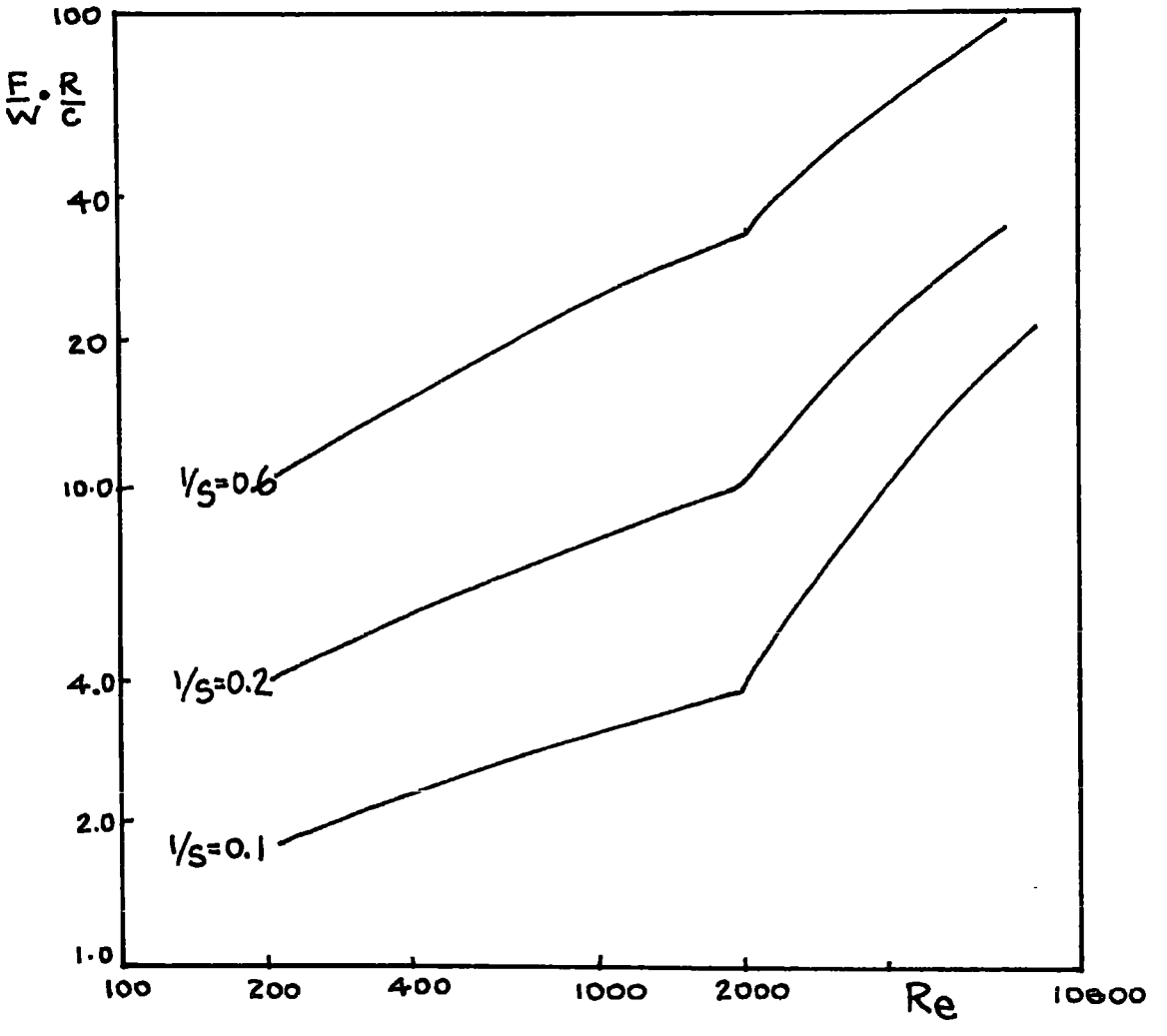

FIG.5 HUGGINS : RESULTS AT CONSTANT S

TURBULENT FRICTION REDUCTION BY HIGH MOLECULAR WEIGHT POLYMERS

1. PREVIOUS INVESTIGATIONS

The phenomenon of reducing frictional losses in turbulent flows by the addition of polymers was first described by Toms (1948) and is generally known by his name. The effect is surprising because of the large reductions caused by low concentrations and because the polymer slightly increases the bulk viscosity of the fluid. The actual reduction depends on many factors, but is typically 50% with 0.001% to 0.01% by weight of added polymer. The fluid remains essentially Newtonian in the laminar regime. Molecular weights of about one million or above are necessary.

It is important to note that only the Toms effect described above will be considered. Some investigators have measured slight drag reductions using polymers which cause noticeable shear thinning or viscoelastic effects; however high concentrations are necessary and the laminar behaviour is affected. It has been found that large additions of wood pulp or glass fibres can cause a drag reduction in turbulent flow. Although these phenomena might involve the same basic mechanism as the true Toms effect, they can be differentiated from it by smaller friction reductions, higher concentrations and modified laminar behaviour.

The solutions that exhibit the Toms effect are not significantly viscoelastic as normally measured, but this does not exclude viscoelasticity as a possible cause. In fact it is certain that the production and dissipation of turbulent energy are affected by the polymer.

A large number of investigations have followed Toms' report. Unfortunately much of the information is conflicting but some generally accepted facts will be presented before detailed results are discussed.

1. Friction reduction begins at a critical value of the wall shear stress which depends on the polymer type, concentration and molecular weight.

2. The greatest reduction is caused by linear polymers with few side branches and flexible linkages. The base fluid should be a good solvent for the polymer.

3. The polymer must be present near the wall for friction reduction and the concentration in this region is important.

4. The polymer increases the thickness of the laminar sublayer without appreciably affecting the flow in the turbulent core.

5. All polymers become less effective at reducing friction after some time. This degradation is probably caused by a reduction in the average molecular weight by mechanical fracture of the polymer chain.

6. Laminar to turbulent transition is not delayed and the friction is always greater than the extrapolated laminar value.

A pipe flow system is probably the simplest way to investigate turbulent drag reduction. Pressure drop measurements can easily be made accurately and a great deal of information is known about this type of flow. Not surprisingly, almost all of the previous investigations used this method and most of these used water as the solvent.

Most of the important features of polymer drag reduction were presented in Toms' paper. However he used a rather unusual solution (polymethyl methacrylate in monochlorobenzene) and some of his results are difficult to interpret. Two later pipe flow studies will be used to illustrate the main features of the effect. Figs. 6 and 7 show the results in the usual friction factor against Reynolds number form.

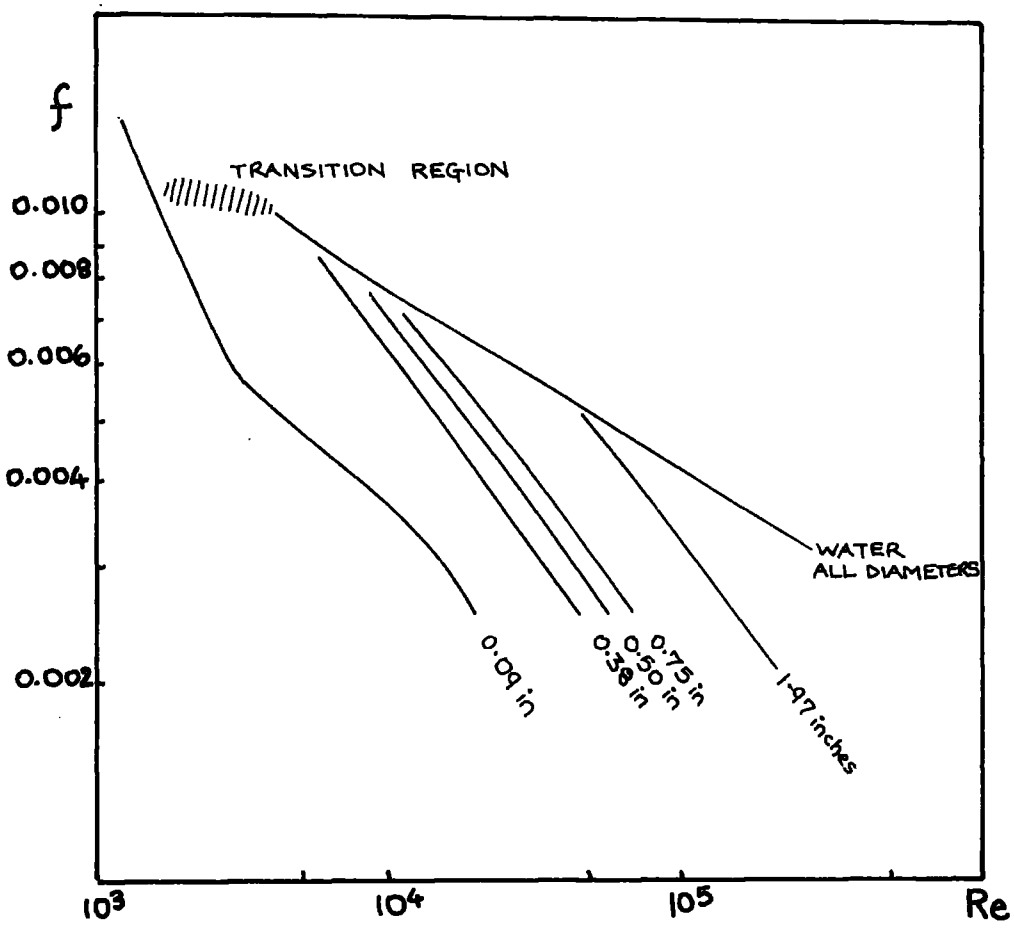

FIG. 6 EXPERIMENTAL RESULTS OF WHITE

VARIOUS PIPE DIAMETERS AS SHOWN
SOLUTION: 480 p.p.m GUAR GUM IN WATER
FRICTION FACTOR, $f = 2\tau_w/\rho V^2$

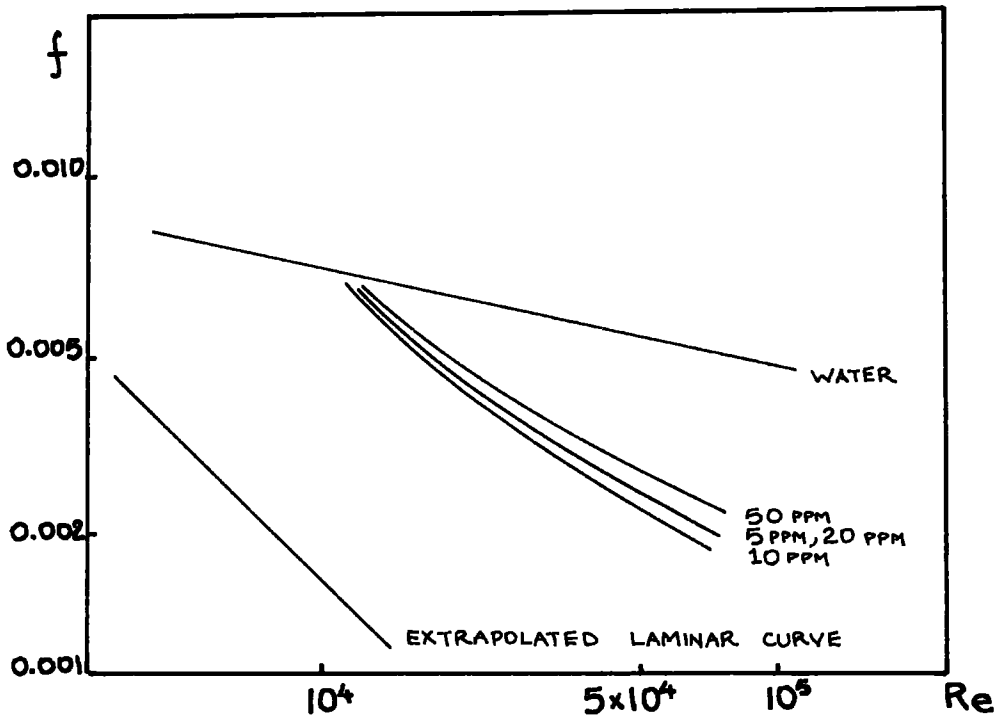

FIG. 7 RESULTS OF GOREN AND NORBURY

PIPE DIAMETER = 5cm
VARIOUS CONCENTRATIONS OF POLYOX WSR 301

From White's results (1966) it can be seen that the polymer does not affect laminar flow and that there is a strikingly sharp change in the friction when drag reduction begins. The onset of the reduction is highly dependent on the pipe diameter, and was shown by White to correspond to the concept of a critical wall shear stress. Taken with some of his other results he has shown that this critical value varies only slightly with concentration. Assuming that Blasius' law is valid for this Reynolds number range i.e. $f \alpha Re^{-0.25}$ then for a particularly polymer $Re_{ONSET} \alpha d^{8/7}$. This expression agrees closely with White's results.

The diameter effect caused some confusion during the early investigations, particularly those using a small diameter pipe for which the results were interpreted as an extension of laminar flow. The practical usefulness of the Toms effect in pipe flow systems is severely limited by the dependence on pipe diameter. Although the flow in large diameter pipe lines, such as those used for oil transportation, is usually turbulent, the wall shear stress can be below the critical onset value.

The results of Goren and Norbury (1967) on Fig.7 again show that the friction is unaffected until a critical point. The slight dependence of the onset on concentration can be seen, as well as a critical concentration which causes the maximum reduction. For the poly(ethylene oxide) used the optimum concentration was about 10 parts per million by weight. White found that for Guar Gum, the drag reduction increased up to the highest concentration used (480 p.p.m.). The greater friction reductions were produced by PEO and it can be concluded that this is a more effective additive than Guar gum.

PEO is commercially available in well defined molecular weight ranges, readily dissolves in water and is non-toxic. It has been widely used for pipe flow investigations particularly in the grade available from Union Carbide Ltd. known as Polyox WSR 301, which has a molecular weight of 4×10^6. Polyox has proved to be an extremely effective drag reducer and seems to

embody all the desirable molecular characteristics. Unfortunately it also degrades very quickly. Guar Gum, a naturally occurring mixture of polymers, is much more stable although not as effective in reducing friction. It is perhaps inevitable that degradation rate and effectiveness go together because of conflicting molecular requirements.

Before considering the results of various other workers, it is worthwhile to note some of the factors that can produce conflicting data. The most important are the effective polymer concentration and the molecular weight. Both wall injection and premixed solution have been used and the method chosen will obviously affect the concentration until well downstream of polymer entry. Uncertainties in the molecular weight might be due to shearing during the mixing process or original errors. These problems, particularly variations in mixing method, have caused poor repeatibility. The molecular characteristics have not been completely specified in many cases, hindering attempts to correlate the observed effects with these properties. Forced transition has been used in a number of pipe flow investigations to ensure a consistent transitional Reynolds number.

Wells and Spangler (1967) carried out a classically simple experiment to show that the polymer only affects flow near to the boundary. They injected a concentrated solution at the centre of a pipe and at the wall. Only in the latter case did friction reduction begin immediately. It took a finite time for the polymer to diffuse from the centre to the wall and then the friction began to fall.

Various investigators have noticed continued friction reduction after the polymer supply has stopped. This led to a wall adsorption theory, but this is generally discredited. The carry-over effect is probably due to the long residence times of polymer near to the walls.

Gadd (1965, 1966, 1967) has carried out a series of experiments to investigate the possibility of viscoelasticity accounting for the Toms effect. A PEO solution will usually form a thread on a rod withdrawn from it, whereas water breaks up into drops to minimise the surface energy. This behaviour is explicable in terms of a normal stress difference which is a characteristic of a viscoelastic fluid. Crudely this means that the pressure is not the same in all directions. There are therefore good reasons to investigate the rheological properties if drag reducing solutions.

A viscoelastic explanation of the Toms effect is possible and various rheological models have been suggested. It would seem however that these are more applicable to concentrated solutions and recently a molecular, rather than continuum explanation is usually put forward.

Gadd found that although freshly prepared Polyox solutions showed measurable viscoelasticity, solutions that had been standing for some time did not. The friction reducing properties were not affected by ageing. He also found that various other polymers that reduce turbulent drag neither have measurable normal stress differences nor form threads; Guar Gum is an example of this type. He suggests that the difference between freshly prepared and aged PEO solutions is that aggregations of molecules are formed during preparation and later break up to give a homogeneous solution.

Gadd carried out experiments on flows without solid boundaries, mainly jets of polymer solution into water. He found that freshly prepared solutions of Polyox behaved differently than water, but that aged solutions were indistinguishable. The aged solutions do not form threads.

It has been suggested that the methods used for the detection of viscoelastic effects are not sensitive enough. Elata and Rubin (1966) investigated the effect of polymers on the formation of Taylor vortices, showing that this instability is very sensitive to viscoelastic properties. They found that the

flow was stabilised by the polymers, but only significantly at high concentrations.

In his later reports Gadd puts forward sublayer thickening as the primary mechanism of drag reduction and suggests that any viscoelastic effects are a secondary phenomenon. He points out that the thickening might possibly be explained in terms of a normal stress difference; thus molecular and continuum explanations are not entirely incompatible.

Several workers have measured the velocity variation across the flow in pipes. The typical results of Wells as presented by Lumley (1967) in his general review of drag reduction are reproduced in Fig.8. There are various problems in calibrating either a pitot tube or a hot-wire instrument for polymer solutions but, particularly for low concentrations, the profile is probably close to the real situation.

The results are presented in the normal way; the thickening of the laminar sublayer is immediately apparent. The slope of the curve for the turbulent core is not affected, but the region near to the wall is extended. A typical effect on the actual flow velocities is shown diagrammatically in Fig.9. It can be seen that the flow is increased for the same wall stress correspondingly to increased friction for the same flow. The polymer affects only the region where turbulent energy production and dissipation are of the same order, although the concentration is constant across the test section (Goren and Norbury, 1967).

Virk et al (1967, 1971) carried out an investigation of the flow of polymer solutions in both rough and smooth pipes, paying particular attention to the correlation between measurable polymer characteristics and the observed effects. They found that the friction reduction increased with molecular weight and proposed a universal correlation. The results for rough pipes are particularly interesting because of the possibility of investigating the

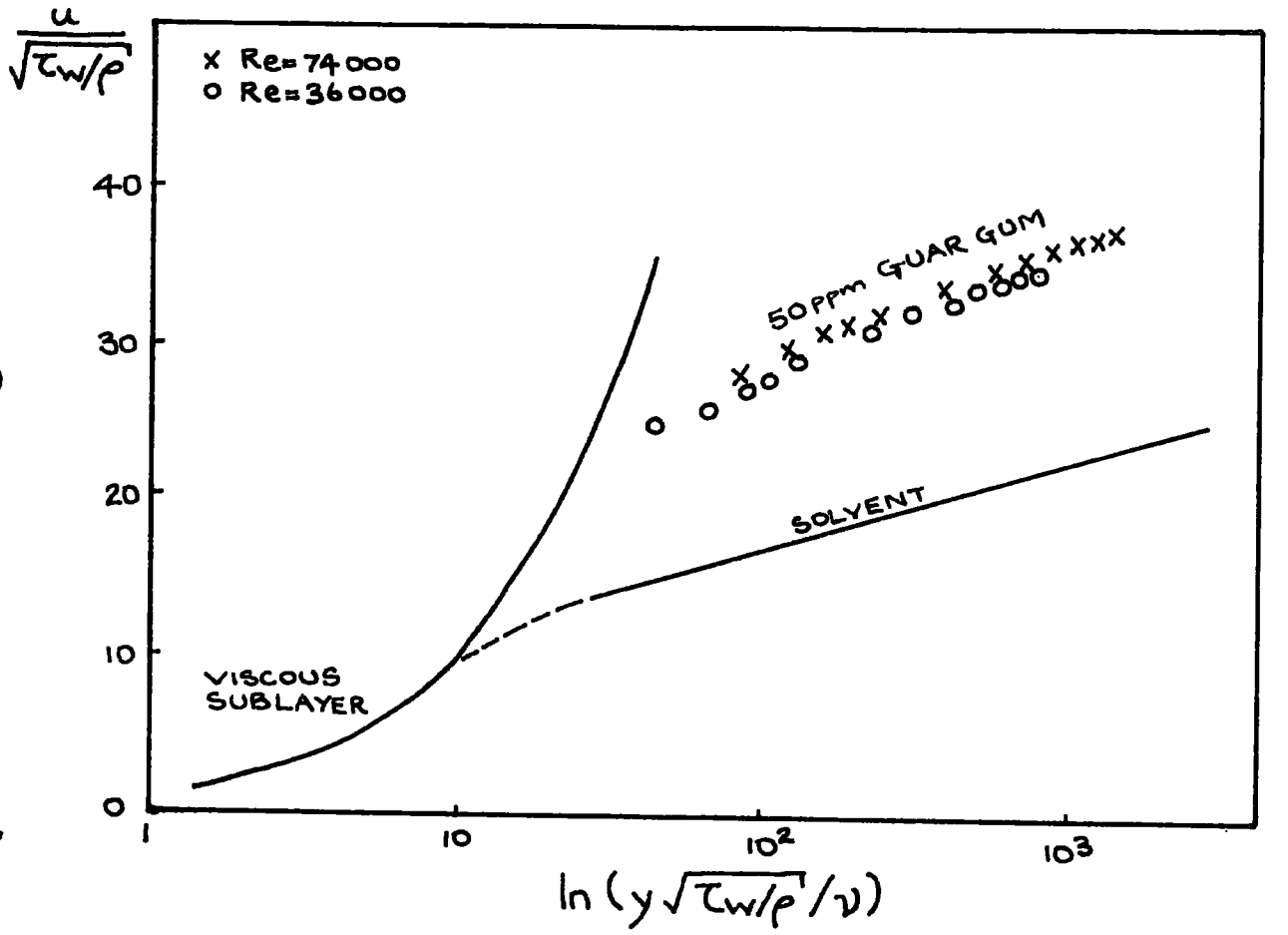

FIG 8. VELOCITY VARIATION ACROSS A PIPE
RESULTS OF WELLS, PLOTTED BY LUMLEY

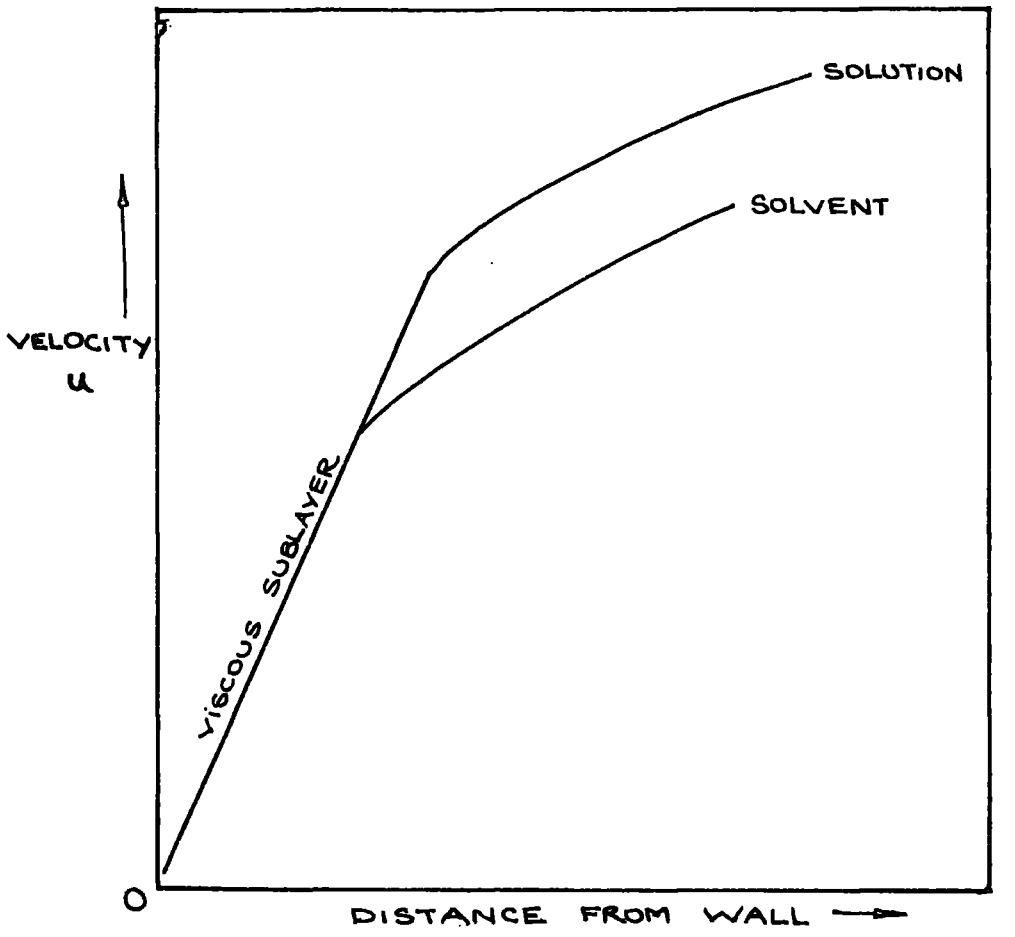

FIG. 9 DIAGRAMMATIC EFFECT OF A FRICTION REDUCING ADDITIVE ON VELOCITY VARIATION NEAR TO A BOUNDARY

effect at the wall from simple friction measurements; they are shown in Fig.10.

Virk (1971) found that there is a limiting value for the drag reduction which is independent of polymer type, concentration or molecular weight. The asymptotic value is always less than for extrapolated laminar flow and can be represented by:

$$f = 0.42\ Re^{-0.55}$$

Fig.10 is produced on the basis of this maximum possible reduction and shows a remarkable similarity between the solvent and the solution. The pipe remains hydraulically smooth until a higher Re for the polymer solution, supporting the concept of a thickened sublayer. The increase is by a factor of about 2.5, which closely corresponds to that from velocity measurements.

Virk found that the onset shear stress varied little with concentration. The critical value for Polyox WSR301 is about 0.5 N/m^2.

The results of Merril et al (1966) are particularly applicable to journal bearings because a co-axial cylinder apparatus was used. A direct comparison with pipe flow results is complicated by end effects. Merril calculated the critical concentration at which polymer molecules begin to affect each other; the value for Polyox WSR301 is given as 400 p.p.m. At concentrations below this the additive hardly increases the bulk viscosity. Although the additions of polymer necessary for friction reduction are a small proportion of the total weight, most of the solvent is affected. The results of part of Merril's work are presented in Fig.11; the effect of varying concentration of WSR301 at about four times transitional speed is shown.

Unfortunately it is difficult to determine the best concentration of Polyox WSR 301 from the published results. Some workers have found that there is an optimum concentration. Merril found 3 p.p.m. gave the most reduction whereas Goren and Norbury, using injection from the pipe walls, specified 10 p.p.m. Both the investigations of Squire et al (1967), and Giles and Petit

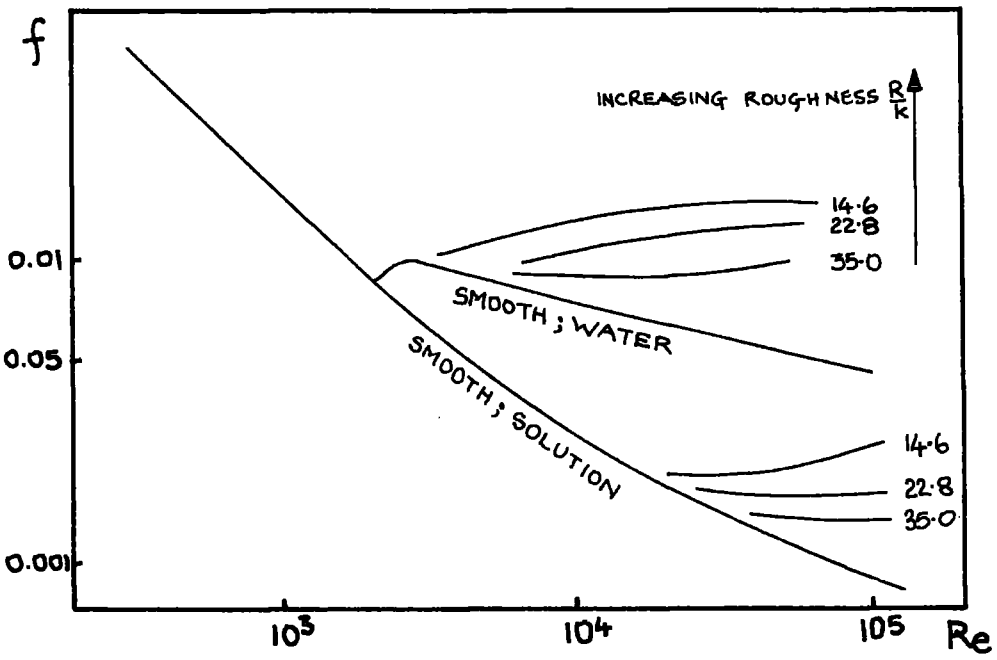

FIG. 10 FRICTION REDUCTION IN ROUGH PIPES : VIRK'S RESULTS

PIPE DIAMETER = 8 mm

MAXIMUM POSSIBLE REDUCTION IS SHOWN

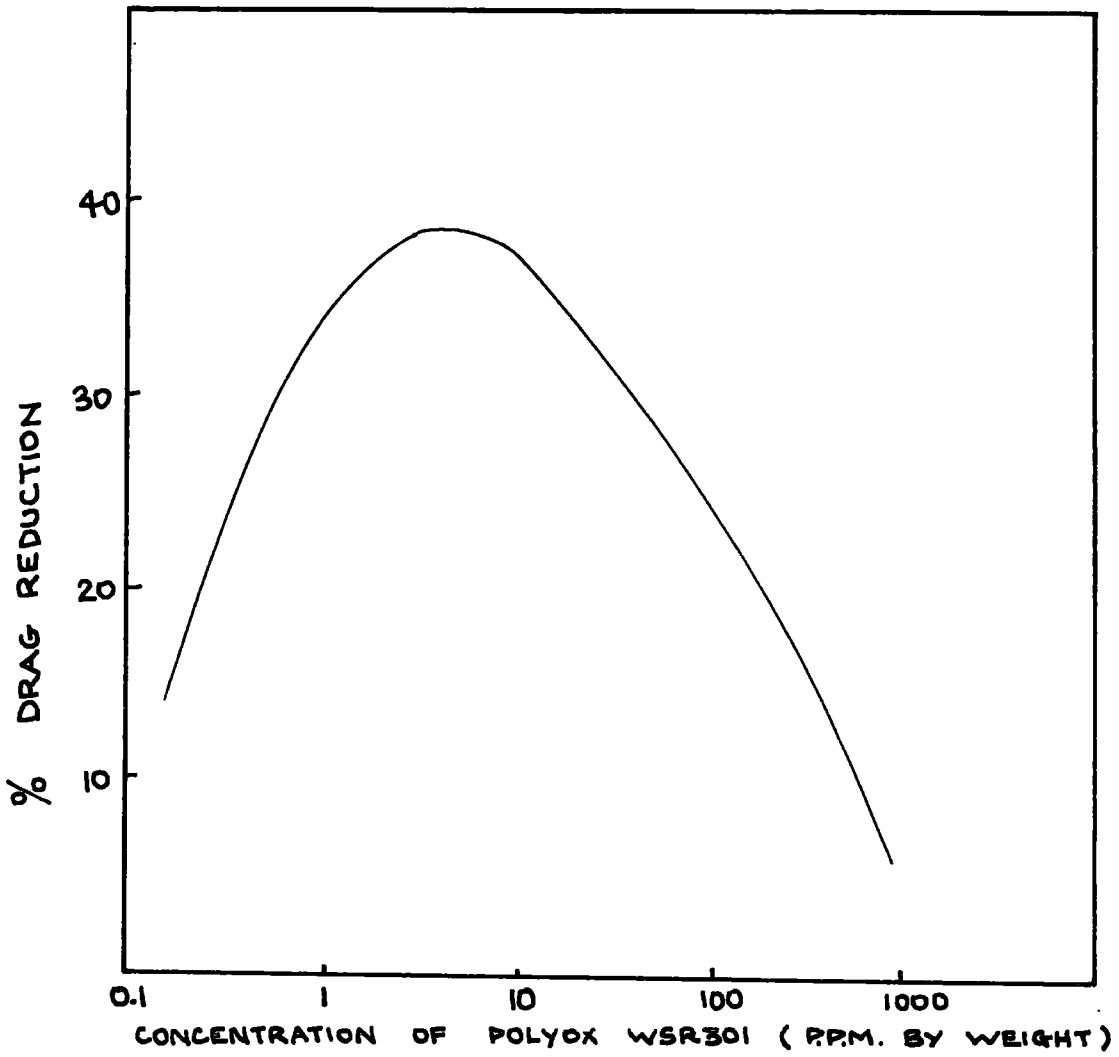

FIG. 11 MERRIL'S RESULTS : DRAG REDUCTION IN COUETTE VISCOMETER

(1967) used a pipe flow apparatus with a premixed solution. They found that the optimum concentration was about 25 p.p.m., but 300 p.p.m. caused the same reduction.

Virk's result was very different from all the others, showing increased reduction up to the highest concentration (500 p.p.m.) used.

The differences between the results are unexplained, but must be due to differences in apparatus or in solution preparation. There does not seem to be any published quantitative information on polymer degradation rate. It is probable, however, that the reduction is effectiveness begins immediately. The measured optimum concentration might therefore be higher than strictly required at each point so that the degradation effect is minimised. If this hypothesis is true then the rate of shearing and the method of solution preparation would affect the optimum concentration.

2. THE MECHANISM OF FRICTION REDUCTION

A definitive explanation of the Toms effect has not yet been put forward. Several fundamentally different theories have been suggested since the original observations were published. It is now generally accepted that thickening of the viscous sublayer is the primary consequence of the addition of polymer.

Relations between the onset and degree of friction reduction and the molecular characteristics have been developed but they are essentially empirical. Thus the correlations cannot be extended with certainty beyond the experimental range. The effective use of the phenomenon will be greatly aided by an understanding of the basic mechanism.

The Toms phenomenon occurs only in turbulent flows; it has been shown not to be an extension of laminar flow. In turbulent flows energy is extracted from the mean flow to maintain the turbulence. The turbulent energy is dissipated into heat and acoustical energy. The effect of the polymer is to reduce the loss of energy but it is not known if the production or dissipation of the turbulent energy is affected. The study of conditions close to the wall is extremely difficult but advances in this direction can be expected to produce valuable information. One conclusion that can be drawn from the experimental observations is that the core of the flow is unaffected by the presence of polymer molecules.

The region of influence of a polymer molecule in a dilute solution is limited to the space occupied. This led to a conclusion that the presence of the polymer becomes noticeable when the smallest scale of the flow becomes comparable to the polymer scale.

Lumley (1967) proposed a mechanism based on the suppression of vortices which exist in the sublayer by anisotropic viscosity. The eruption of these vortices into the core is recognised as fundamental in producing turbulence. The polymer chains are normally tangled into balls by thermal agitation and

van der Waal's forces. Under the high shear conditions occurring at the edge of the sublayer the molecules will be elongated and will rotate. The elongated molecules, according to Lumley, hinder the transmission of energy across them. In essence this is a continuum mechanism; the effect being achieved through the overall solid-like behaviour of the molecules. This excludes a interaction based on scales and so an interaction with the production of turbulence is questionable.

From a molecular viewpoint, the primary cause of the Toms effect is probably an interaction with the dissipation of energy. The polymer presumably inhibits the transfer of energy from large scale to more vigorous turbulence.

3. THE PRACTICAL USE OF FRICTION REDUCING POLYMERS

Polymers have been found that exhibit turbulent drag reduction in a variety of fluids, including water and mineral oils; but the effect has not been exploited to the extent that might be expected. There are various problems hindering the practical use of the Toms' effect, which is obviously attractive.

Experiments have been carried out on both small scale and full sized ships. Using Polyox injected from the sides of a minesweeper, Canham (1970) found that a power reduction of about 15% could be obtained with a concentration of about 10 p.p.m. in the boundary layer. This is obviously wasteful although degradation effects are not important, and it is difficult to properly distribute the polymer round the hull. The system was found to be too bulky and too expensive for continuous use in commercial vessels, but it might be useful for short bursts of speed from warships. It has recently been discovered that some of the fastest fish secrete a friction reducing substance in times of necessity, (Rosen and Cornford, 1971). In this way, as in many others, Nature anticipated Modern Technology.

The use of friction reduction in transportation pipe lines is hindered by the diameter effect and by the degradation of the polymer which occurs if large distances are involved. One of the most successful applications is in fire fighting systems. A large quantity of water has to be passed once at high flowrates through small diameter hoses - an ideal situation for the use of Polyox.

The limiting factor in most systems is undoubtedly degradation. More stable polymers will probably be developed in the future, and a better understanding of the basic mechanism might allow the design of friction reducing materials for specific applications. It might be possible for molecules to recombine after shearing or for particles rather than molecules to provide large friction reductions.

The critical onset shear stress in journal bearings occurs at a speed far below the transition to turbulence, thus the advantages of polymer addition should be available throughout the turbulent regime. The length corresponding to the diameter in pipes is the radial clearance which is always small. However, before the present project it was not obvious if the high shearing rate would degrade the polymer too quickly for a significant reduction in friction.

THE EXPERIMENTAL RIG

The investigation was carried out on a plain journal bearing machine designed by the author and built in the University workshops. The test section of the shaft is nearly 0.1m in diameter and is supported by a plain slave bearing at either end. The operating ranges are from 10 to 170 r/s and from 0 to 5 kN load. The following parameters were measured:

bearing friction torque
shaft speed
applied bearing load
pressures at various points round the test bearing
lubricant flowrate, feed pressure and outlet temperature.

Figs. 12, 13, 14 and 15 show the machine.

1. THE DRIVE SYSTEM

The machine is powered by an 11 kW, 25 r/s Induction motor. This drives a PYE TASC UNIT at 60 r/s by means of a TURNERS POLY-VEE belt. The TASC UNIT provides a maximum of 7.5 kW at variable speeds up to 53 r/s; it is essentially a type of magnetic clutch using the feedback from a tachogenerator to regulate the output speed. The output speed could not be closely maintained at low values because of hunting. The test shaft is driven by means of a STEPHENS MIRACLO belt. This is of nylon-reinforced leather construction; it was chosen so that small diameter pulleys could be used and because it slides off at a well determined point in the event of a bearing seizure.

The motor and TASC unit are carried on a steel channel platform which can be tilted to tension the belt to the test shaft. The motor moves in slots to tighten the other belt. The test head is bolted to the top of a framework which carries the motor platform underneath.

Fig.14 shows the layout.

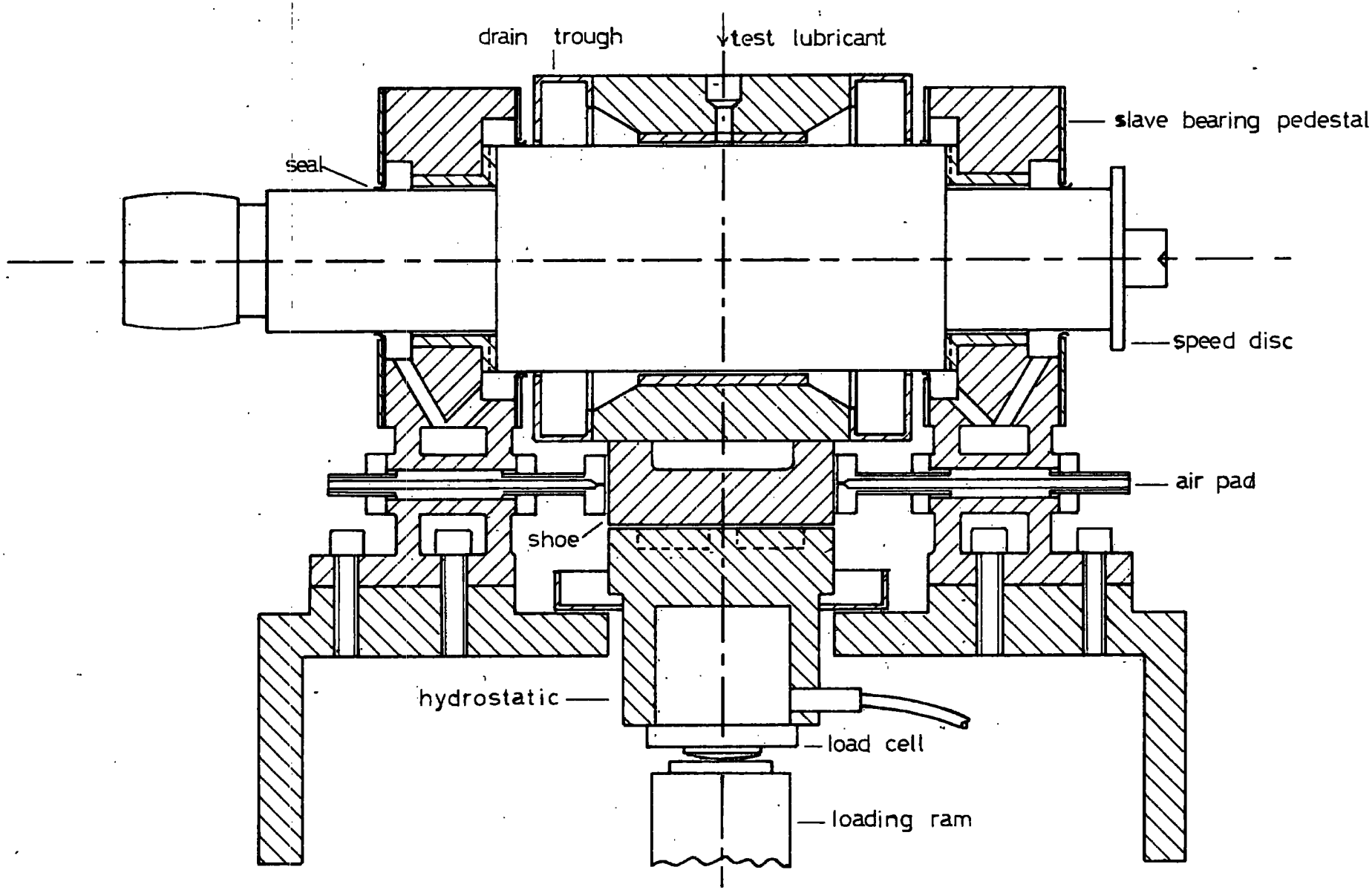

FIG. 12 SECTION THROUGH TEST HEAD

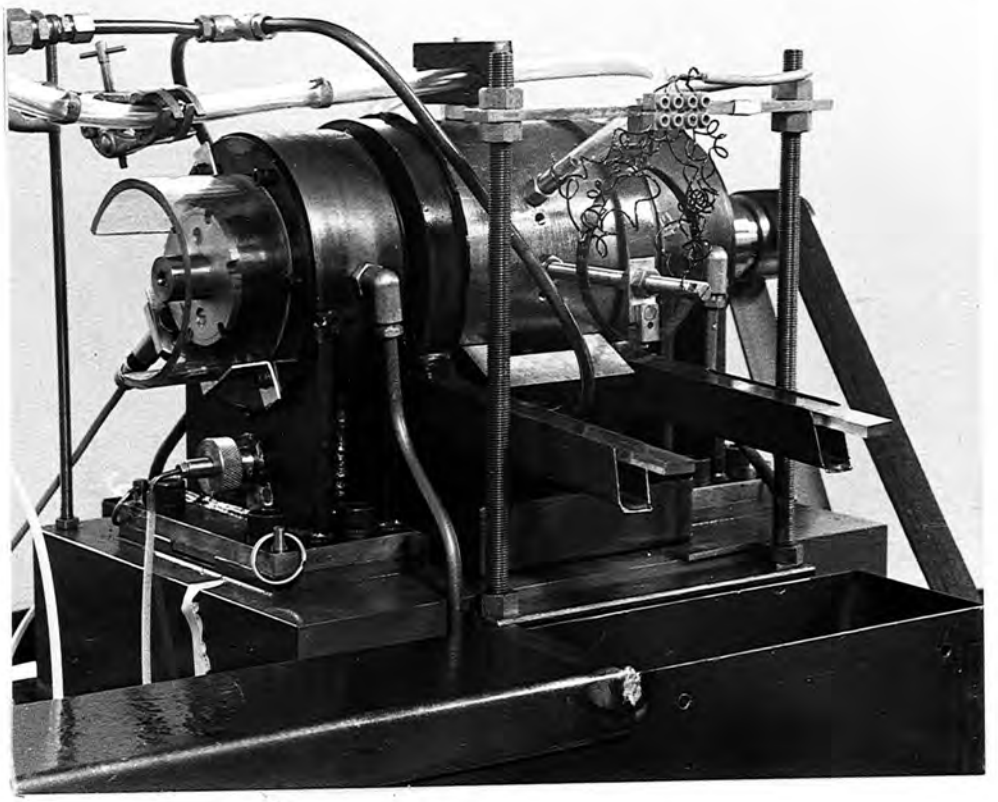

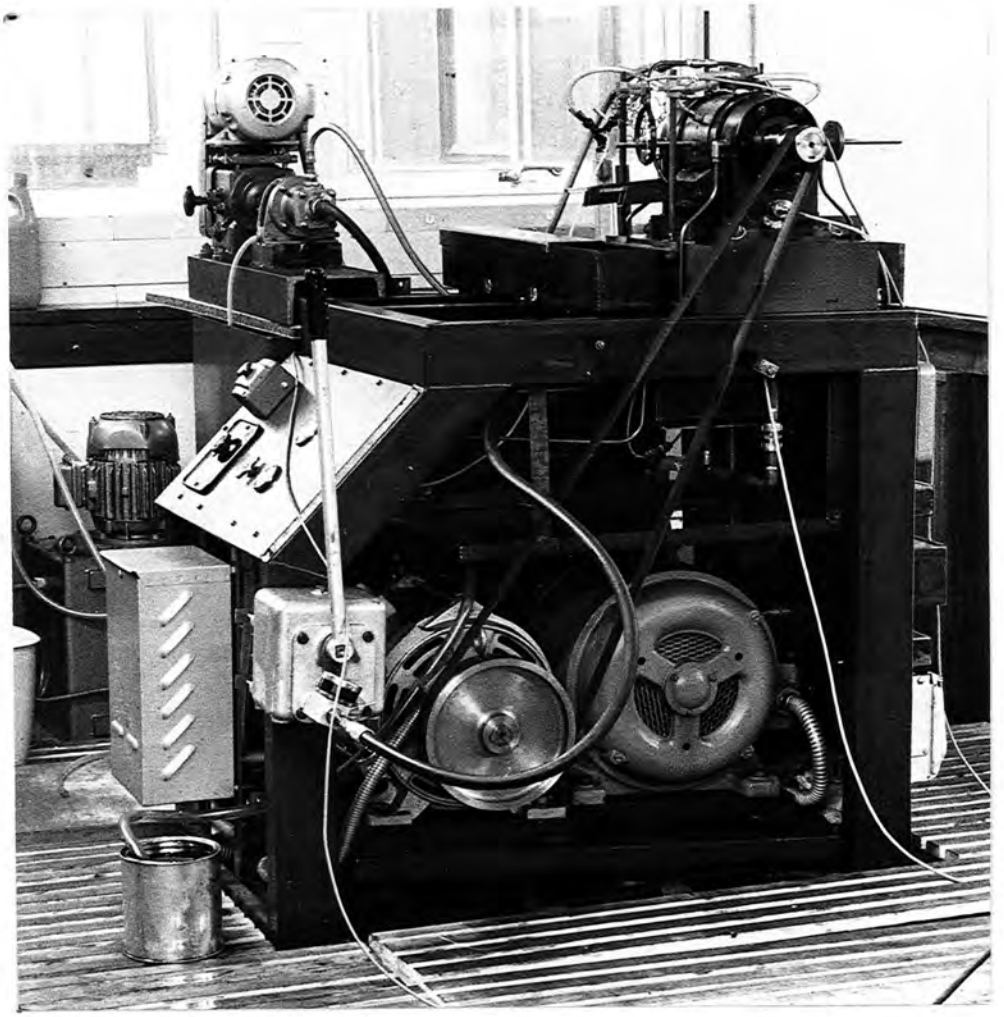

FIGURE 13 and FIGURE 14 - THE TEST RIG without belt guard

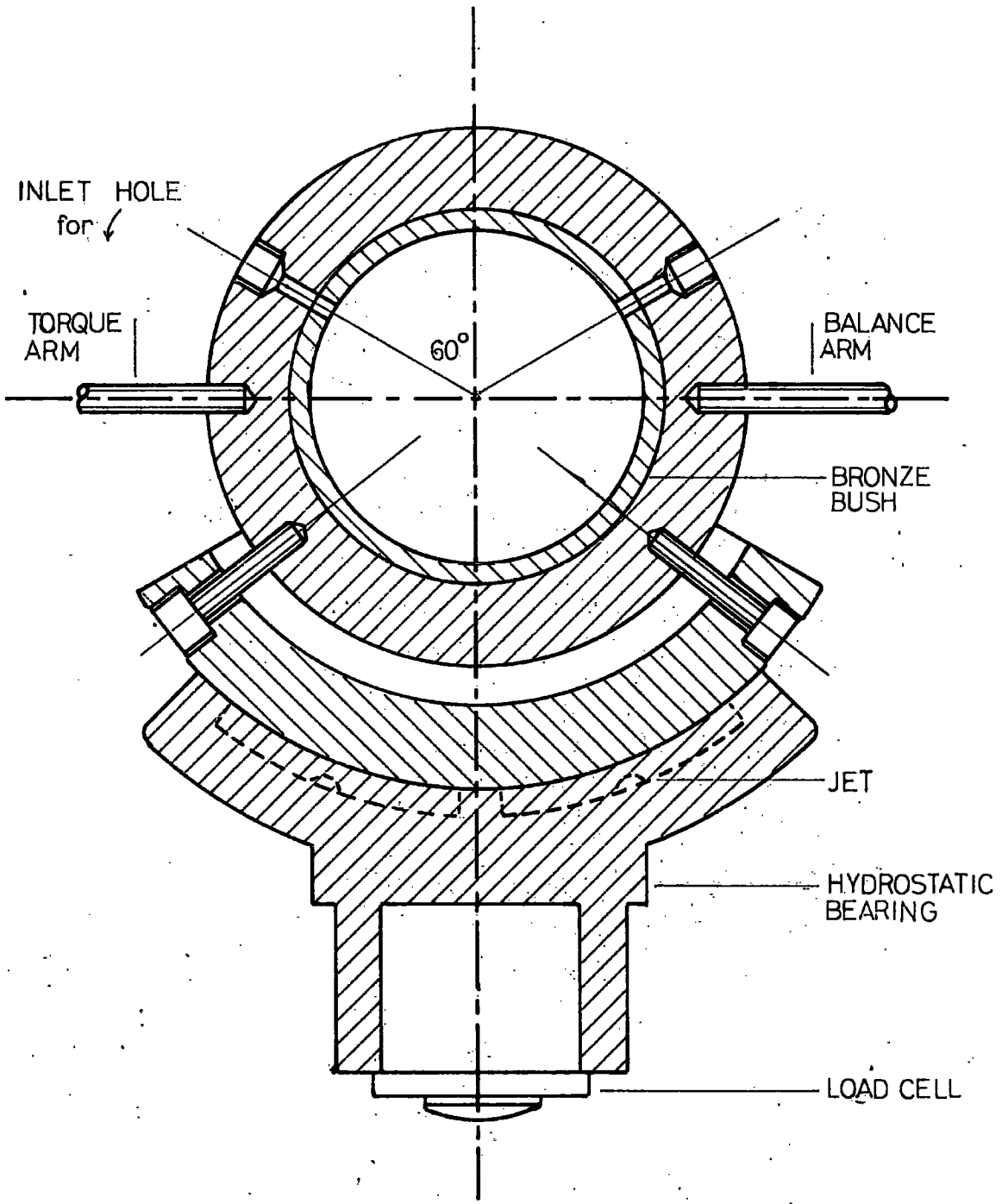

scale : half size

FIG.15 SECTION THRO' TEST BEARING

2. THE SHAFT AND THE SLAVE BEARINGS

The shaft is supported in two plain bearings, one on either side of the test bearing. This arrangement keeps the shaft deflection to a minimum over the test section, although assembly is more difficult. The pedestals are bolted to a substantial cast-iron base and located by dowels; both slave bearings were bored through together when in position. The bearings are both 6.25×10^{-2} m diameter with a diametral clearance of 1×10^{-4} m; they were designed to operate well within the laminar regime. The bronze bushes are lined with white metal; the inner face of each locating the shaft in the axial direction. A driving pulley is keyed to one end of the mild steel shaft, it is slightly crowned to keep the flat belt in position.

A gear pump supplies mineral oil via a 20 micron filter to each bearing. There are two feed grooves at 90° from the vertical to allow rotation in either direction; both are supplied although only the leading groove is strictly necessary. The oil drains into a pocket at each end of the bearing and then downwards through slots into a compartment inside the pedestal. A suction pump returns the lubricant to the supply tank through tubes which are screwed into the bottom of each pedestal and pass through holes in the base.

Seals made of thin rubber are fitted to both ends of the bearings, they are simply rings glued to the inside of the end oovers and turned outwards. In practice these seals were not completely adequate because, under certain conditions, oil built up in the pockets and leaked out. It was thought that the increased friction of more effective seals would heat the shaft too much and so the leakage was tolerated.

During initial tests it was found that the thrust faces acted as centrifugal pumps, flooding the drainage system at that end of the bearing and starving the other end. The bearings were successfully modified by cutting large radial grooves in each face destroying the pumping action.

Plain slave bearings were chosen because the maximum speed and load are beyond that recommended for suitable rolling element bearings. In retrospect a deep groove ball bearing and a roller bearing lubricated by oil mist would probably be more suitable because high speeds were only required for short periods. This would have avoided the drainage sealing and starting difficulties of plain bearings. One advantage of the plain bearings is that the test head can be dismantled very quickly for maintenance and modification.

3. THE LOADING SYSTEM

The loading system had to be carefully designed to that it would not interfere with the measurement of friction, which was of prime importance. Friction coefficients as low as 0.001 are not unusual for plain bearings, and if the line of action of the load just misses the bearing centre or if the loading mechanism exerts a small force on the test bearing then there will be a torque produced of the same order as the bearing-shaft friction. The couple due to the geometrical errors of the system can be accounted for by taking friction readings for both directions of rotation.

It is important to make the friction in the loading system as small as possible if reliable results are to be obtained. The neatest and most effective way is to use a hydrostatic bearing. This interposes a film of pressurised fluid between the loading device and the test bearing so that shear forces cannot be transmitted. The present design uses a hydrostatic bearing which is 90° of a cylinder and has a projected area of $1.75 \times 10^{-2} m^2$; it acts against a shoe of 120° arc bolted to the test bearing. The arrangement can be seen in Fig.15. The channel section of the shoe enables pressure measurements to be taken in that part of the bearing.

The oil is pumped at high pressure through AMAL jet orifices into four symmetrical pockets, this maintains a constant film thickness over the whole

hydrostatic bearing and so accurately fixes the load direction. If the bearing tilts it will reduce the film thickness at some point; this will reduce the flow from the associated pocket and so decrease the pressure drop across that jet. The pocket pressure will rise and force the film thickness to increase until equilibrium is reached. The procedure will be reversed in the part of the bearing with increased film thickness, so helping the return to the correct position. A certain degree of compensation could be obtained from the supply lines alone, but the jets accentuate the effect and can easily be changed to give correct control.

The test bearing thus floats on a film of oil and is automatically kept in the position whereby the load acts through a vertical line through the bearing centre. As the load is altered, with the supply pressure constant, the point of application moves along this line.

The pocket pressure and size, and the jet characteristics were chosen to give good compensation with a high stiffness. The oil is filtered and supplied to the bearing at about 2×10^6 N/m^2. It drains from the sills of the hydrostatic bearing into a trough; a suction pump returns the flow to the supply tank via a water cooled heat exchanger. A five micron filter is needed as this type of bearing is susceptible to jet blockages and to grit being trapped between the surfaces. Taking readings in both directions eliminated any effects due to misalignment or asymmetrical flows.

The loading ram sits on an I-beam bolted to the underside of the test head base. A hand pump pressurises the ram and a needle valve locks it in position. A load cell is located in the bottom of the hydrostatic bearing; it has a curved face which acts against the flat top of the ram. The cell is a fully temperature compensated strain gauge unit made by VIBROMETER SA; it is connected to a PEEKEL A.C. bridge from which the load can be read with an accuracy of 2%. A cell of 10 kN capacity was used for most of the

experimental tests, but others of 25 kN and 50 kN capacity were available.

Published papers by Neal (1967) and Raimondi and Boyd (1957) were consulted during the design of the loading system.

4. SPEED MEASUREMENT

A disc with six notches is attached to one end of the test shaft. An electro-magnetic pickup is positioned adjacent to this disc such that voltages are induced by the notches moving past. The speed is read off directly in r/min on an electronic counter arranged to count the number of peaks over ten seconds. The lead had to be carefully screened to avoid pickup from the induction motor.

5. TORQUE MEASUREMENT

The test bearing is restrained from rotating by an arm projecting from it and acting against a ring dynamometer. The ring is made from Beryllium-Copper strip, which has the advantages of high yield stress, low Young's modulus and very low mechanical hysterisis. Four small strain gauges are arranged in a full bridge circuit to give the best temperature compensation possible; they are connected to a PEEKEL A.C. bridge from which the friction can be read with a repeatable accuracy of about 2%. The full range of frictional force can be measured with small deflections of the ring; the whole device has proved to be very linear with no measurable hysterisis. The ring and arm are connected in such a way that both pushes and pulls can be measured, and the arm can be easily disconnected for zeroing. Another arm projects from the other side of the bearing, it carries a movable weight which is used for initial balancing. Any remaining out of balance force is eliminated by taking friction readings for both directions of rotation.

The torque measuring device is shown in Fig.13. Great care was taken to ensure accurate friction measurements because these were particularly important. The system was originally calibrated using balance weights and checked again using a single weight before each test. The strain bridge was zeroed at each change of scale required as well as at the start.

6. LUBRICANT TEMPERATURE MEASUREMENT

A copper-constantan thermocouple projects into each of the drainage troughs attached to the test bearing. These are connected to a HONEYWELL recorder such that the average temperature is shown directly and the variation recorded on a chart. The readings are used for the calculation of the mean viscosity used in analysing the results. Comparison with thermometers of known accuracy showed the instrument to be accurate to $1^{o}C$.

7. MEASUREMENT OF TEST LUBRICANT FLOWRATE AND SUPPLY PRESSURE

This flowrate is measured by a GAPMETER, which depends on the drag on a plug moving in a tapered glass column. The instrument was calibrated by weighing timed samples. During the test runs, some anomalous flow values were recorded with polymer solutions. It seems that the operation of the meter is affected by the friction reducing properties and so it was recalibrated for the solutions used in the bearing tests.

The pressure is measured by a Bourdon gauge situated after the flowmeter.

8. TEST LUBRICANT SUPPLY

A variable speed, positive displacement pump is used so that polymer containing lubricants are not degraded more than is necessary before reaching the bearing. A CARTER variable speed unit drives a MONO-PUMP. The inlet temperature of the lubricant is not carefully controlled, but as a once

through system is usually used this is not important. The temperature of the lubricant in the supply tank can be altered to give the required Reynolds number range.

The flexible pipes to the test bearing and to the hydrostatic bearing are positioned so that no unnecessary forces are transmitted through them. The feed to the test bearing lies axially from a clamping block situated on the top; the arrangement can be seen on Fig.13.

9. LOCATION OF THE TEST BEARING

The test bearing is located axially by two air pads acting against the sides of the shoe, these can be seen on Fig.12. Air is supplied at 3×10^5 N/m^2. The clearance between the pad and the shoe has to be small for satisfactory operation; otherwise the shoe sticks against one pad because of a Bernoulli effect.

The hydrostatic bearing is not located sideways. After the initial setting, the ram forces it into the correct position.

10. ECCENTRICITY MEASUREMENT

It was originally intended to measure the eccentricity of the bearing with electrical gauges mounted on the housing. A set of inductances gauges were supplied for this purpose by Vibrometer Ltd. but proved to be more sensitive to temperature changes than displacement. This is a common problem with this type of measurement.. Unfortunately the environment of the test bearing could not be compensated for and the attempt had to be abandoned. Although friction measurements are the most important in this case, eccentricity measurement would have been particularly useful during the development of the rig and might have revealed interesting details of the bearing behaviour.

11. THE TEST BEARING HOUSING AND DRAINAGE

The length of the test bearing bush is 7.62×10^{-2} m and the diameter of the shaft passing through 1.016×10^{-1} m; during the project various bearing clearances and supply grooving arrangements were used.

The bush is mounted in a large steel housing to which the shoe is bolted. The ends of the housing are cut away to act as pockets for the leakage flow. A drainage trough is bolted to each end; it directs the lubricant out at right angles to the shaft axis. The flow then drains away through another trough either to the supply tank or to waste as required. It was originally intended to drain the test bearing through short troughs along the axis and so avoid any applied moment due to the liquid, but for the flowrates that eventually proved to be becessary this is not possible in the space available. The force due to the actual design shown is only a small proportion of the bearing friction at other than very low speeds; it was accounted for by taking the readings in both directions.

Pressure tappings 1.6×10^{-3} m diameter were drilled radially through the test bearing housing at the various positions shown on Fig.30. They are threaded for ENOTS connectors. The bushes were drilled through as required and the tappings connected by small bore nylon tubing to a selection of Bourdon gauges.

THE DEVELOPMENT OF THE TEST BEARING

1. ORIGINAL INTENTIONS

As the project was originally conceived, it was intended to investigate the behaviour of a loaded bearing over a large Re range using several lubricants and polymers. By altering the bearing clearance and fluid viscosity it seemed possible to cover operating conditions from purely laminar to far into the turbulent regime. Any effect due to the addition of a polymer is most noticeable at high Reynolds numbers.

The published reports on turbulent journal bearing behaviour do not indicate that any problems can arise in using larger than normal clearances. In particular precise control of the operating parameters, such as lubricant flowrate, did not seem to be necessary. In practice, constant development of the test bearing and the experimental method was required before repeatable friction results of the expected form could be obtained. The polymer could not be added to the lubricant until any changes could be definitely attributed to that factor alone.

The problems encountered were due to the investigation of a large scale effect on small scale apparatus and the project had to become less ambitious. However, several interesting aspects of journal bearing behaviour were noticed during the development and the difficulties involved with the tests provide important information for future work.

The test bearing was originally in the form shown in Fig.12. A bronze bush, lined with white metal, was pressed into the steel housing. An axial oil groove was milled into the top of the bush at a point opposite the loading position. During tests with this arrangement it became obvious that mineral oils could only be used for laminar operation. The bearing was still laminar at the highest speeds even using a very low viscosity oil with a radial

clearance of 5×10^{-4} m. Increasing the clearance actually reduced the flow Reynolds number because the flowrate increased and the film temperatures were less, increasing the mean viscosity. Original calculations had overestimated the heating effects and the reduction in viscosity.

Journal bearings are self designing to some extent. Thus if the lubricant viscosity is reduced then the film temperatures fall and the mean viscosity in the load carrying film is not significantly affected. It is therefore difficult to force a small journal bearing into the turbulent regime without significantly departing from normal practice.

It was considered important to continue with hydrocarbon lubricants so that the polymers which are effective in these fluids could be tested. A kerosene oil with a normal viscosity of 4×10^{-3} Ns/m^2, that is about four times as viscous as water was used in a bearing with a radial clearance of 2.5×10^{-4} m. Calculation indicated that a Re of 3000 or above could be obtained with this combination; but during testing the white metal flaked off the bearing making further modifications necessary. The possible Reynolds number was not high enough and the whole approach needed to be changed before the polymers could be tested.

2. THE CONCENTRIC BEARING

The first tests using a loaded bearing were disappointing, and the whole concept was reconsidered in an attempt to ascertain if friction reducing polymers were effective.

A transparent plastic bearing, constrained to be concentric by narrow lands, was installed. The design is shown in Fig.16 below.

The lands closely fitted the shaft and so were laminar at all speeds; whereas the centre section would usually be turbulent. The small contribution to the total frictional torque due to the lands would not have been important as only the change due to the polymer was of interest.

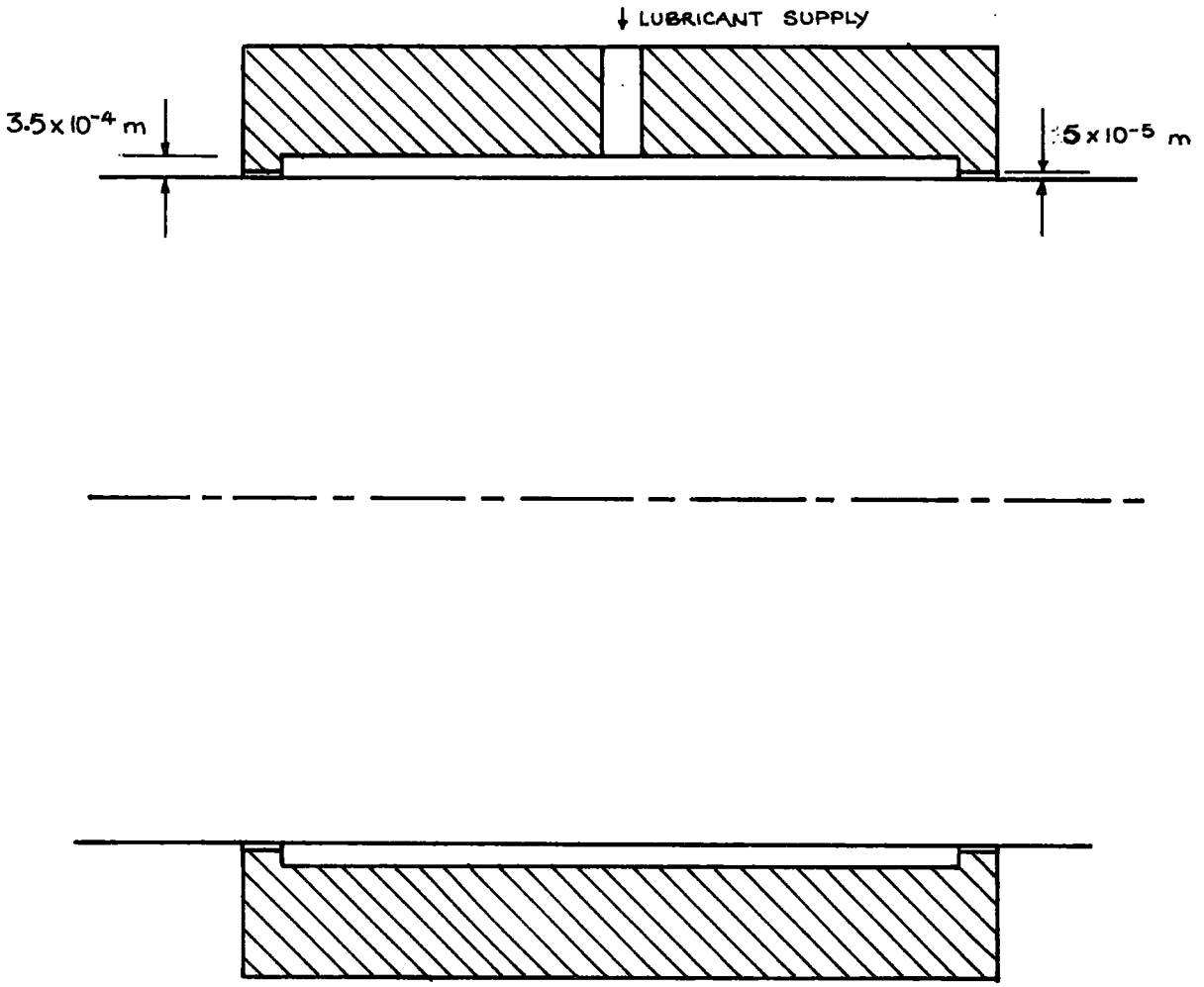

Fig.16 CONCENTRIC TEST BEARING

The bearing was supplied with kerosene and the friction measured over the speed range. Although the turbulent regime was evident by an increased torque/speed gradient, the results were too inconsistent for precise experimentation. It could be seen that the interior of the bearing became opaque at high speeds. Examination with a stroboscopic light source showed a multitude of small bubbles being carried round by the shaft. Careful observation established that the bubbles first formed next to the lands. The lands operated as normal journal bearings carrying the bearing weight and presumably developed cavitated regions which introduced air into the centre section.

The bearing was tested using water as the lubricant with similar results. A dilute Polyox WSR301 solution was also used but only a 5% reduction in friction could definitely be attributed to the additive. If the bubbles were

the source of the lack of repeatability then complete immersion of the bearing would have to be necessary. This would have involved considerable development and so the loaded bearing design was reconsidered as it is nearest to normal practice.

3. FILM EXTENT VARIATION: THE TRANSPARENT BEARING

Smith and Fuller obtained useful results from a water lubricated bearing and so their example was followed in an attempt to obtain satisfactory turbulent operation.

The advantage to be gained from the use of water as the lubricant in an experimental bearing are given below.

1. High Reynolds numbers can be obtained with small clearances and low speeds.
2. The low viscosity reduces the power requirements and the film temperatures.
3. The small viscosity variation with temperature reduces errors in the mean viscosity used in calculations.
4. A great deal of information has been obtained on the effectiveness of polymers dissolved in water.

However, there are also certain disadvantages:

1. Steel parts tend to rust - this process can be retarded by the addition of sodium nitrite to the water.
2. Water is an extremely poor boundary lubricant. It was necessary to carry the weight of test bearing on the loading ram during starting and stopping to avoid damage.
3. Although low clearance ratios can be used it is difficult to evaluate how unrealistic the situation becomes. It is

obviously the combined effect of clearance and viscosity which determines the behaviour.

Tests were undertaken with the original pattern of white metalled bearing with a radial clearance of 2.5×10^{-4} m. Water was supplied at a head of 1 m through a single hole opposite the load position. A gravity feed system was chosen to avoid any unnecessary degradation when the polymer additives were used.

Friction measurements taken at loads just sufficient to suppress whirling did not show the expected increase at high speeds. At low speeds, the torque increased linearly with speed as is expected for laminar operation. At higher speeds the gradient fell; in some cases an increase in speed produced no noticeable increase in torque. The bearing was obviously not entering the turbulent regime. Apart from this obvious defect the friction measurements were not repeatable and the behaviour was irregular.

In order to investigate this behaviour, a transparent version of the bearing was made. A large tube of TRYLON polyester resin was cast and then machined to the same dimensions as the metallic bearing. Although this process was eventually successful, great care was necessary at all stages to avoid the formation of cracks. The resin had to be cured very slowly in a flexible mould to prevent stressing.

The material dimensionally affected by both water absorption and heating, but friction measurements with the transparent bearing showed the same behaviour as the original. Temperature measurements proved that the effect was not caused by changes of viscosity.

Under the same conditions as before, the film could be observed to become smaller as the speed increased. The breakdown of the full film showed the characteristic cavitation streamers. The position of the cavitation

region remained almost static while the start of film moved into the loaded region as the speed increased. At low speeds the film attained its full width just after the supply hole and there was a small amount of reverse flow. A typical variation in flow pattern is shown in Fig.17. At high speeds the film became less distinct and churning seemed to be taking place. The shortest film extent observed was approximately 120^{o} although accurate measurements were impossible.

The shortening of the film accompanied the changes in friction and it is certain that the behaviour was caused by the diminishing area of sheared fluid. As the film moved into the small clearance region the mean Re would fall preventing a transition to turbulence. This behaviour is another example of the modification of the operating conditions such that the required characteristics were unobtainable.

The transparent bearing was used to investigate the behaviour of the bearing with the intention of correcting it. However the observations encouraged an examination of the conditions controlling the start of the film. It has often been reported that there is a delay in the formation of the film although a satisfactory explanation has not been put forward. The numerical analysis based on the Reynolds equation given in Appendix 1 shows that a minimum friction condition can be applied. It is shown that the friction is a minimum when the film extent is about 130^{o} and that if possible the bearing will adopt this configuration.

The transparent bearing was modified in stages in order that the design could be improved until the film shortening was controlled and operation in the turbulent regime was possible. An increased supply pressure affected some improvement but most of the extra flow left the bearing in the region near to the supply; an axial groove rather than a hole exacerbated this effect. However an axial groove at 90^{o} to the load direction kept the start of the film static for a greater speed range.

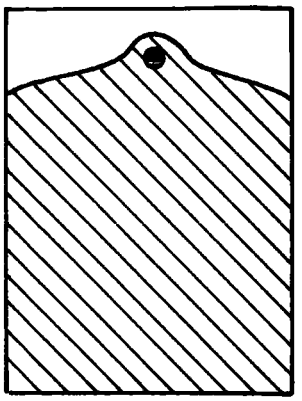

500 r/min

SMALL AMOUNT OF REVERSE FLOW

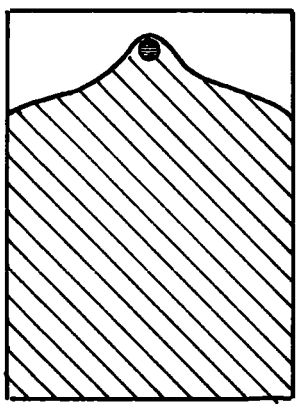

800 r/min

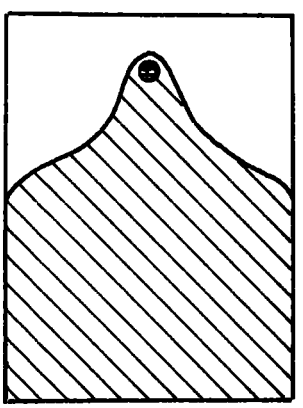

1200 r/min

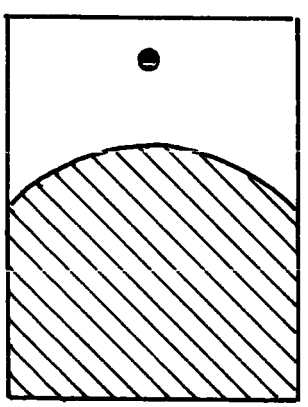

1800 r/min

FILM BROKEN AWAY FROM HOLE
FLUID TRICKLING DOWN SURFACES

FIG. 17 TYPICAL VARIATION OF INLET FILM

With the information gained from these tests the final version of the test bearing could be derived.

4. THE FINAL DESIGN OF THE TEST BEARING

The dimensions of the test bearing which was successfully used in the polymer tests are given below.

RADIAL CLEARANCE	7.62×10^{-5}m
CLEARANCE RATIO	1.5×10^{-3}
AXIAL WIDTH	7.62×10^{-2}m
LUBRICANT SUPPLY	1 cm holes positioned at 60° on either of the top of the bearing.

Calculations established that the position of the supply hole would be slightly after the maximum film thickness for the intended loads and speeds. Only the leading hole was used during the tests. The bore is less than 2×10^{-5}m out of parallel with the shoe surface which faces the loading system.

A synthetic bearing material was originally chosen for the bearing to alleviate the problems introduced through water lubrication. The material used, 'DELRIN', offers a high stiffness, a low coefficient of dry friction and dimensional stability. However friction measurements with this design proved to be irregular although turbulent behaviour was apparent. The scatter was too great for a quantitative investigation of friction reduction. The problem probably arose from variations of the dimensions, particularly the clearance. The inability of water to wet the material might have also affected the results. Although Delrin is more suitable than most other plastics its properties are far less favourable for precise investigation than metal.

A lead-bronze bearing material was used for the tests which are described in the following sections. Special precautions were necessary to avoid bearing seizure at low speeds.

The clearance ratio used limits the possible Re to 6000. This value offers a reasonable balance between controlling the film extent and testing friction reducing polymers at conditions far into the turbulent regime where their effects are most noticeable.

Throughout the development of the test bearing, the design had to be made more normal and the original ambitions restricted. The range of Re was reduced and only one lubricant could be used. The modifications were necessary because of the difficulties involved in operating a bearing under abnormal conditions and in obtaining consistent results. A larger bearing diameter would have undoubtedly simplified the requirements.

EXPERIMENTAL RESULTS AND DISCUSSION

Tests with the bronze bearing described previously, established that the operating conditions had to be carefully controlled in order to obtain repeatable results of the required form.

The test procedure is given in Appendix 4.

The Reynolds number used is based on the mean radial clearance and the lubricant viscosity at the outlet.

1. THE EFFECT OF LUBRICANT FLOW RATE ON BEARING FRICTION

The bearing friction was found to be dependent on the lubricant flowrate; the effect was accentuated by the large clearance ratio and the low lubricant viscosity.

There is not an obvious way of controlling the flow to give good experimental results. The external variables are supply pressure and feedrate; the relation between them is dependent on the speed, load and viscosity. Ideally the film extent should be controlled at either of two values: that corresponding to minimum dissipation and zero pressure supply, as discussed in Appendix 1; or starting immediately after the supply point, corresponding to a high pressure supply as often used in practical systems. The requirement for experimentation is a simply controlled condition; it is obviously impossible to specify the internal conditions directly.

The lubricant pump supplies a flow which is almost independent of the back pressure. Fig.18 shows the friction results at different flowrates and a constant load. The tests were all taken in the same direction of rotation and so the values of T^*, the non dimensional torque, have not been corrected for imbalance of the bearing. However the shape of the curves is more important than the absolute values.

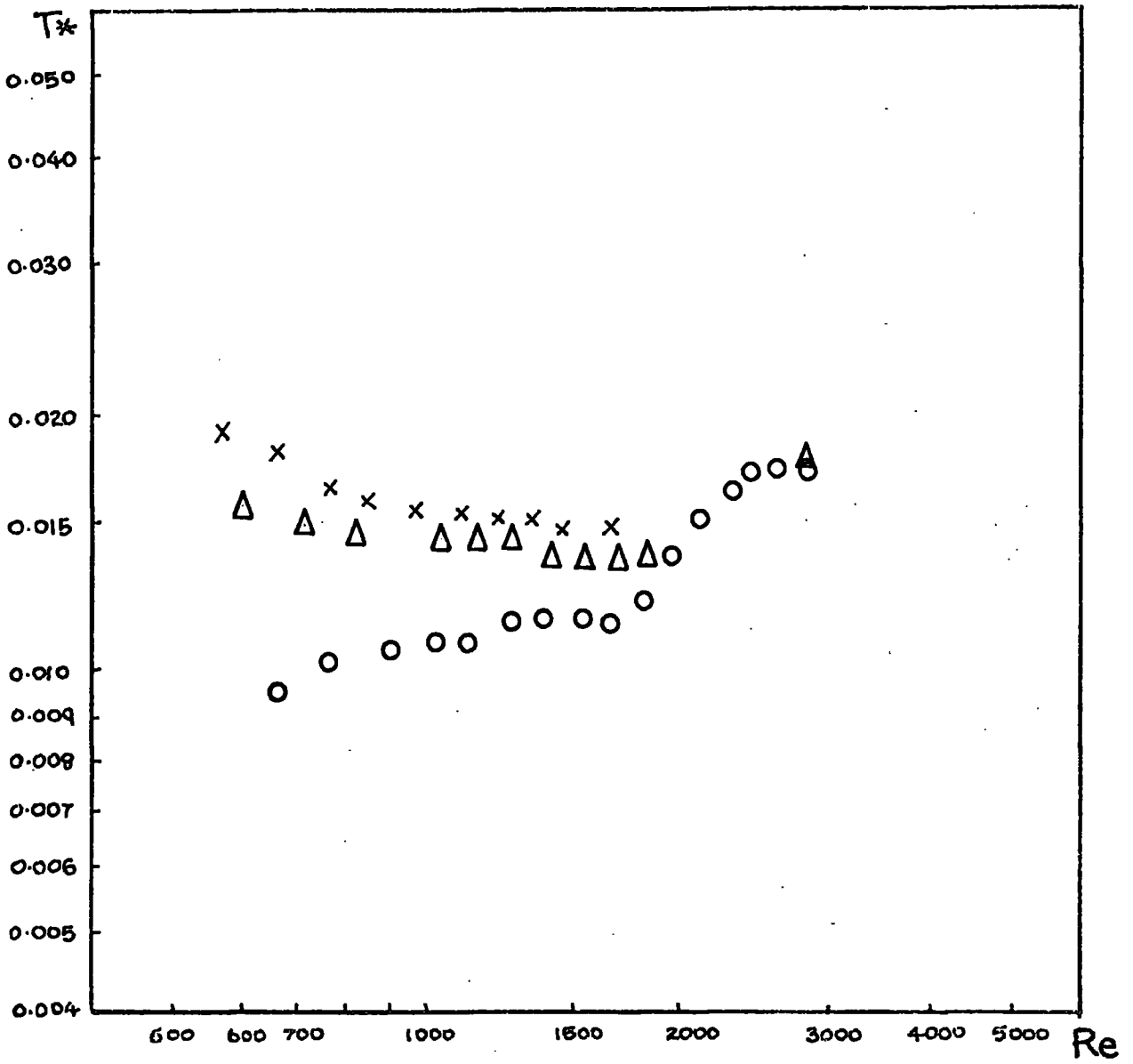

FIG. 18 TEST RESULTS : LOG-LOG PLOT T* vs. Re

LUBRICANT : WATER

SUPPLY PRESSURE : VARIABLE

LOAD: 910 NEWTONS

NOTES: APPROX. CONSTANT FLOWRATE DURING EACH TEST, RESULTS AS MEASURED

KEY :

O	TEST 01 U	FLOW ≈	0.022 kg/s
×	TEST 03 U		0.045
Δ	TEST 02 U		0.034

The curves are very different from the expected form of a linear region followed by a transition to turbulence. As the speed increased during each test the supply pressure rose; the pressure measurements are given in Appendix 2. A change in the pressure has less effect on the friction at high speeds than at low speeds. In order to produce more satisfactory results the flow should be greatest at low speeds; this is a consequence of the higher eccentricity ratio.

The friction at each speed varied roughly linearly with the supply pressure. Manipulation of the results show that a constant supply pressure would give more normal behaviour. This conditions is often used for experimental tests on bearings because it is the simplest condition. It also helps to control the film extent as the eccentricity changes.

The optimum supply pressure proved to be 2×10^5 N/m^2. This is an unusually high value. The pressure tapping was situated before the feed pipe from the flowmeter to the test bearing, but losses before the bearing were small. Pressure measurements in the bearing indicated low values just round the bearing from the supply. Therefore the flow must have been dominated by the axial flow due to the supply pressure, and so most of the side leakage and losses occurred near to the supply point. The film presumably attained its full width almost immediately.

2. THE EFFECT OF LOAD ON BEARING FRICTION

It was originally intended to use a constant bearing load throughout the tests. However the small loads required to avoid overloading at low speeds were not satisfactory at higher speeds. The friction torque fell at a certain critical speed and rose if the speed was immediately reduced. Typically the torque was reduced by a factor of 0.5 at a speed of 70 r/s with a load of 400N. The critical speed and the degree of reduction were irregular; in general the

speed increased as the load was increased. The fall in torque was sudden and so was not caused by a shortening of the film or a reduction in the viscosity.

During one of the tests the speed was increased beyond the critical value resulting in a complete bearing seizure. Eventually the occurrence was associated with a small whirling motion. Larger scale conical whirling was also observed under certain conditions, but this was not accompanied by reduced torque. Although translational whirling at half shaft speed causes a complete loss of load capacity it would not be expected to reduce the friction. The mechanism could have involved a breakdown of the film due to the squeeze film effect, followed by metallic contact and seizure. The behaviour would be accentuated by large clearance and low viscosity. A particular load could only be used for part of the speed range if whirling was to be avoided.

Fig.19 shows friction measurements at various loads with a supply pressure of 2×10^5 N/m^2.

The curves are again different from the expected shape. The differences are caused by the varying flowrate rather than the effect of the eccentricity ratio. The results suggest that the load should increase as the speed increases.

A worthwhile advantage can be gained by using a constant Sommerfeld number. The interpretation of T^* vs. Re curves is simplified but strictly the condition is impossible to maintain. The method used was to base the load at each speed on a value calculated to give constant S with an assumed variation in viscosity. The temperature variation was determined from previous experience. During the tests described in the following sections the combinations of load and speed successfully restricted the variation of S.

The increased load at high speeds controls the film extent in a similar manner to the manipulation of the supply pressure. The use of constant supply pressure for a roughly constant eccentricity is justifiable if the main component of the flow is that forced from the bearing by the supply pressure

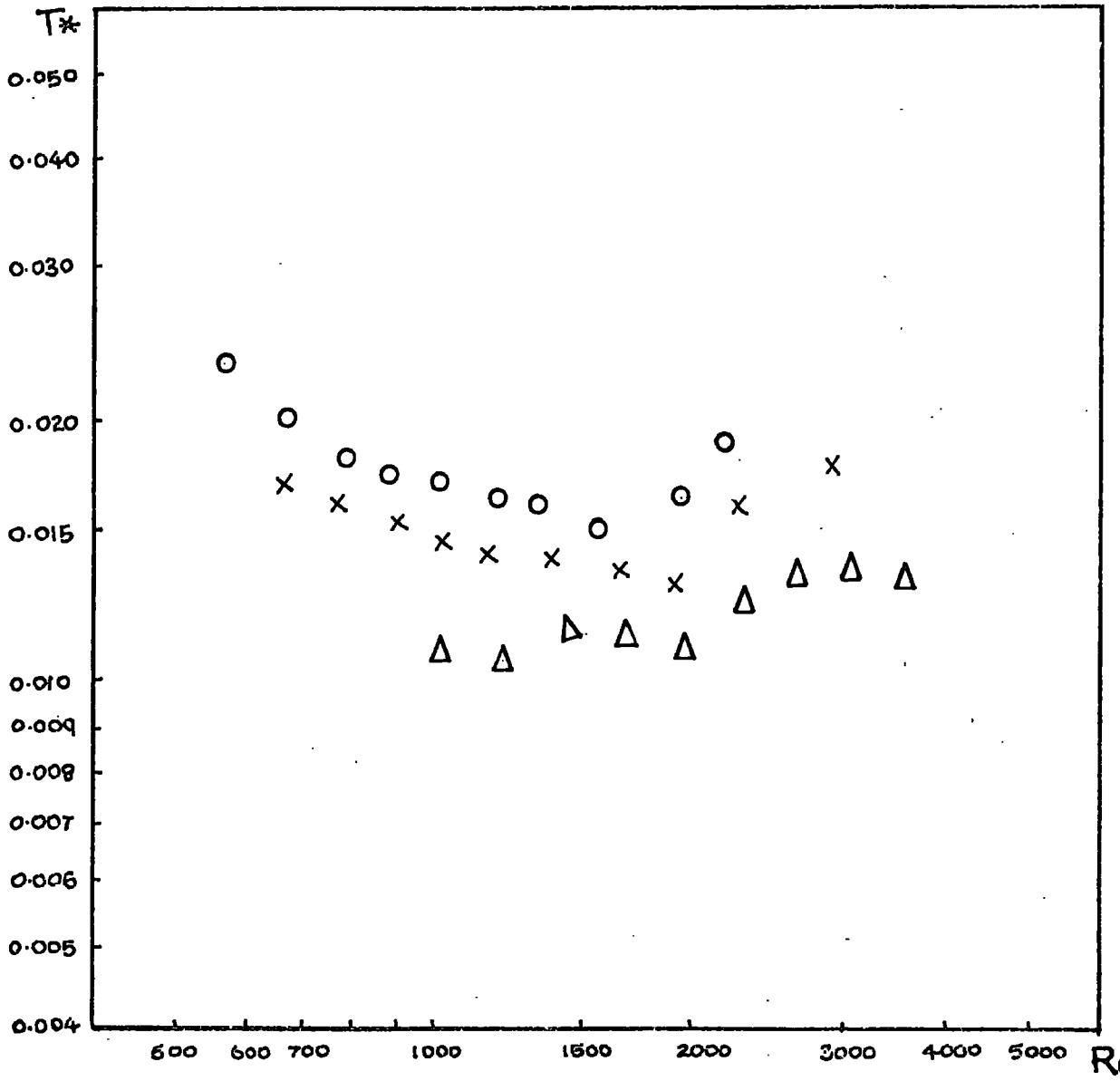

FIG. 19 TEST RESULTS : LOG-LOG PLOT T* vs. Re

LUBRICANT : WATER

SUPPLY PRESSURE : 2.0×10^5 N/m^2

LOAD: CONSTANT DURING EACH TEST

NOTES: RESULTS AS MEASURED

KEY :

O	TEST	04U	LOAD = 910 N
×	TEST	05U	LOAD = 1120 N
Δ	TEST	06U	LOAD = 1433 N

not the component due to the film pressures.

The parameters could be controlled in other ways to produce different behaviour but the friction results indicate that constant supply pressure and constant S produce normal behaviour. This is normal in terms of practical bearings for which control is less critical.

The value of S chosen for the tests corresponds to an eccentricity ratio of approximately 0.5 according to laminar theory. The bearing is thus only moderately loaded. For turbulent operation and for lubrication with polymer solutions the relation between eccentricity and S will be different than for laminar operation. A constant value of S does not therefore indicate constant eccentricity when the flow regime changes, but the effect is small according to the results of Smith and Fuller. In practice there was a tendency for S to increase as the speed increased because of a difference between the assumed and real temperatures. This partially compensates for the increase in load capacity at a given eccentricity ratio caused by turbulence. The test results indicate that the friction is most affected by load and flowrate in the laminar regime for which the eccentricity could be most carefully controlled.

3. FRICTION RESULTS WITH WATER LUBRICATION

A. THE TORQUE DUE TO THE LOADING SYSTEM

Friction measurements were taken at the chosen series of loads and speeds. Tap water was supplied at 2×10^5 N/m^2 to the leading supply groove for each direction. Fig.20 shows the plot of T^* vs. Re for both directions of rotation. The frictions are not the same for the two directions, which are signified by 'U' or 'D'. The displacement between the curves is constant indicating that the difference in torque increases with speed. Alternatively this can be interpreted as increasing with load.

Fig.21 shows the difference in bearing friction plotted against bearing load for Reynolds number up to 2000. The tests 08U and 10D were considered because the lubricant outlet temperatures were the same and so the difference is not due to viscosity variations. The difference in friction increases linearly with load, suggesting that the operation of the loading system is not entirely satisfactory. The effect could be accounted for by a displacement of the load direction of 2.6×10^{-4} m from the bearing centre. The error can be compensated by subtracting or adding a proportion of the load so that the laminar regions coincide.

Fig.22 shows the results displaced according to Fig.21. The results for the two directions correspond throughout the speed range not only for the section used for the calculation of the correction. The adjustments to the friction measurements account for any error in the initial balancing of the bearing as well as loading defects.

B. THE TORQUE DUE TO THE ANGULAR MOMENTUM OF THE LUBRICANT

The most noticeable aspect of the corrected curves shown in Fig.22 is that the torques are greater than the Petroff values. The discrepancy is too large to be accounted for by errors introduced by the simplifications of the equation. The main differences between the test bearing and normal laminar

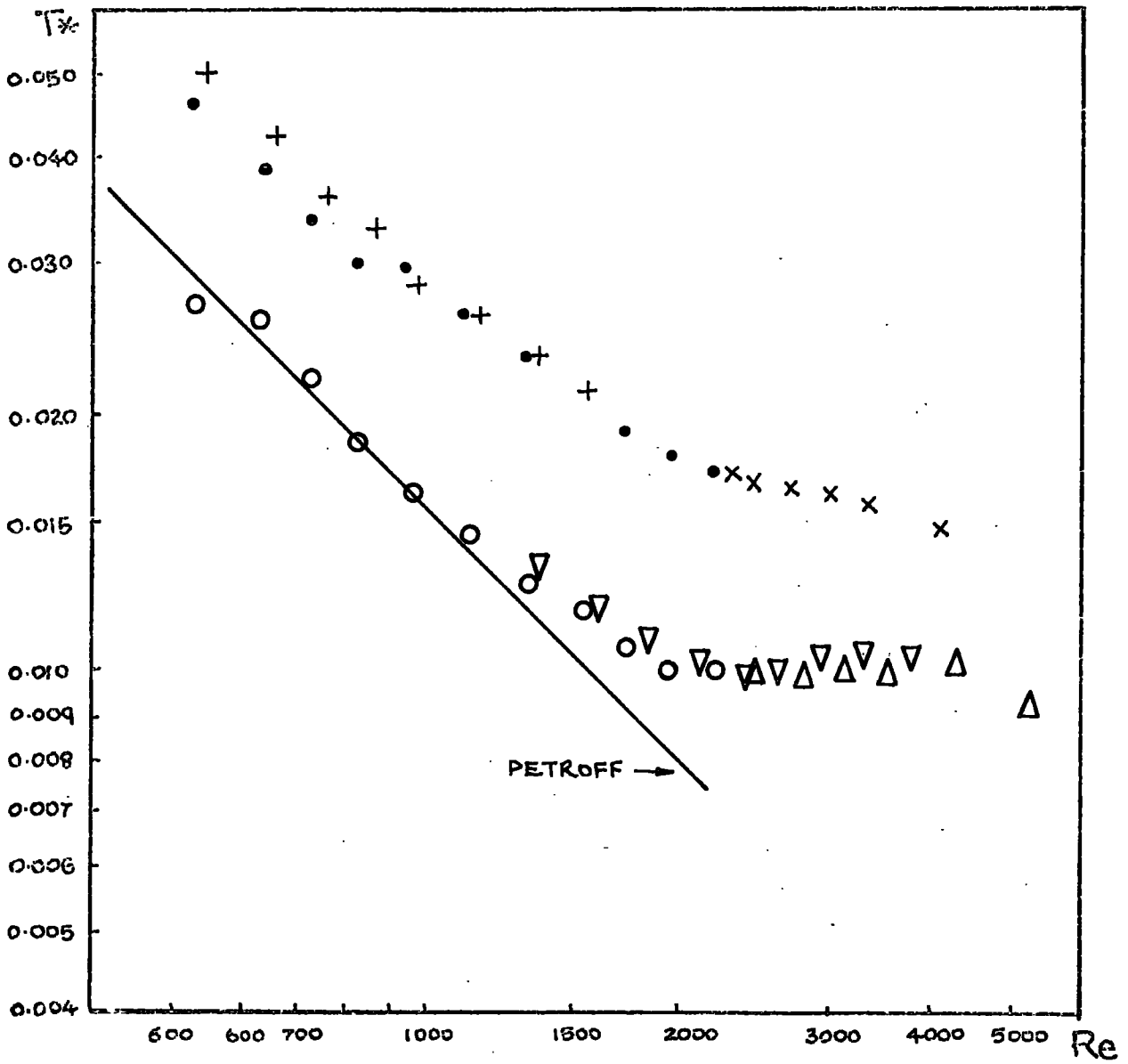

FIG. 20 TEST RESULTS : LOG-LOG PLOT T* vs. Re

LUBRICANT : WATER

SUPPLY PRESSURE : 2.0×10^5 N/m²

LOAD: VARIABLE

NOTES: RESULTS ARE AS MEASURED

KEY :

•	TEST	10 D
X		11 D
+		12 D
O		08 U
∇		09 U
Δ		09 U

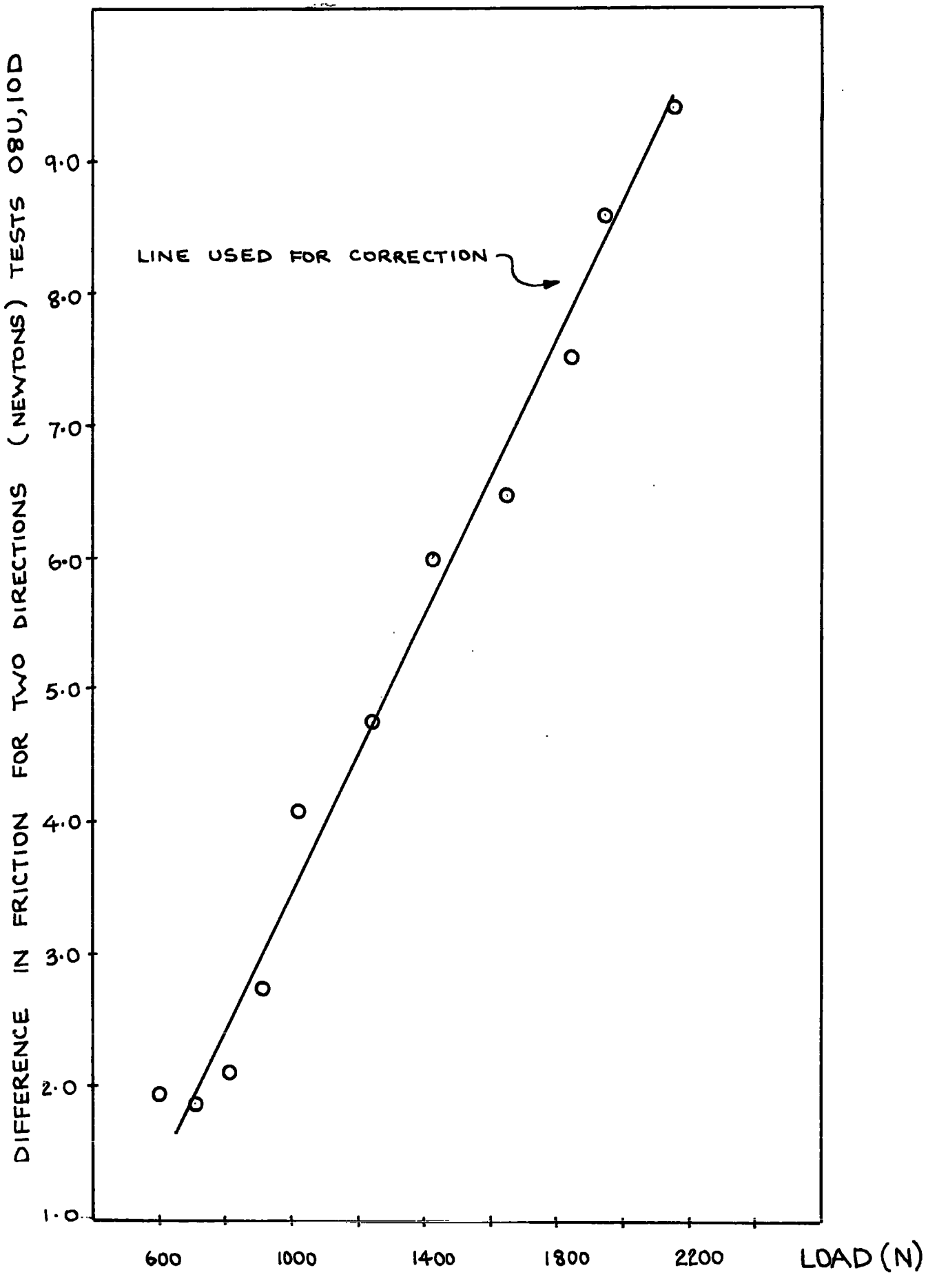

FIG. 21 TORQUE DUE TO THE LOADING SYSTEM

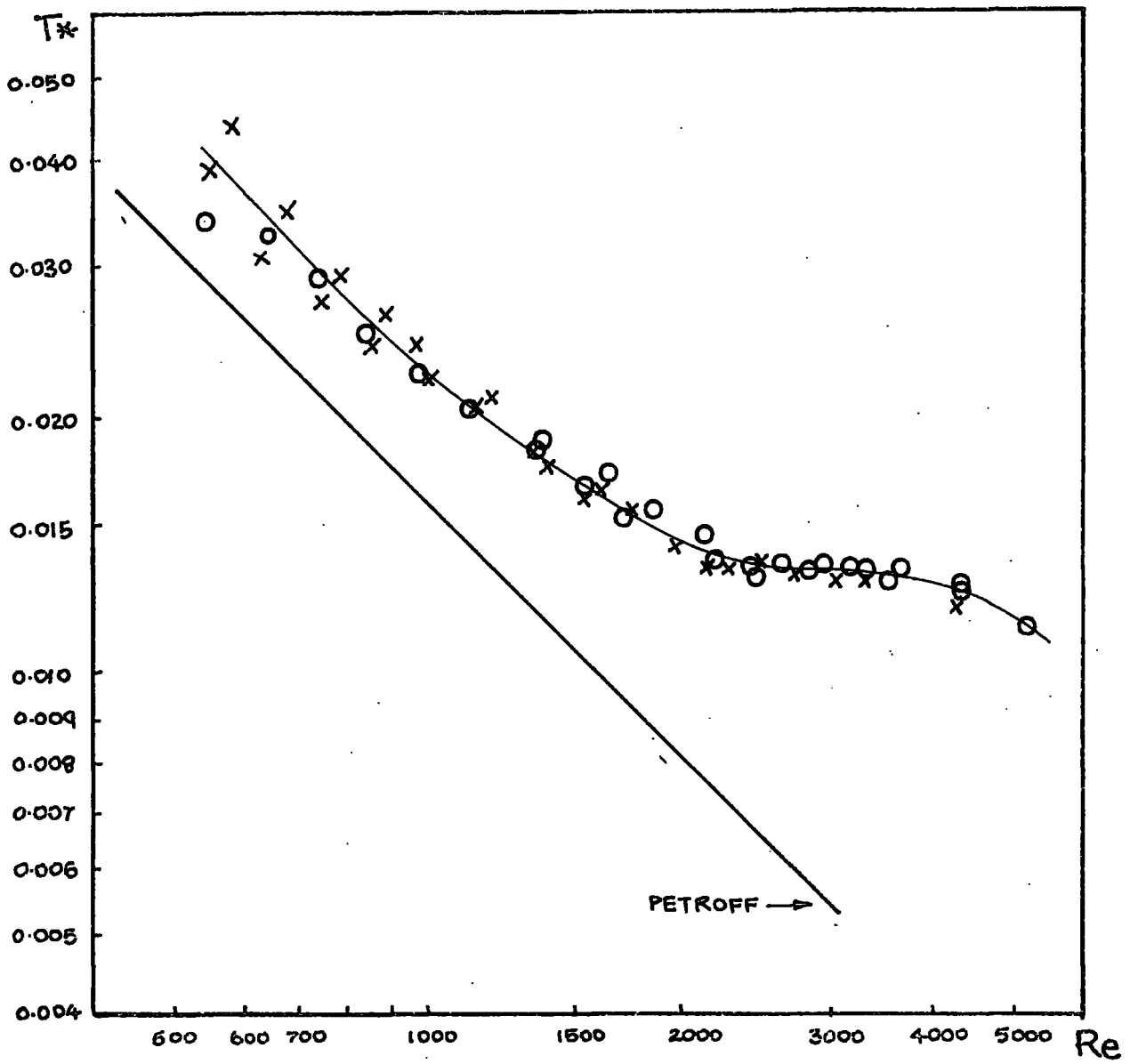

FIG. 22 TEST RESULTS : LOG-LOG PLOT T* vs. Re

LUBRICANT : WATER
SUPPLY PRESSURE : 2.0×10^5 N/m^2
LOAD: VARIABLE

NOTES: RESULTS CORRECTED FOR DEFECTS OF LOADING SYSTEM

KEY :

O TESTS 08U, 09U, 07U

X TESTS 10D, 11D, 12D

bearings, which closely correspond to Petroff, are higher speed and higher flowrate. The lubricant enters the bearing without angular momentum and must be accelerated by the shaft. There will thus be a component of the shaft torque from this source as well as the shearing of the fluid. This component proves to be significant in the present case.

The increase in shaft torque will depend on whether the lubricant leaves the bearing along the shaft or down the edges of the bush. The mean velocity is different for these cases.

If all the flow has to be accelerated to the surface velocity then the additional shaft torque will be given by:

$$\Delta T = \dot{m}\omega R^2 = 2\pi\dot{m}NR^2$$

If all the flow trickles down the edges of the bearing bush then the mean velocity will be half of the surface velocity of the shaft. Both the bearing and shaft torques will then be increased by $\Delta T/2$.

Because of the high shaft speed and the high flow rate of the test bearing it is probable that the largest proportion of the flow is flung off the shaft. The angular momentum would then be transmitted to the drainage troughs and so increase the bearing torque by an amount ΔT. This would increase the non-dimensional torque T^* by an amount given by:

$$\Delta T^* = \frac{\dot{m}r}{8\rho R^2 L}$$

Fig.23 shows the results modified by subtracting this contribution so that the shearing force alone can be considered.

C. COMPARISON WITH PREVIOUS INVESTIGATIONS

The results shown in Fig.23 indicate that the friction increases linearly with speed up to Re = 1000. After this point the gradient increases;

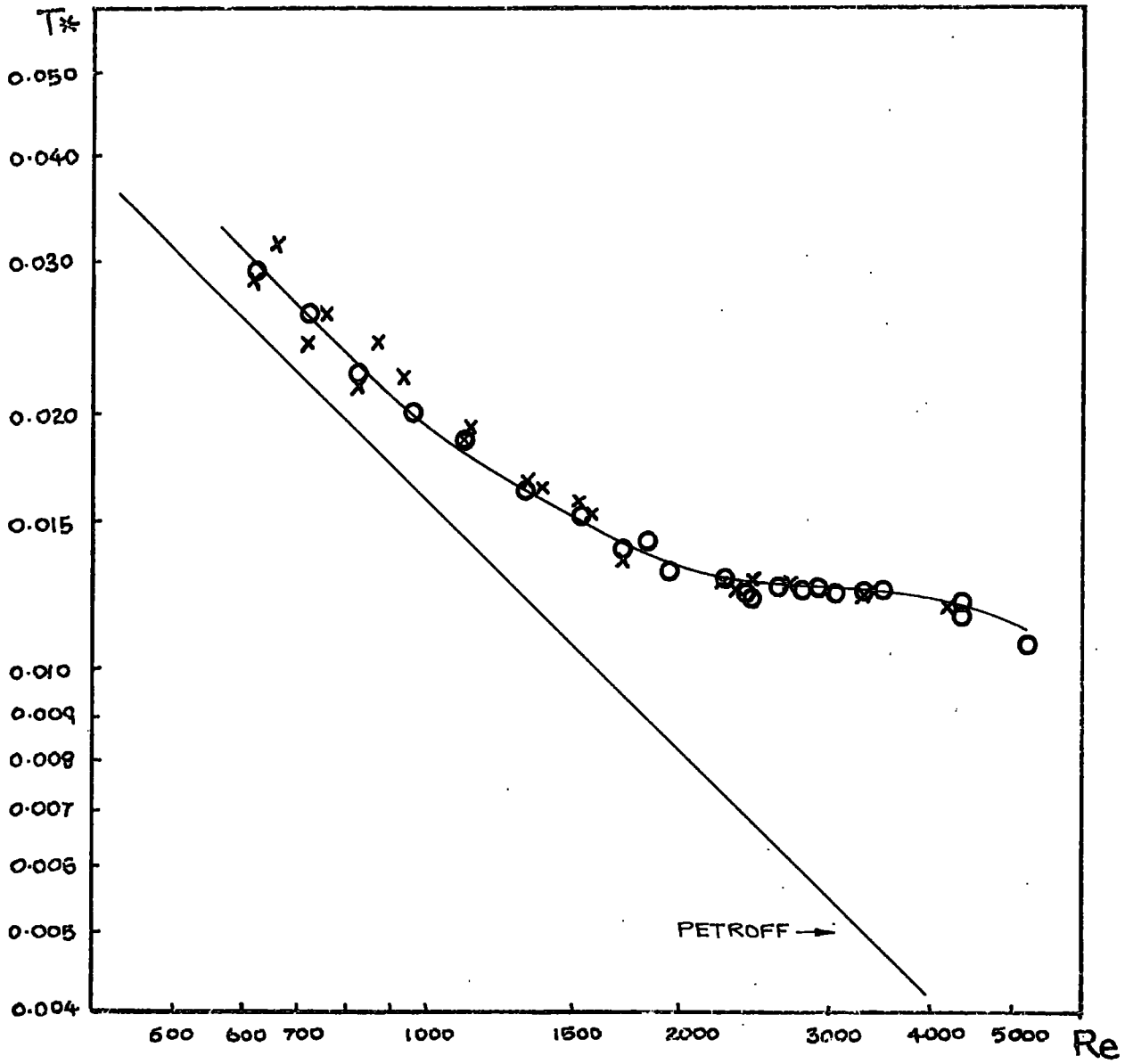

FIG. 23 TEST RESULTS : LOG-LOG PLOT T* vs. Re

LUBRICANT : WATER

SUPPLY PRESSURE : 2.0×10^5 N/m²

LOAD: VARIABLE

NOTES: RESULTS CORRECTED FOR DEFECTS OF LOADING SYSTEM AND ANGULAR MOMENTUM OF LUBRICANT

KEY :

o TESTS 08U, 09U, 07U

x TESTS 10D, 11D, 12D

the friction becomes proportional to the square of the speed at Re = 2000. The transition to full turbulence therefore occurs at the expected point.

The predicted Reynolds number for the formation of concentric Taylor vortices is 1050 although eccentricity and axial flow would be expected to increase this value. The departure from laminar flow before full turbulence is more gradual than has been observed for secondary flow and the region Re = 1000 to 2000 more probable represents the growth of turbulence.

Turbulent flow will begin in the large clearance region near to the supply and then spread into the loaded region of the bearing as the shaft speed increases. The transition at an Re of 2000 signifies complete turbulence confirming that mean clearance and outlet viscosity are satisfactory parameters for prediction. The clearance in the loaded region is of course less than the mean but the viscosity will be lower, and so Re could be the same as the mean value. Therefore turbulence could spread and then suddenly encompass all of the film.

Fig.23 is similar to the curve shown in Fig.2 obtained by Wilcock from a bearing fed with oil at the leading groove. The transition is smoother for that investigation perhaps because constant load, and so varying eccentricity, was used.

The friction measurements in the turbulent region are lower than those obtained by Smith and Fuller. This could be a consequence of eccentric operation directly, or of a shorter film. The loads used by Smith and Fuller were so small that the bearing could have been completely full with the Sommerfeld pressure distribution. This could also have caused the transition to be more distinct than in the present case.

The results are tabulated in Appendix 2. The Sommerfeld number was not kept constant but the small variations did not cause significant scatter of the friction measurements. The results are sufficiently consistent for any appreciable effect due to the polymer to be detected.

4. THE EFFECTS OF A POLYMER ADDITIVE ON BEARING PERFORMANCE

A. FRICTION

Measurements of the bearing friction were taken with various concentrations of Polyox WSR301 under the same conditions as for plain water. The method of solution preparation is given in Appendix 3. The lubricant passed through the bearing to waste.

Fig.24 shows the results for both directions of rotation at a concentration of 50 p.p.m. The curves were brought together by adding or subtracting a fraction of the load as determined from the water results. The close agreement between the two directions supports the conclusion that the displacement is due to defects of the loading system.

Fig.25 shows the same results with the angular momentum contribution subtracted. The shape of the curves is not greatly affected by this correction proving that the additive affects the shearing of fluid within the bearing.

The polymer begins to reduce the frictional torque at an Re of 1000. As Re increases the reduction increases. This behaviour substantiates the concept of growing turbulence in the film. As expected the lubricant flow rate was slightly higher for the polymer solution; the reduction cannot therefore be caused by a shortened film.

The water results shown on Figs. 24 and 25 were taken in between the polymer tests for comparison.

The results show that the onset shear stress for friction reduction is reached before transition in a journal bearing and that the friction is greater than the extrapolated laminar value.

Fig.26 shows the reduction in power loss caused by the addition of the polymer in typical tests.

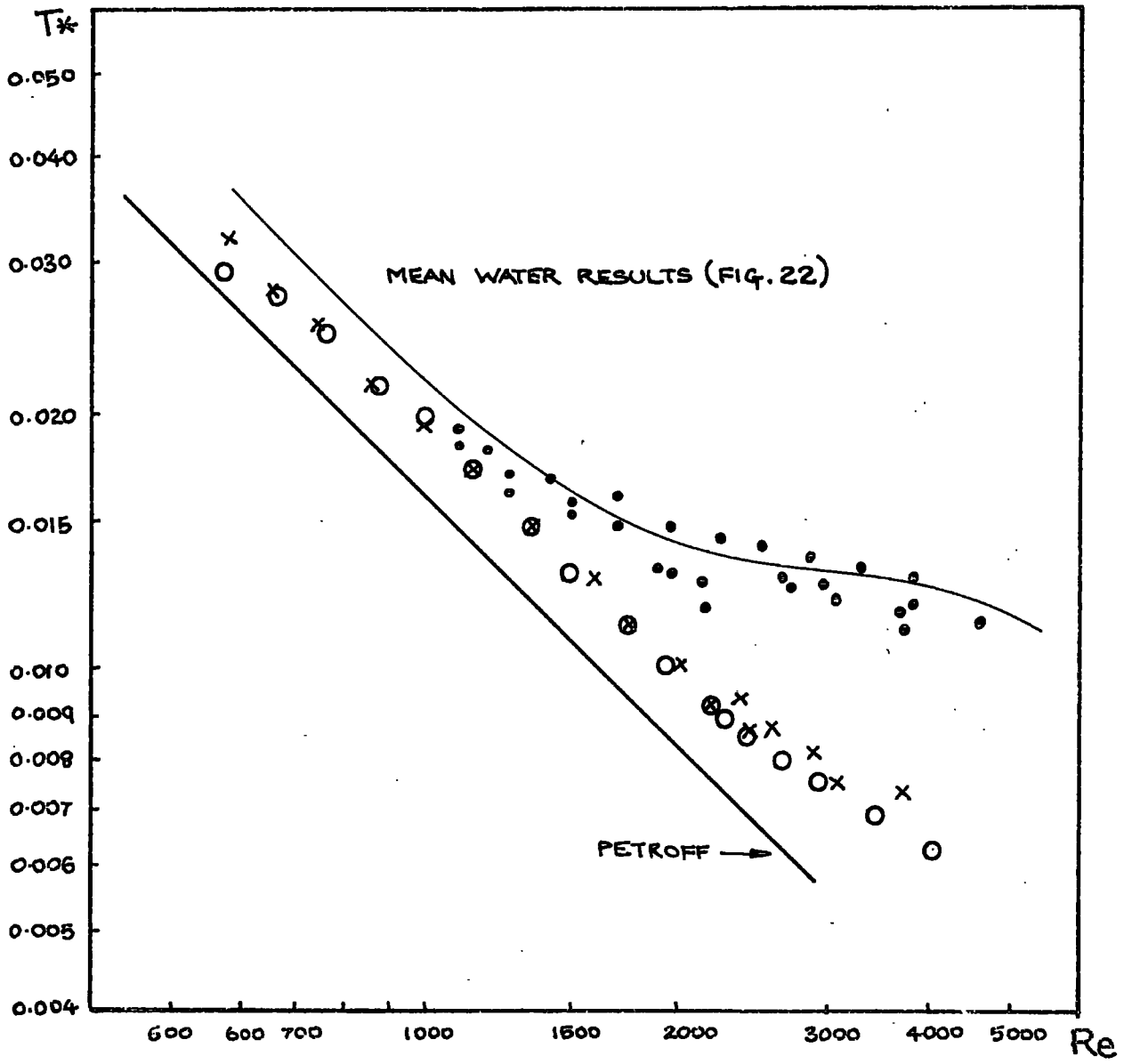

FIG. 24 TEST RESULTS : LOG-LOG PLOT T* vs. Re

LUBRICANT : WATER + VARIOUS CONCNS POLYOX WSR 301

SUPPLY PRESSURE : 2.0×10^5 Kg/m^2

LOAD: VARIABLE

NOTES: RESULTS CORRECTED FOR DEFECTS OF LOADING SYSTEM

KEY :

⊙	TESTS	17U, 18U, 19U	WATER
O	TESTS	13U, 14U	50 ppm POLYOX
×	TESTS	15D, 16D	50 ppm POLYOX

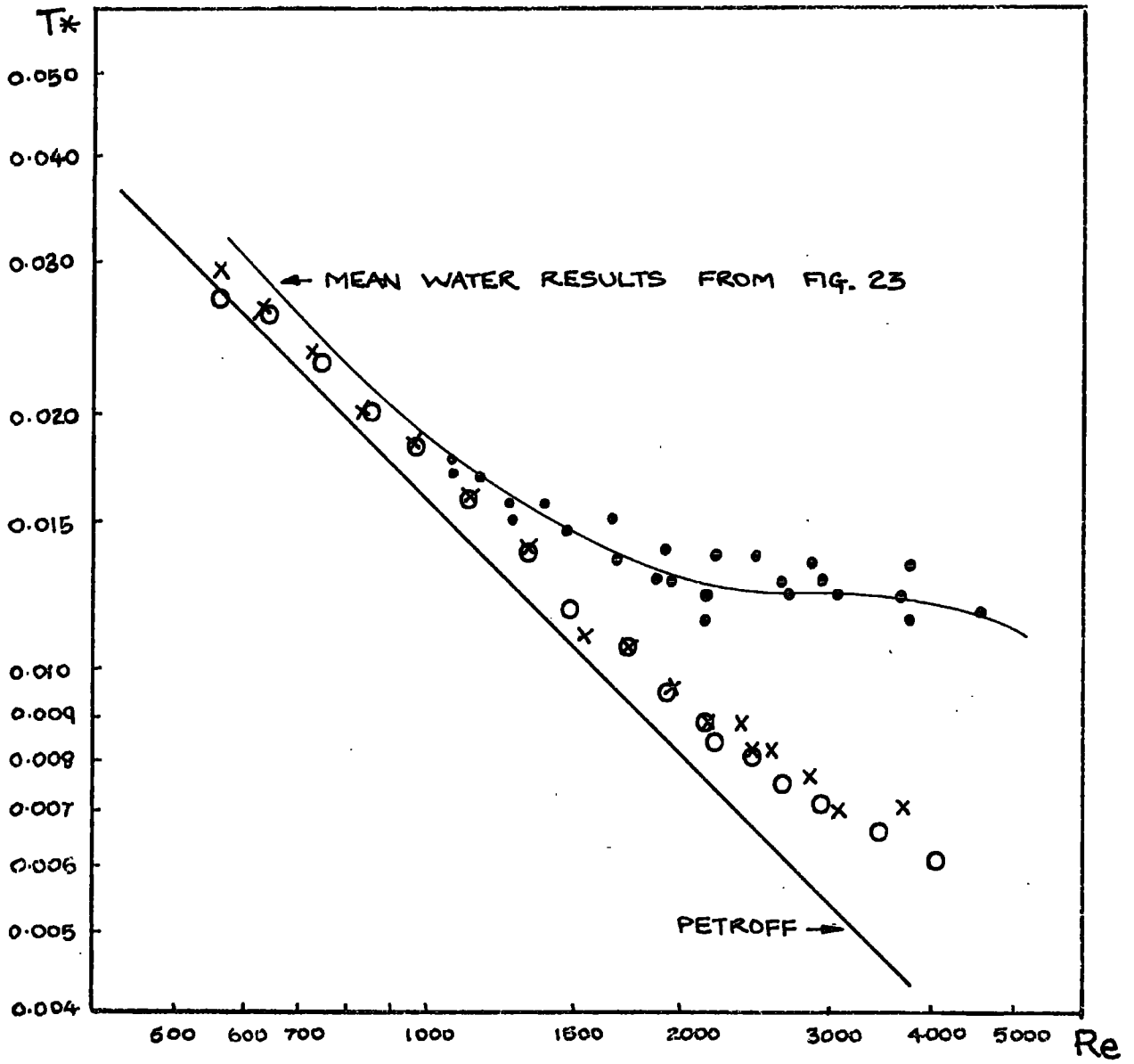

FIG. 25 TEST RESULTS : LOG-LOG PLOT T* vs. Re

LUBRICANT : WATER + VARIOUS CONCNS POLYOX WSR301

SUPPLY PRESSURE : 2.0×10^5 N/m^2

LOAD: VARIABLE

NOTES: RESULTS CORRECTED FOR ANGULAR MOMENTUM OF LUBRICANT AND DEFECTS OF THE LOADING SYSTEM

KEY :

•	TESTS 17U, 18U, 19U	WATER
O	TESTS 13U, 14U	50 ppm POLYOX
×	TESTS 15D, 16D	50 ppm POLYOX

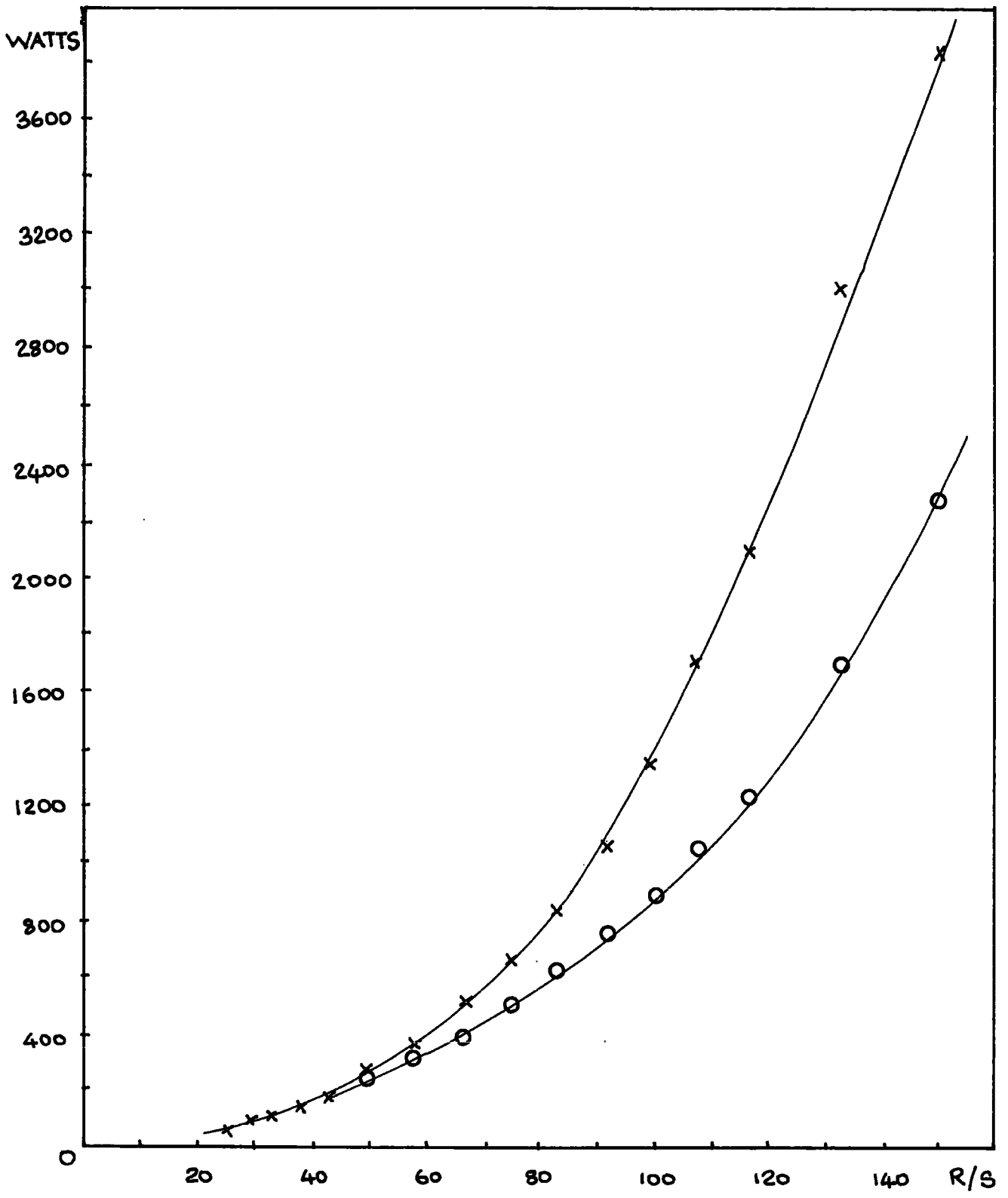

FIG. 26 BEARING POWER LOSS vs. SHAFT SPEED

O TESTS 13U, 14U 50 ppm POLYOX

× TESTS 08U, 09U WATER

RESULTS CORRECTED FOR LOADING SYSTEM TORQUE

Fig.27 shows the variation in the reduced friction coefficient with Re. This plot represents the variation in the efficiency of the lubricating film. The friction coefficient for water lubrication is essentially constant until the transition when it begins to increase. The addition of the polymer lowers the value for turbulent operation. Although the value of S is substantially constant for all the points plotted, the eccentricity ratio is not necessarily constant. Therefore a penalty in the load carrying capacity might have to be paid for the reduction in friction. However if the capacity was reduced to the laminar value then the efficiency would still have been increased.

The friction results for other concentrations from 5 p.p.m. to 214 p.p.m. are shown in Fig.28. Water was supplied to the bearing for some time after each test to eliminate effects due to retention of polymer.

The variation in friction reduction with concentration is shown in Fig.29 for two values of Re. The optimum concentration is about 50 p.p.m. in both cases. It is interesting that the friction for 5 p.p.m. approaches that for water alone at high Reynolds numbers. This could be due to polymer degradation occurring at higher shear rates. The optimum concentration might be that which compensates for degradation. The friction reduction is less for the higher concentrations, presumably because of the slightly increased viscosity.

B. WHIRL STABILITY

During the friction measurements, it was noticeable that the readings were less erratic and that the test bearing was more stable when the additive was used. These observations prompted quantitative tests on the whirl stability of the bearing.

With the shaft rotating at 92 r/s and lubricant supplied at 2×10^5 N/m^2, the bearing load was reduced until vibration could be observed. The instability

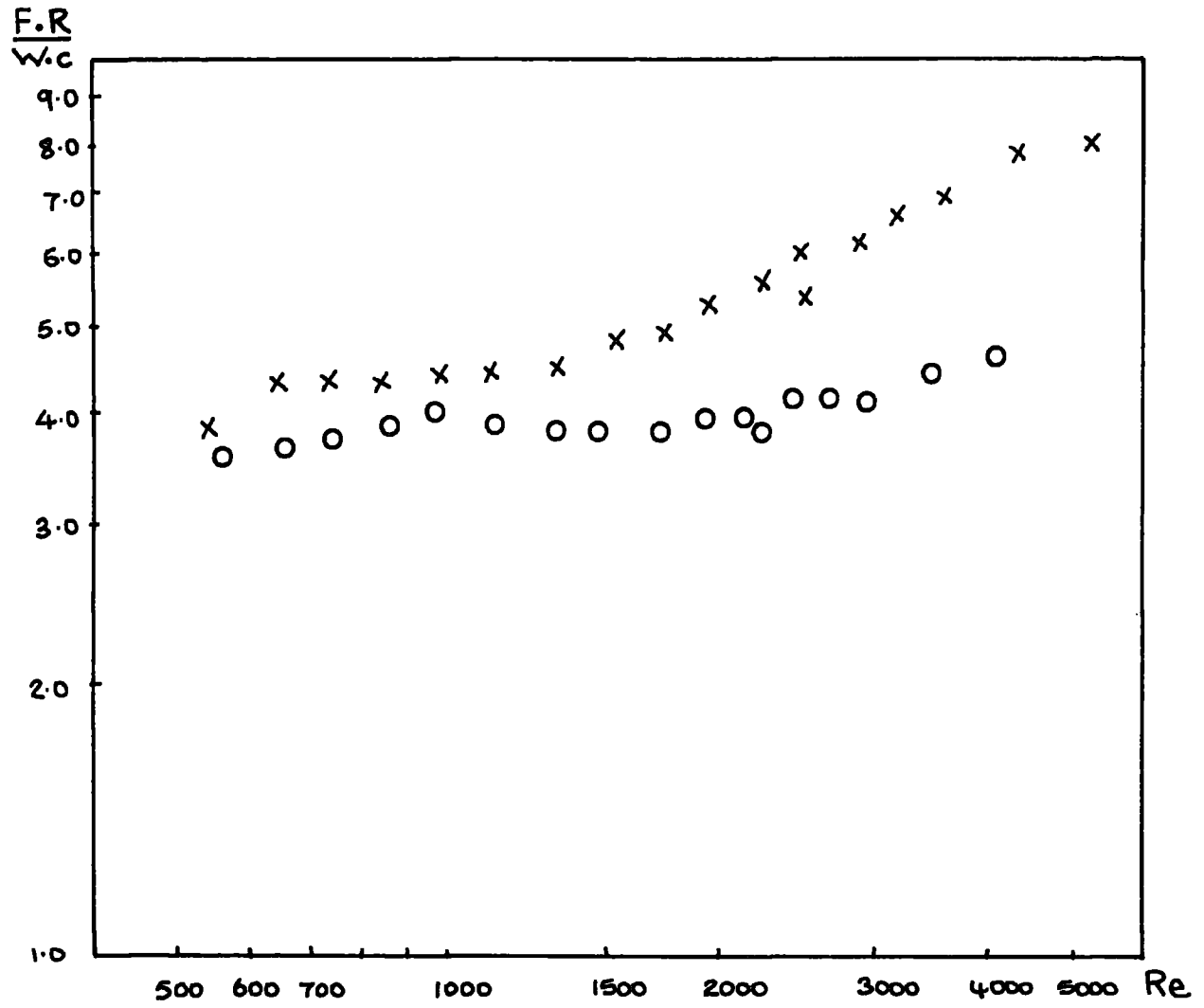

FIG. 27 FRICTION COEFFICIENT vs. REYNOLDS NO.

O TESTS 13U, 14U 50 ppm POLYOX

X TESTS 08U, 09U WATER

ALL RESULTS CORRECTED FOR LOADING SYSTEM TORQUE

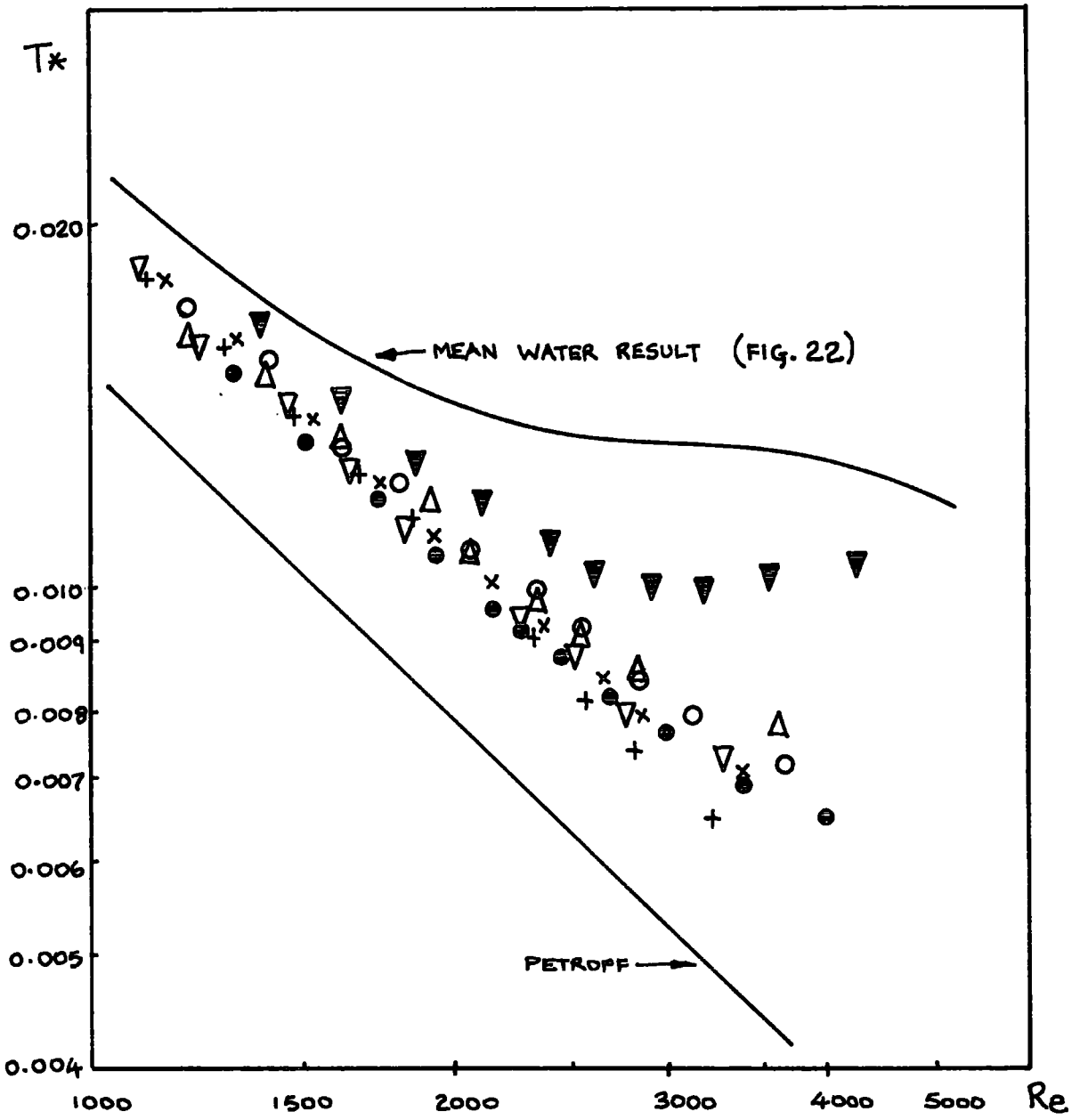

FIG. 28 T* VS. Re VARIOUS CONCNS POLYOX

▼	5·1 PPM	POLYOX	TEST 25U
Δ	15·7 "		24U
▽	28 "		23U
+	63 "		22U
×	121 "		21U
●	50 "		13U, 14U
O	214 "		20U

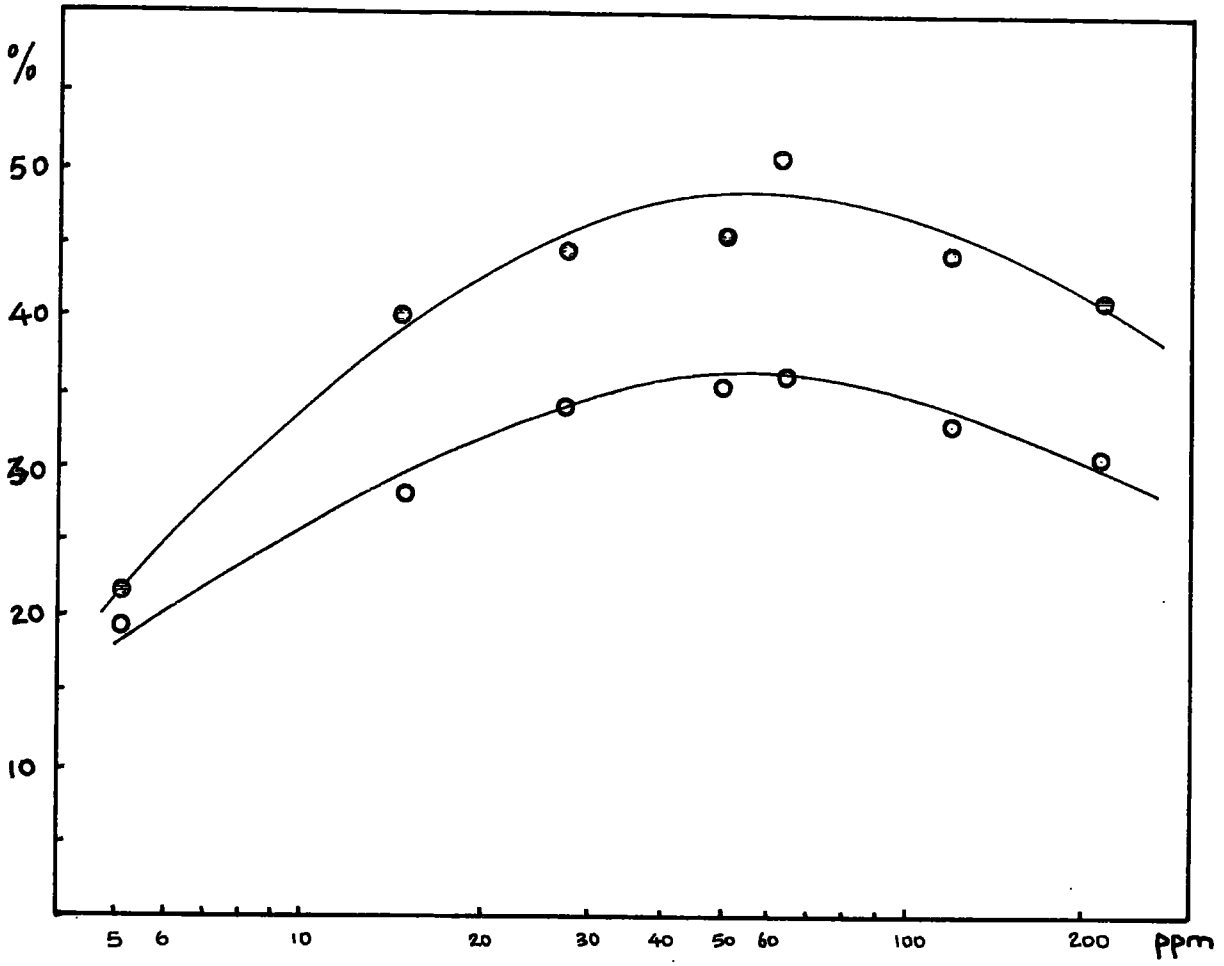

FIG. 29 % FRICTION REDUCTION vs. CONCN.

o Re= 3500

o Re= 2500

took the form of conical whirling; it was also noticeable on the friction measuring instrument. A number of tests confirmed a repeatable lowering of the whirl load with a 50 p.p.m. Polyox solution. This is equivalent to a raising of the whirl speed at constant load. The results are given below in non-dimensional form to account for viscosity variations.

WHIRL LOAD (N)	1224	1015	952	931
Re	2551	2498	2664	2724
1/S	0.225	0.276	0.277	0.277
	water	Polyox WSR301 50 p.p.m.		

The addition of the polymer caused a 23% rise in the value of 1/S at the onset of whirling. This is a significant stabilisation and the effect would be a very useful benefit, in addition to friction reduction, if it occurred in a practical bearing.

Unfortunately the results cannot be readily applied to other bearings. The free test bearing is dynamically different from the normal situation, and the hydrostatic bearing will affect both the stiffness and the damping. It is impossible to estimate the effect of a polymer on the stability of an oil lubricated bearing, but the results encourage a rigorous investigation. The control of whirl remains a major problem in bearing design.

There are several possible explanations of the stabilisation. The eccentricity ratio could be increased by the addition of the polymer or the damping could be increased. The mechanism might be a combination of these two factors. The first stage of an investigation would definitely involve the accurate measurement of eccentricity.

It was unfortunately not possible to determine if the bearing was stabilised in the laminar regime because the actual bearing load could not be accurately measured at low loads.

C. PRESSURE DISTRIBUTION

Since the eccentricity ratio cannot be measured on the test rig in its present form, it was thought that some indication could be obtained from pressure measurements round the bearing.

Readings were taken at the points shown on Fig.30 with the following operating conditions:

shaft speed 92 r/s

load 2166N

supply pressure 2×10^5 N/m^2

The off-centre tappings were used to ensure that the shaft and bearing axes were parallel, resulting in a symmetrical pressure variation across the bearing. The centre-line value was calculated assuming a parabolic variation.

The pressure profile obtained is indicated in Fig.30. The sharply peaked shape, characteristic of laminar flow, is evident. No significant changes was caused by the addition of Polyox. This suggests that the eccentricity is not greatly affected but is not conclusive proof. The form of the pressure distribution and the eccentricity might both be affected by the polymer and the two effects might have cancelled out. Alternatively the whirl stabilisation could have been caused by an increase in the eccentricity too small to noticeably affect the pressure profile.

D. POLYMER DEGRADATION

The reduction in effectiveness caused by the shearing of polymer solutions is the most important consideration in the application of friction reducing additives to journal bearings. The friction results have shown Polyox WSR301 to be an extremely effective additive, but in all the tests the solution passed only once through the bearing. Under the conditions of high shear rate encountered, the friction would gradually increase in a recirculating system.

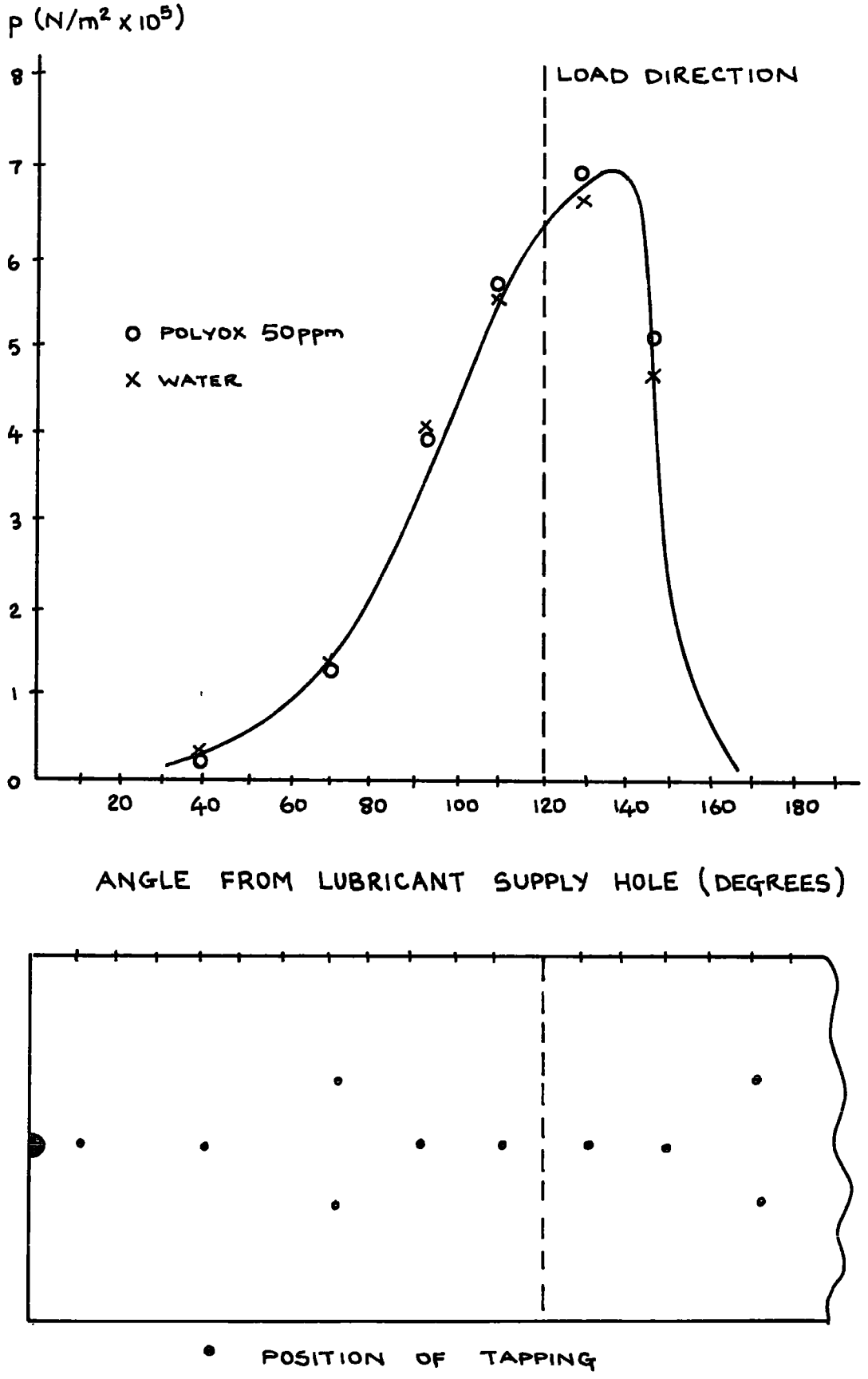

FIG. 30 PRESSURE DISTRIBUTION

The degradation rate was investigated at 92 r/s and 2166N load, corresponding to a Reynolds number of about 2500. The polymer solution, at 50 p.p.m. concentration, was fed to the bearing at 2×10^5 N/m^2. The outlet flow from one test was collected and used as a supply for the next; samples of the solution were taken at each stage. To ensure consistent shearing some of the lubricant was discarded at the beginning and end of each test.

After the first test the solution did not form threads although the friction reducing properties were not affected. The restricted supply (40 kg) limited the number of tests that could be done because of the necessity for wastage and sampling. The inlet temperature increased as the lubricant was recycled; this complicates the comparison of the friction results because the effect of varying viscosity on the torque and on the Reynolds number has to be considered. Fig.31 shows the change in the ratio of the measured friction to the value previously recorded for a freshly prepared solution at the same Re.

The effectiveness of the solution is reduced in passing through the bearing. After the fourth pass the lubricant gave the friction reduction produced by a freshly prepared solution at 15 p.p.m. concentration. If the results can be extrapolated then the friction would approach that for water after approximately twenty passes. The polymer will be degraded in the pump and in the feed pipe but the bearing is the most damaging because of the high shear rate.

It was intended to measure the distribution of molecular weight at each stage using a Gel Permeation Chromatograph. However the polymer could not be successfully transferred from water to the solvent required in the process. If the lubricant had been a mineral oil then it could have been used directly. The determination of the changes in molecular weight produced by shearing in the various parts of the system is probably the most informative method of investigating degradation. The results could be correlated with the change in friction reduction.

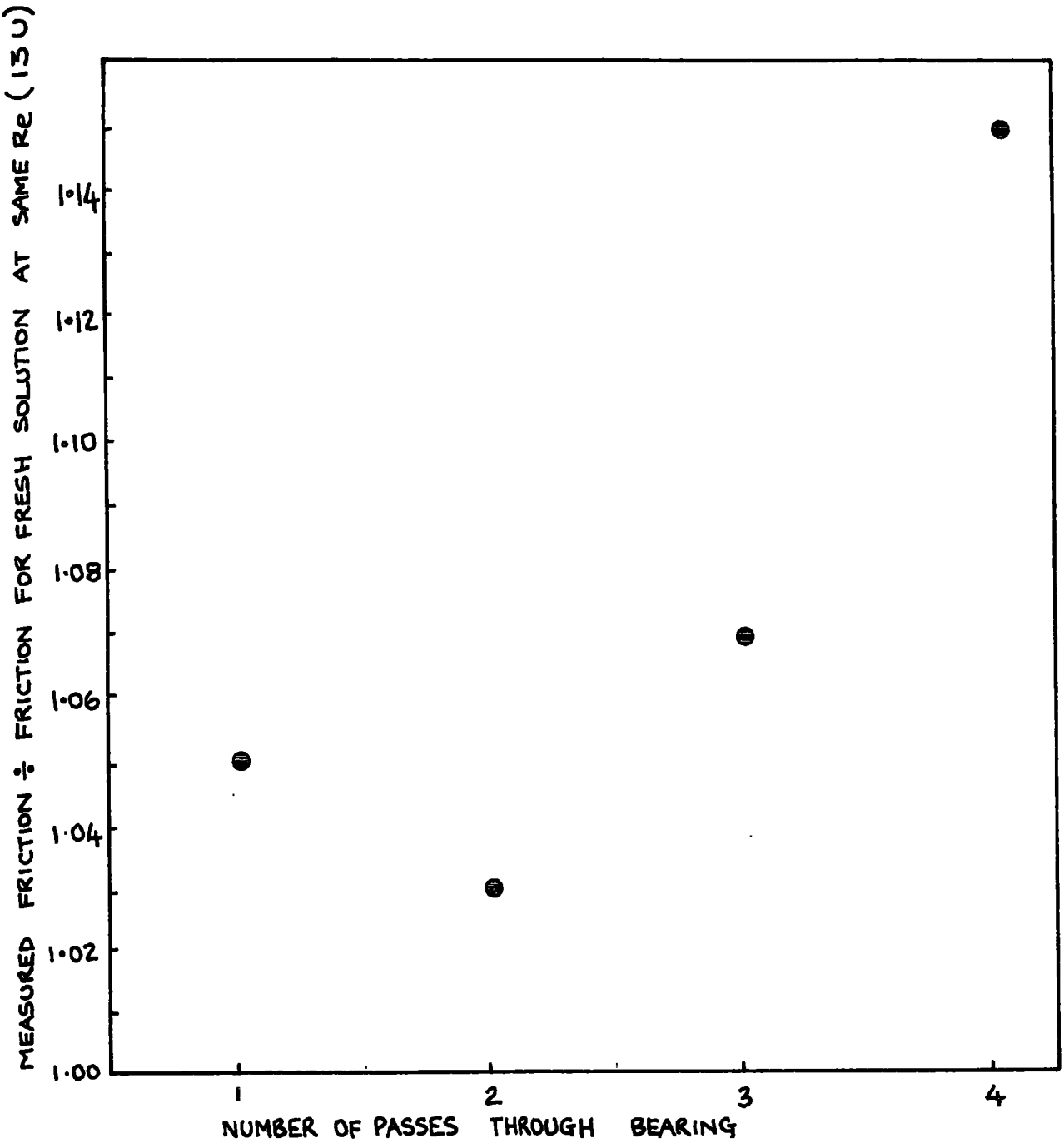

FIG. 31 DEGRADATION OF THE POLYMER

LUBRICANT : 50 ppm POLYOX

It would also be useful to investigate the reduction in effectiveness as a polymer solution passed through a long length of small diameter tubing. The results could not be directly related to conditions in a journal bearing but the time scale involved would be of interest.

Polymer degradation will undoubtedly be the factor limiting commercial use of frictional reduction in journal bearings. The effectiveness of the lubricant could be prolonged by the addition of fresh polymer but the rise in viscosity would diminish the gain in power consumption.

E. LUBRICANT FLOWRATE

The flow through a bearing can be most simply considered as a combination of two components:

1. That due to the supply pressure forcing fluid through the clearance. This occurs even without rotation and is known as the zero speed flow.
2. That due to the pressures generated in the lubricating film.

In reality there will be an interaction between these two components.

Under laminar conditions, the flow through a bearing is constant at constant eccentricity ratio if the zero speed flow dominates. Fig.32 shows the variation of flowrate with Reynolds number for two typical tests taken at approximately constant Sommerfeld number. For water lubrication the flow remains constant until an Re of 1000 when it begins to fall. Thus the flow rate is reduced by the onset of turbulence.

The reduction in flow could have been caused by reduced eccentricity or by turbulence near to the supply hole. The effect of the addition of polymer is to restore the laminar flowrate; this could be due to either increased eccentricity or to a modification of the turbulence in the leakage flow.

The most important consequence of this result is that the friction reductions observed cannot be attributed to a change in the flowrate.

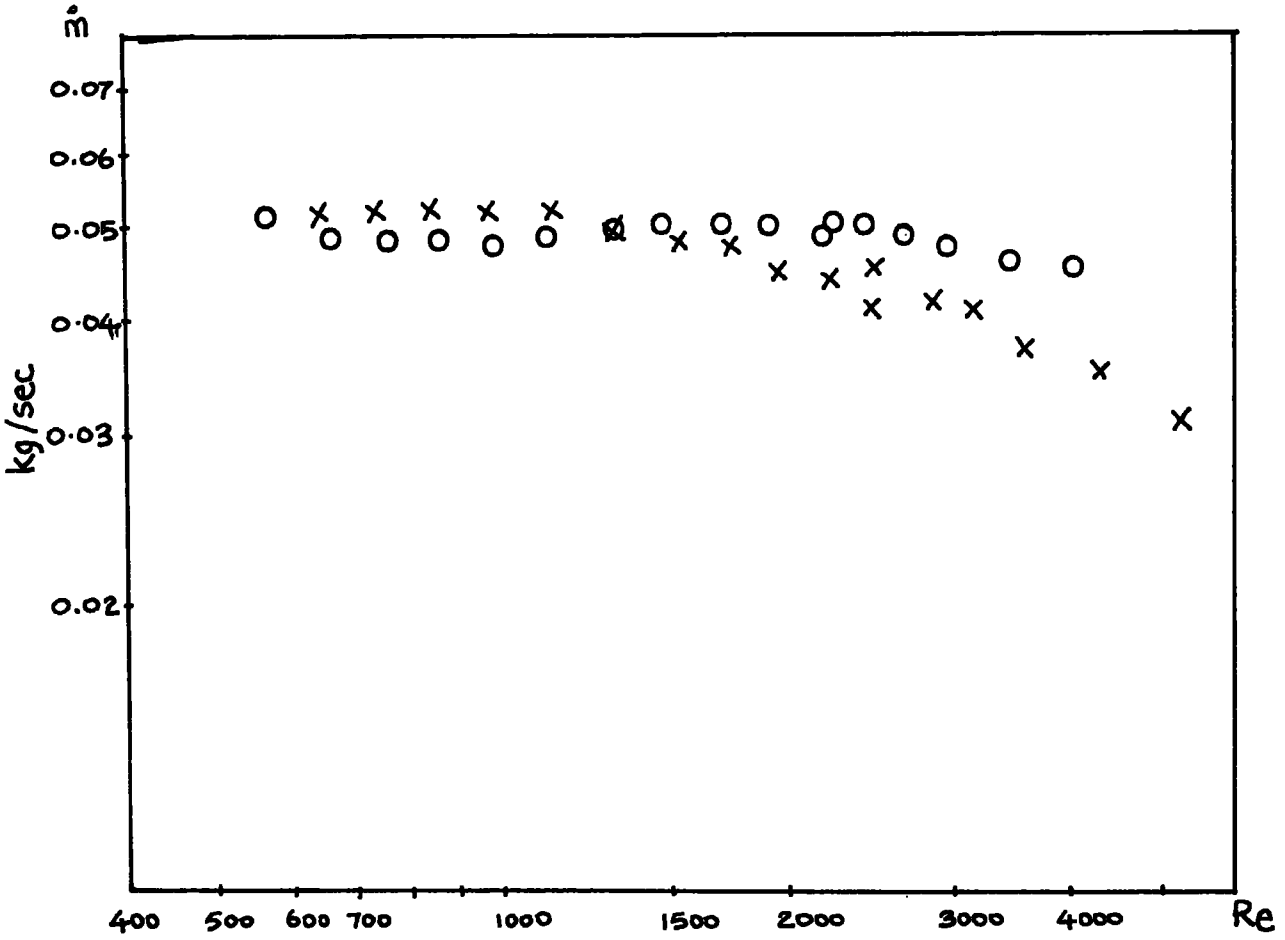

FIG. 32 LUBRICANT FLOWRATE VS. REYNOLDS NO.

O TESTS 13U, 14U 50 ppm POLYOX

X TESTS 08U, 09U WATER

CONCLUSIONS

1. The frictional torque of a journal bearing operating in the turbulent regime can be significantly reduced by the addition of a high molecular polymer to the lubricant.

2. The reduction begins immediately after the onset of turbulence but the friction is always greater than the extrapolated laminar value.

3. The optimum concentration of poly(ethylene oxide) in a water lubricated bearing was found to be 0.005% by weight. This reduced losses by 45% at a Reynolds number of 3500.

4. The additive increased the whirl speed at constant load.

5. The pressure distribution was not affected by the additive.

6. Transition to turbulence caused a reduction in the flowrate of water through the bearing; it could be restored by the addition of the polymer.

7. The polymer became less effective as it was sheared in the bearing; after 20 passes the friction rose to the value for water lubrication. Degradation of the polymer will be the limiting factor in exploitation of friction reduction in bearings.

8. There was little evidence of the formation of a secondary flow of the Taylor vortex type.

9. The investigation of turbulent behaviour on a small diameter bearing necessitates a large clearance ratio and low viscosity lubricant. These departures from normal practice increase the dependence of the friction on flowrate and load due to varying film extent.

10. The angular momentum of the lubricant leaving the bearing appreciably increased the measured bearing friction.

11. An analysis based on Reynolds equation indicates that the formation of the lubricant film is controlled by a minimum dissipation principle. The observed delay after the maximum film thickness can be explained on this basis.

FUTURE WORK

The results encourage further research into the addition of friction reducing polymers to bearing lubricants. The following suggestions seem to be the most important.

1. The investigation of the effects of polymers suitable for mineral oils. Poly-iso-butylene would probably be useful. A larger diameter bearing would be necessary.

2. A comprehensive study of polymer degradation. The measurement of molecular weight distribution would be the most valuable method.

3. An investigation of the whirl stabilising effect. Accurate eccentricity measurement would be necessary to determine if increased eccentricity is the cause. It would also be interesting to find if a penalty in the load capacity has to be paid for friction reduction.

4. Visual observations and friction measurements could be used to verify that a minimum dissipation principle controls film formation. The effects of supply pressure and feed position could be studied. It would be also interesting to investigate if turbulence affects the hypothesis.

APPENDIX 1

FILM EXTENT IN JOURNAL BEARINGS

During the development of the test bearing it was found that the torque was dependent on the film extent which decreased as the shaft speed increased. The breakdown of the film was almost static whereas the position where the film reached its full width moved 130° from the supply hole.

Cole and Hughes (1956) observed a delay in the film formation of up to 70° after the maximum film thickness. This phenomenon has not been satisfactorily explained. It was thought that an investigation of the conditions controlling the start of the film would facilitate the experimental testing and provide valuable information concerning bearing behaviour.

A. BASIC THEORY

The basic equations governing the behaviour of hydrodynamic lubricating films have become well known since the classical paper of Reynolds was published in 1886.

The simplest form of the Reynolds equation, considering no side leakage i.e. infinitely wide, is:

$$\frac{dp}{dx} = 6U\eta \frac{h-\bar{h}}{h^3}$$

$\bar{h}$, a constant integration, is defined by $h = \bar{h}$ where $\frac{dp}{dx} = 0$

The variation of film thickness round a journal bearing can be expressed quite accurately as:

$$h = c(1 + \epsilon\cos\theta)$$

A solution of the differential equation given above will be possible when the boundary conditions have been specified. The correct conditions have been a

source of discussion throughout the development of the theory of lubrication. The simplest are those due to Sommerfeld who assumed a completely full bearing and so a continuous variation in pressure. Fig.33 shows that this predicts negative pressures for the half of the bearing with diverging clearance. Experimental measurements of friction and pressure indicate that the Sommerfeld model is not realistic.

Liquids can normally withstand only small negative pressures before gas bubbles form. The negative half of the Sommerfeld model is only possible in bearings carrying very low loads. It would be possible at higher eccentricites if the lubricant were supplied at the point of lowest pressure or if the ambient pressure was increased. Neither of these basically similar conditions is practical. In air lubricated bearings the negative pressure restriction does not apply.

A nearer estimate of the load capacity can be calculated by considering only the positive pressures predicted by Sommerfeld. However this solution is basically unsatisfactory because it involves a discontinuity of flow at the end of the pressure film.

The generally accepted boundary condition for the end of the film is:

$$\frac{dp}{d\theta} = p = 0 \quad \text{at} \quad \theta = \pi + \alpha'$$

This condition was discussed by Reynolds and is known by his name. The resulting pressure distribution is shown in Fig.33

For the infinitely wide bearing the falling part of the Reynolds pressure distribution is anti-symmetrical about $\theta = \pi$. Pressure measurements closely agree with this shape although surface tension causes a small negative loop just before the film ends.

After the end of the pressure curve, the film breaks up into fluid streamers which decrease in width as the clearance increases. The flow in this cavitated area was observed by Cole and Hughes.

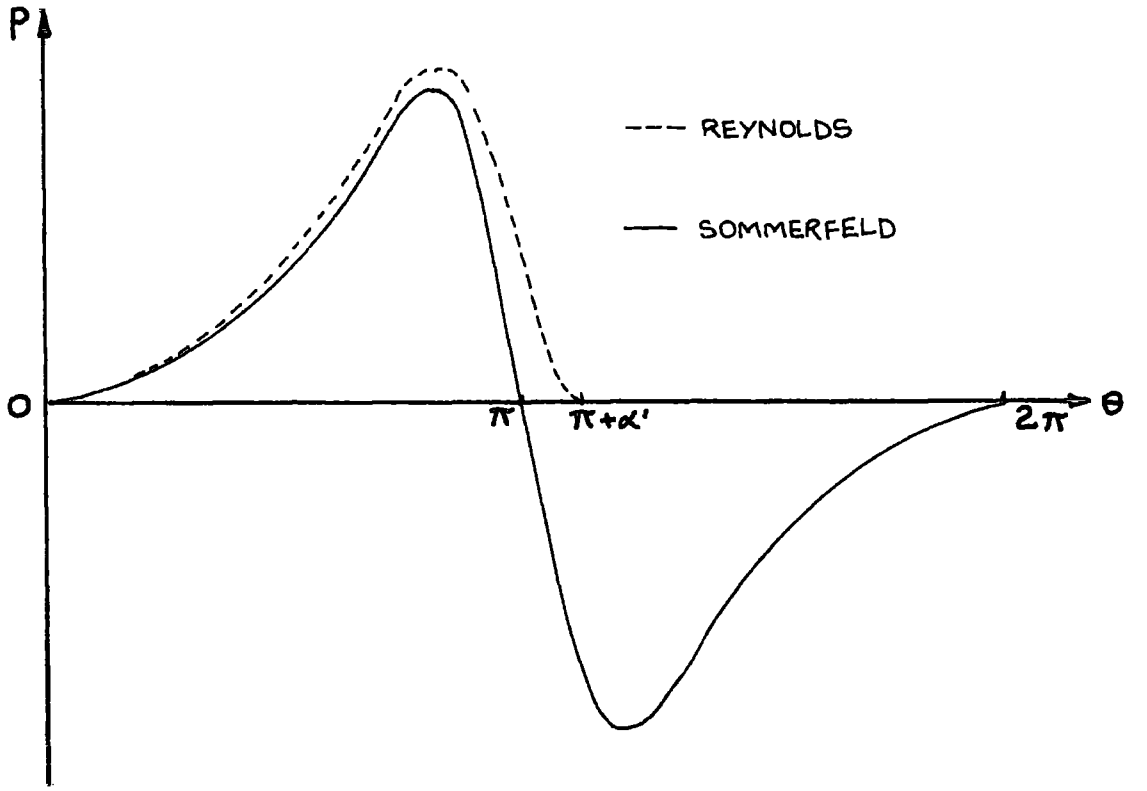

Fig.33 Sommerfeld and Reynolds pressure distributions

The boundary condition at the start of the film where the pressure begins to rise and lubricant first covers the whole bearing width, has received comparatively little attention. It is usually assumed that the film begins at the maximum film thickness ($\theta = 0$). This simplifies the solution of the Reynolds equation and the predicted load capacity is realistic when the lubricant is supplied at either of the two usual points: opposite the load ($\theta = -\psi$) or at $\theta = (\pi/2 - \psi)$. The pressure gradient is low at the start of the film and so the load capacity is not greatly affected by errors in the position.

In a real bearing the axial leakage causes the pressure to vary approximately parabolically across the film. The two dimensional Reynolds equation is:

$$\frac{\partial}{\partial x}\left(h^3 \frac{\partial p}{\partial x}\right) + \frac{\partial}{\partial y}\left(h^3 \frac{\partial p}{\partial y}\right) = 6U\eta \frac{dh}{dx}$$

The no side leakage case can be solved analytically using an integral substitution, but the two dimensional equation is best solved by numerical methods using a digital computer. The boundary conditions discussed for the infinite bearing also apply to the side leakage case. The film breakdown occurs slightly earlier because of the side leakage. The pressure is usually assumed to be ambient outside the complete film.

Cameron (1966) has suggested that the observed delay in the formation of the film can be explained by the finite time necessary for the gases to redissolve. However it seems unlikely that there is a cycle of cavitation and solution. Once the streamers have formed, the gas bubbles could be stable with the lubricant by passing them.

B. THE MINIMUM DISSIPATION PRINCIPLE

A minimum dissipation principle has proved to be useful in the analysis of viscous flow situations. Helmholtz proved that for laminar flow of a Newtonian fluid between known boundaries with specified velocities, the velocity distribution throughout the fluid corresponds to minimum energy dissipation. It can be shown that this is a necessary and sufficient conditions for the equations of motion to be satisfied.

The principle of minimum dissipation is analogous to Castagliano's theorem in solid mechanics. Energy dissipation corresponds to elastic strain energy. The minimum strain energy principle is based on the linearity of stress and strain and so the minimum dissipation principle presumably does not apply to turbulent or non-Newtonian flow.

Although there is not a general proof, it has been shown that for a number of cases the general principle holds for less rigid boundary conditions than those specified by Helmholtz.

Christopherson and Dowson (1959) considered the fall of a ball in a slightly wider tube filled with liquid. They found that the ball falls eccentrically whilst rotating in a direction opposite to that required for rolling down the nearest wall. This result was shown to be consistent with a theoretical analysis based on minimum dissipation.

Christopherson and Naylor (1955) investigated wire drawing with a die pressurised by hydrodynamic action. The wire adopted an eccentric position which was again consistent with minimum dissipation.

A generally applicable minimum dissipation principle would be particularly valuable in lubrication theory as laminar is usual. Christopherson (1957) has shown that the Reynolds condition for the breakdown of lubricating films corresponds to minimum dissipation.

The film extent in a steadily loaded journal bearing has been analysed in the light of these examples. An exact analytical solution is not possible even for the infinitely wide bearing, but numerical methods can be employed to establish the relationship between film extent and energy dissipation.

C. NO SIDE LEAKAGE CASE

It is often worthwhile to investigate the behaviour of real bearings using the simplified model based on no side leakage. The differential equation, given previously, can be most easily solved using the Sommerfeld transformation:

$$\cos \gamma = \frac{\epsilon + \cos \theta}{1 + \epsilon \cos\theta}$$

The solution with the film start angle at the maximum film thickness ($\theta = \gamma = 0$) is well documented. Considering the start at $\gamma = \beta$, $\theta = \theta_1$ and the breakdown at the Reynolds position $\gamma = \pi + \alpha$, $\theta = \theta_2$, the equations are as follows:

$$\epsilon = \frac{2(\cos\alpha(\pi + \alpha - \beta) - (\sin\alpha + \sin\beta))}{(\pi + \alpha - \beta) - (\cos\alpha \sin\alpha) - \sin\beta(2\cos\alpha + \cos\beta)}$$

$$Wy^* = W^* \sin\Psi = \frac{\cos(\pi + \alpha - \beta) - (\sin\alpha + \sin\beta)}{(1 + \epsilon\cos\alpha).(1 - \epsilon^2)^{0.5}}$$

$$Wx^* = W^* \cos\Psi = \frac{\epsilon/2(\cos\alpha + \cos\beta)}{(1 - \epsilon^2)(1 + \epsilon\cos\alpha)}$$

$$F^* = \frac{2\eta URL(\pi + 2\epsilon((\pi + \alpha - \beta)\cos\alpha - (\sin\alpha + \sin\beta)))}{c(1 - \epsilon^2)^{0.5}(1 + \epsilon\cos\alpha)}$$

F^*, the shaft friction, includes the contribution from the streamers in the cavitated region. Their fractional width was calculated as (available flow)/(flow to fill clearance), which assumes a rectangular cross section.

A computer programme was written to calculate the value of F^* at various film extents for a series of specified loads. The load cannot be fixed before solution and so it was necessary to use an iterative method. For given values of α and β the eccentricity ratio was successively modified by linear interpolation until the error in the value of W^* was less than 0.1%. The film co-ordinates were converted to angles in real space and the results plotted.

Fig.34 shows the variation in F^* with θ_1. The value of θ_2 does not change significantly as the film extent decreases. It can be seen that there is a minimum friction for the high and low loads. No minimum seems to exist for the intermediate loads; this will be shown to be a consequence of the infinite width. The eccentricity ratio is dependent on the film extent; as the film shortens the eccentricity increases and so the pressure gradients rise.

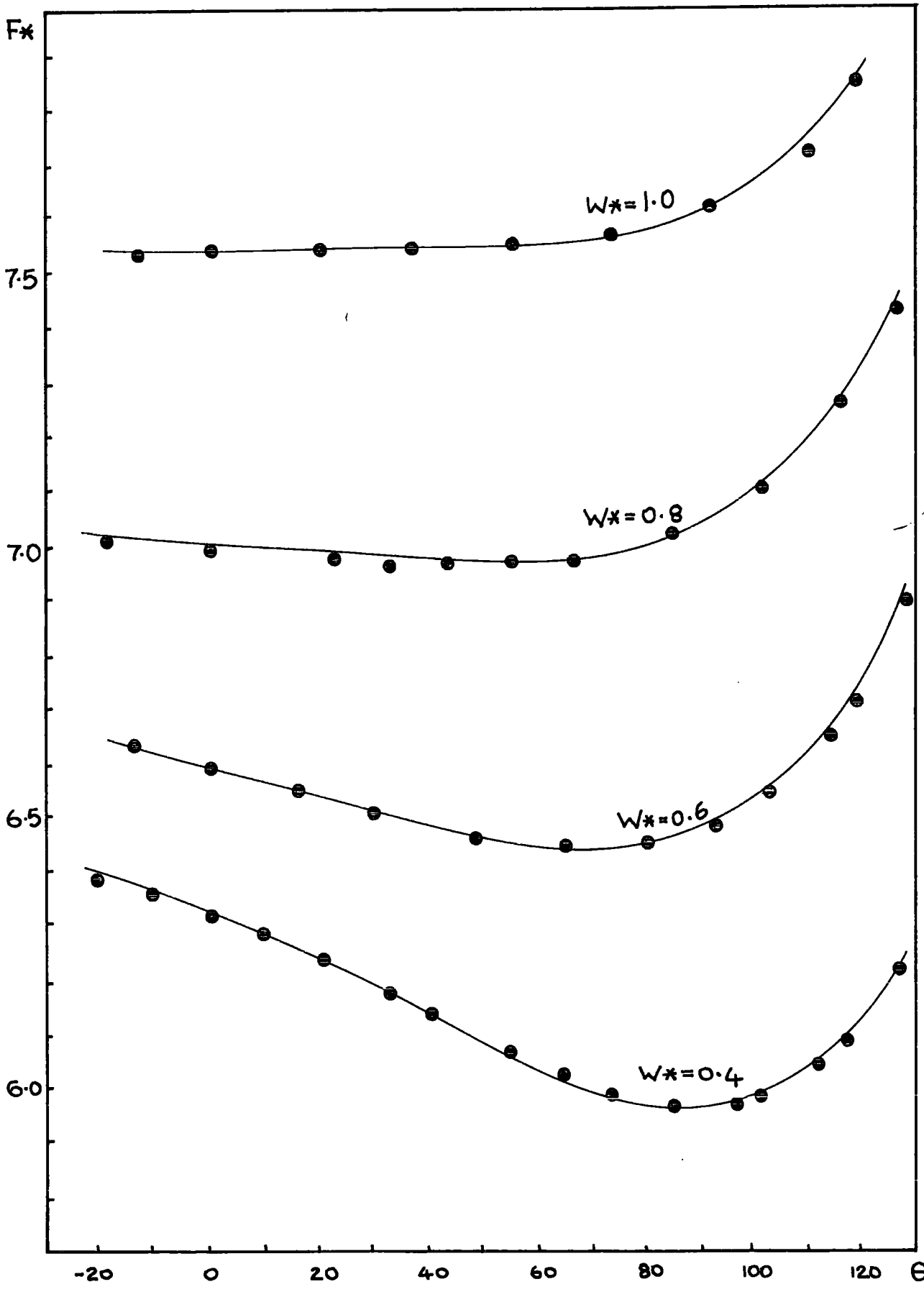

FIG. 34A F* VS. θ_1 AT VARIOUS LOADS L/D= ∞

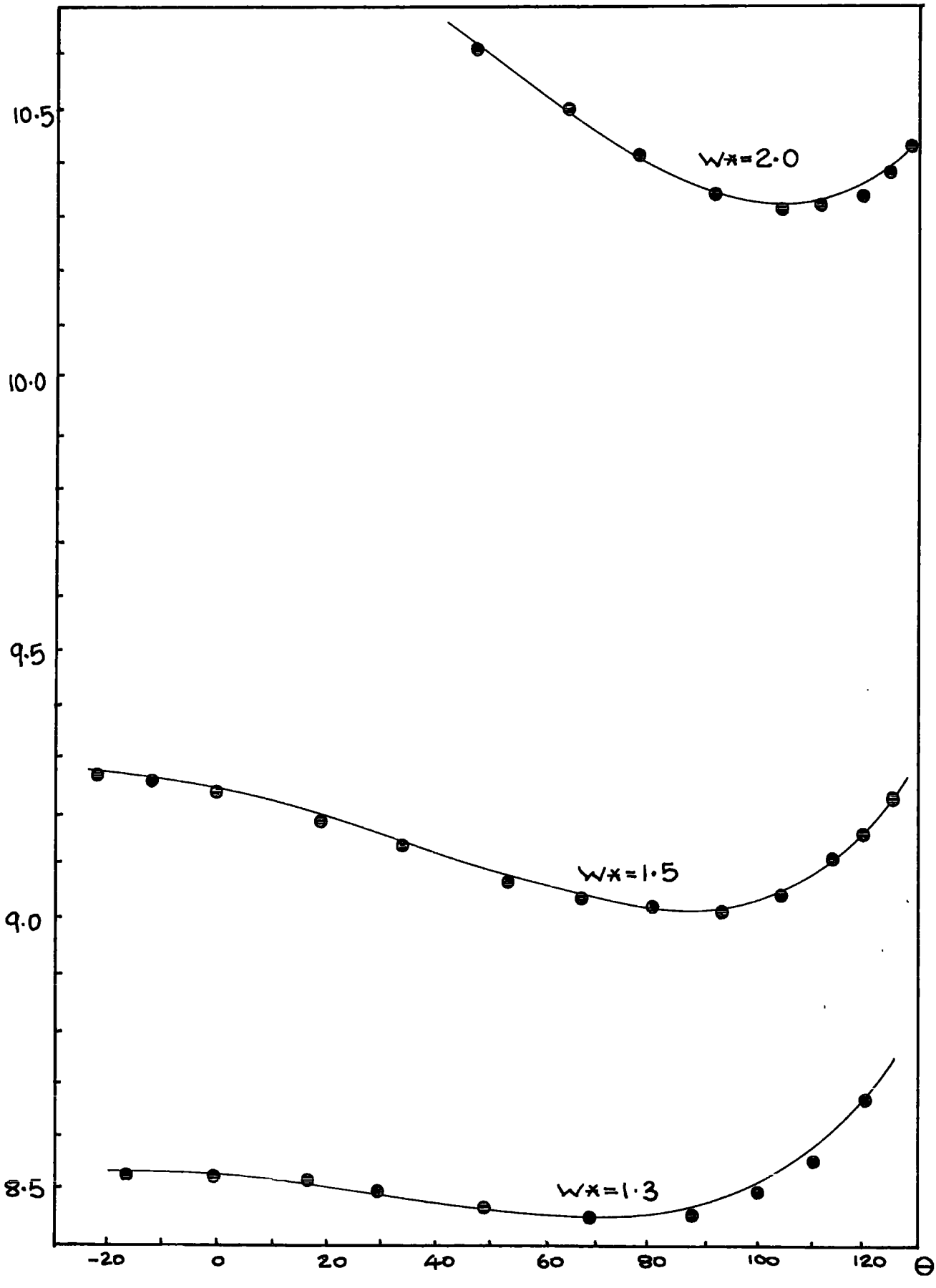

FIG. 34 B F* VS. θ_1 NO SIDE LEAKAGE : L/D= ∞

D. SIDE LEAKAGE CASE

The solution of the two dimensional Reynolds equation is complicated by considering various film extents and loads. The differential equation is usually represented by a finite difference approximation and the set of linear equations for the mesh solved by an iterative procedure. For the purpose of calculation it is convenient to modify Reynolds' equation by replacing p by $M = ph^{3/2}$. High pressures are associated with small film thicknesses and so this modification reduces the gradients and enables a coarser mesh to be used. The index 3/2 offers a simplification in the resulting equation. Written in terms of M, the non-dimensional Reynolds equation becomes:

$$\frac{\partial^2 M^*}{\partial \theta^2} + \left(\frac{R}{L}\right)^2 \frac{\partial^2 M^*}{\partial y^{*2}} = -\left\{\frac{3(2\epsilon\cos\theta + \epsilon^2(\cos\theta)^2 + \epsilon^2\cos 2\theta)}{4(1 + \epsilon\cos\theta)^2}\right\} - \frac{\epsilon\sin\theta}{(1 + \epsilon\cos\theta)^{1.5}}$$

when the film thickness relationship is included.

The equation was solved by a method similar to that suggested by Osbourne (1966). It was represented by a five point finite difference equation and then a Liebmann relaxation method was used to give the values of M^* for one half of the symmetrical bearing. The Reynolds breakdown condition was imposed by immediately reducing to zero any negative pressures produced.

An initial test showed that a 61 x 11 mesh offered a reasonable balance between computing time and accuracy for a bearing with L/D = 1. The 61 points were between the chosen starting point and $\pi/2$ after the minimum film thickness, which is beyond the possible breakdown point. The 11 points were across half of the bearing width.

A computer was programmed to sweep through the interior of the mesh and calculate an improved pressure at each point from the four surrounding values. The initial values were all zero and the boundaries were unchanged throughout the solution. The basic relaxation procedure converges very slowly for a fine mesh and so Aitken's δ^2 method was used to accelerate the process. The method

used involved a sequence of 40 iterations for the whole mesh followed by the calculation of an improved estimate from the three final values at each point. This was repeated until the largest change along the centre line was less than 0.001% between successive iterations. The total computing time was reduced by a factor of almost 2 by the Aitken process but the storage required was increased.

The load was found by an integration of the M* values. Simpson's rule was used axially and the Trapezoidal rule circumferentially.

The shaft friction was calculated by including the contribution from the cavitation streamers. The analysis is exact for both infinitely wide and finite bearings. The starting points are:

$$\frac{du}{dz} = \frac{1}{\eta}\frac{dp}{dx}\left(z - \frac{h}{2}\right) + \frac{U}{h}; \quad \tau = \eta \frac{du}{dz}$$

Integration yields:

$$F^* = 3\epsilon W^* \sin\Psi + I/(1 - \epsilon^2)^{0.5}$$

$$I = \int_{\theta_1}^{\theta_2} \frac{d\theta}{(1 + \epsilon\cos\theta)} + \int_{\theta_2}^{2\pi+\theta_1} \frac{(1 + \epsilon\cos\theta_2)}{(1 + \epsilon\cos\theta)^2}\, d\theta$$

The second part of I is the contribution from the streamers. The whole integral can be solved using the Sommerfeld substitution. It yields:

$$I = \left\{\pi + \alpha - \beta + \left\{\frac{((\beta + \pi - \alpha) - (\epsilon\sin\beta + \epsilon\sin\alpha))}{(1 + \epsilon\cos\alpha)}\right\}\right\}$$

The expression given previously for the infinitely wide bearing can be obtained by substituting for W* in the equation above.

The contribution to the friction from the supply flow was also calculated assuming zero supply pressure and a feed opposite the load. A volumetric flow balance was used to give the extra area of sheared fluid.

The side leakage i.e. supply flow can be calculated by integrating along the edges of the film or by subtracting the flow at the end from the flow at the start. The latter method was used, considering the pressure gradient at the start of the film. This is sometimes neglected but is important at high eccentricities or for short films. The equation is:

$$Q^* = \epsilon(\cos\theta_1 - \cos\theta_2) - (1 + \epsilon\cos\theta_1)^3 \int_0^1 \left\{ \frac{dp}{d\theta} \right\}_{\theta = \theta_1} dy^*$$

The contribution to the friction from the supply flow was calculated by a method similar to that used for the cavitation streamers.

Since the load is one of the final results, an iterative method must be used to determine the conditions at specified loads. Improved values of the eccentricity ratio were calculated from initial estimates using linear interpolation. The process was repeated until the actual load was within 0.1% of the set value. From 2 to 6 eccentricity changes were necessary to obtain this degree of accuracy. Once the load was acceptable the eccentricity ratio was used in the calculation of the shaft friction before advancing the film start angle. The average computing time for a particular load and film extent was 90 seconds on the IBM 360/67 machine employed.

Fig.35 shows the variation of F^* with θ_1 for various values of W^*, the non-dimensional load. The higher frictions at each load include the supply flow component. The results are tabulated at the end of this appendix with the computer programme.

Certain discrepancies are noticeable in the tabulated results which cause irregularities in the curves. The film extent and so the friction cannot change smoothly because of the mesh. This becomes finer as the extent decreases but there will be an error in fixing the breakdown point. The centre-line value of θ_2 was used in the calculation of the friction and the

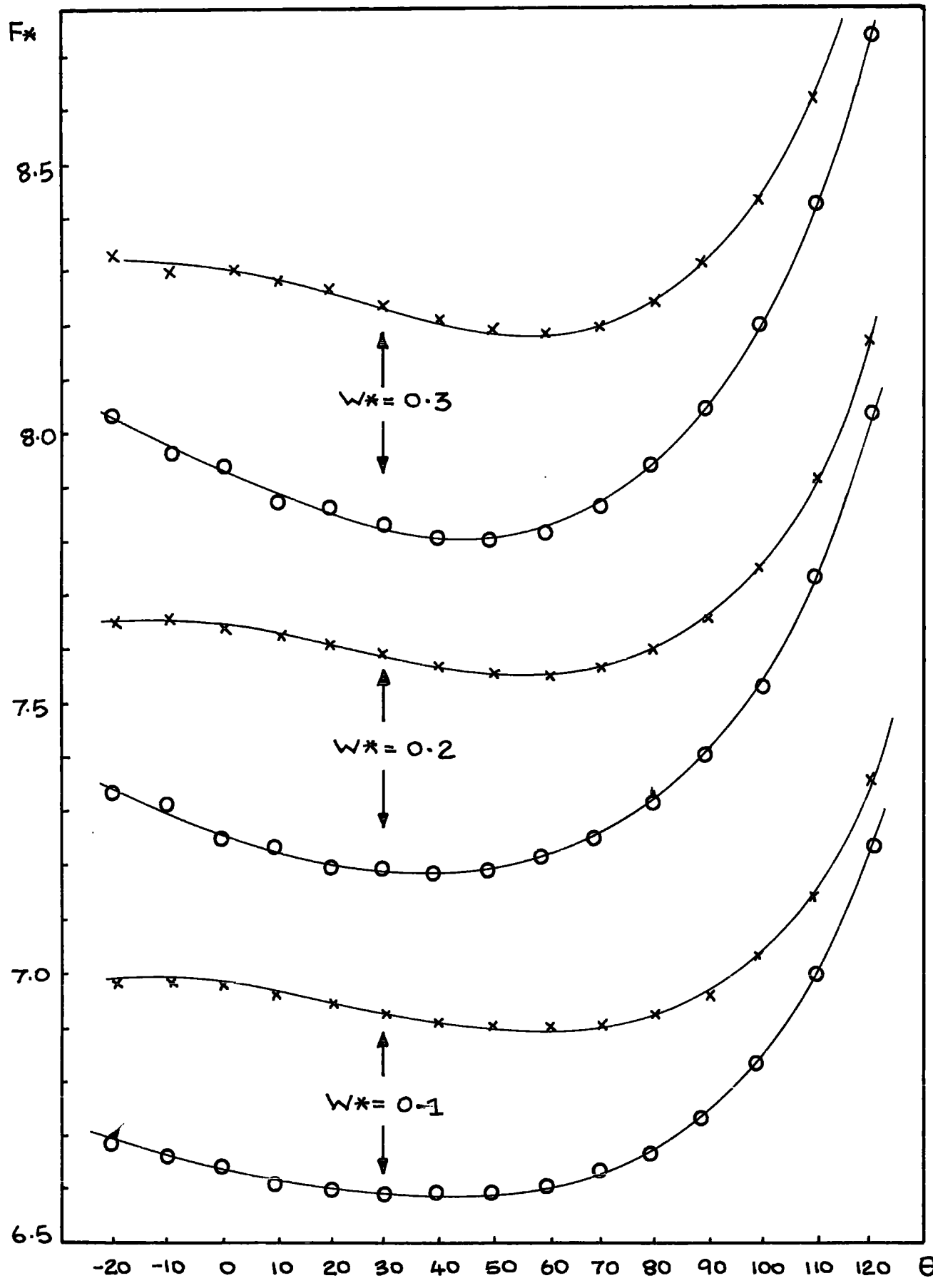

FIG. 35A F* VS. θ_1 L/D= 1 AT VARIOUS LOADS

X INCLUDES SUPPLY CONTRIBUTION

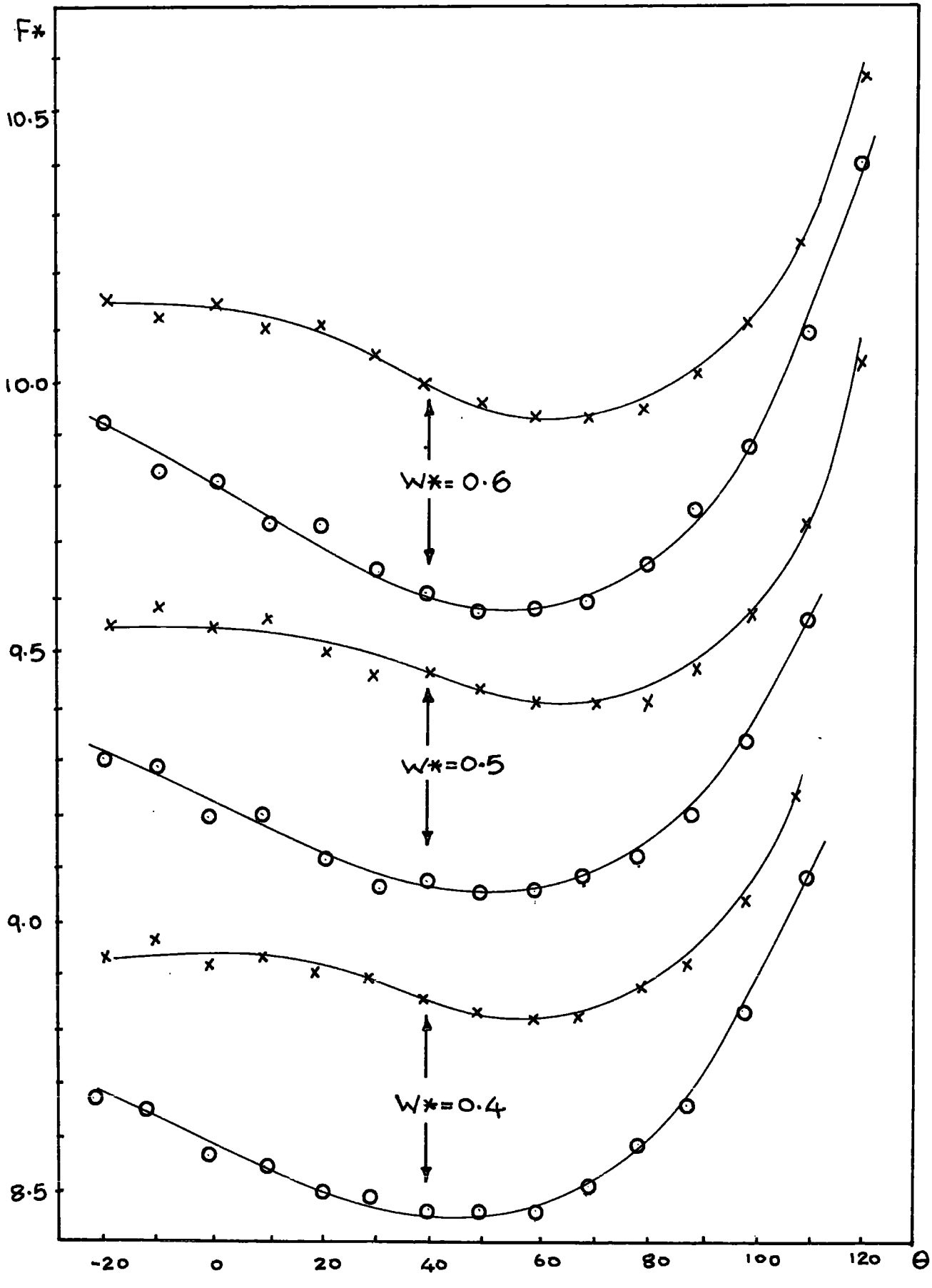

FIG. 35B F* vs. θ1 L/D= 1

× INCLUDES SUPPLY CONTRIBUTION

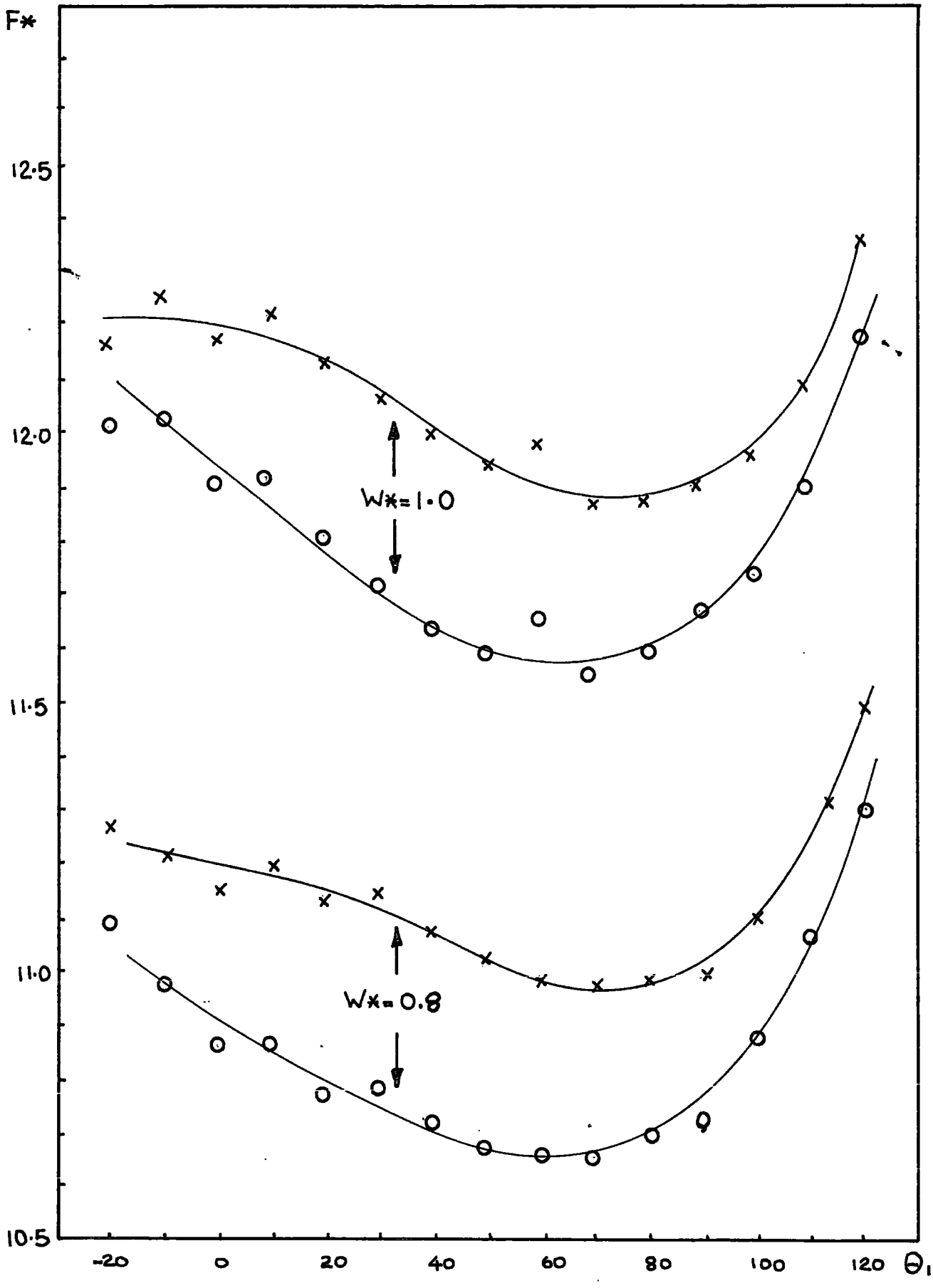

FIG. 35c F* vs. θ_1 L/D=1

X INCLUDES SUPPLY CONTRIBUTION

flowrate; this introduces a small error due to the earlier cavitation at the edges of the bearing. Another error is introduced by the variations in the load; it is difficult to differentiate this effect from that due to errors in the eccentricity ratio. At low values of θ_1 the eccentricity ratio changes little or even not at all as the extent decreases. Theoretically ϵ must increase as the film shortens but accumulated errors mask this behaviour.

The irregularities caused by the finite difference approach could be reduced at the expense of computing time but the form of the curves would not be changed.

E. DISCUSSION

The results of the side leakage calculations demonstrate that for a given value of the non-dimensional load there is a value of the film extent that results in minimum friction.

The hypothesis is that a bearing will tend to operate with that film extent that corresponds to minimum energy dissipation.

The variation in friction is small for most of the starting positions but this does not affect the basic principle. For the loads considered the optimum value of θ_1 is between 55° and 65° when the supply flow contribution is included. At both ends of the θ_1 range considered the difference between the two conditions decreases: in one case the start is near to the supply point and in the other the flowrate is small because of the short film.

Fig.36 shows the results of Cole and Hughes plotted with the present theoretical results. Their bearing had a feed position and L/D ratio similar to the theoretical model and so the results are comparable. They observed the maximum delay in the film start angle at the lowest feed pressures as expected. It can be seen that the minimum friction results closely agree with the experimental results for the film start angle.

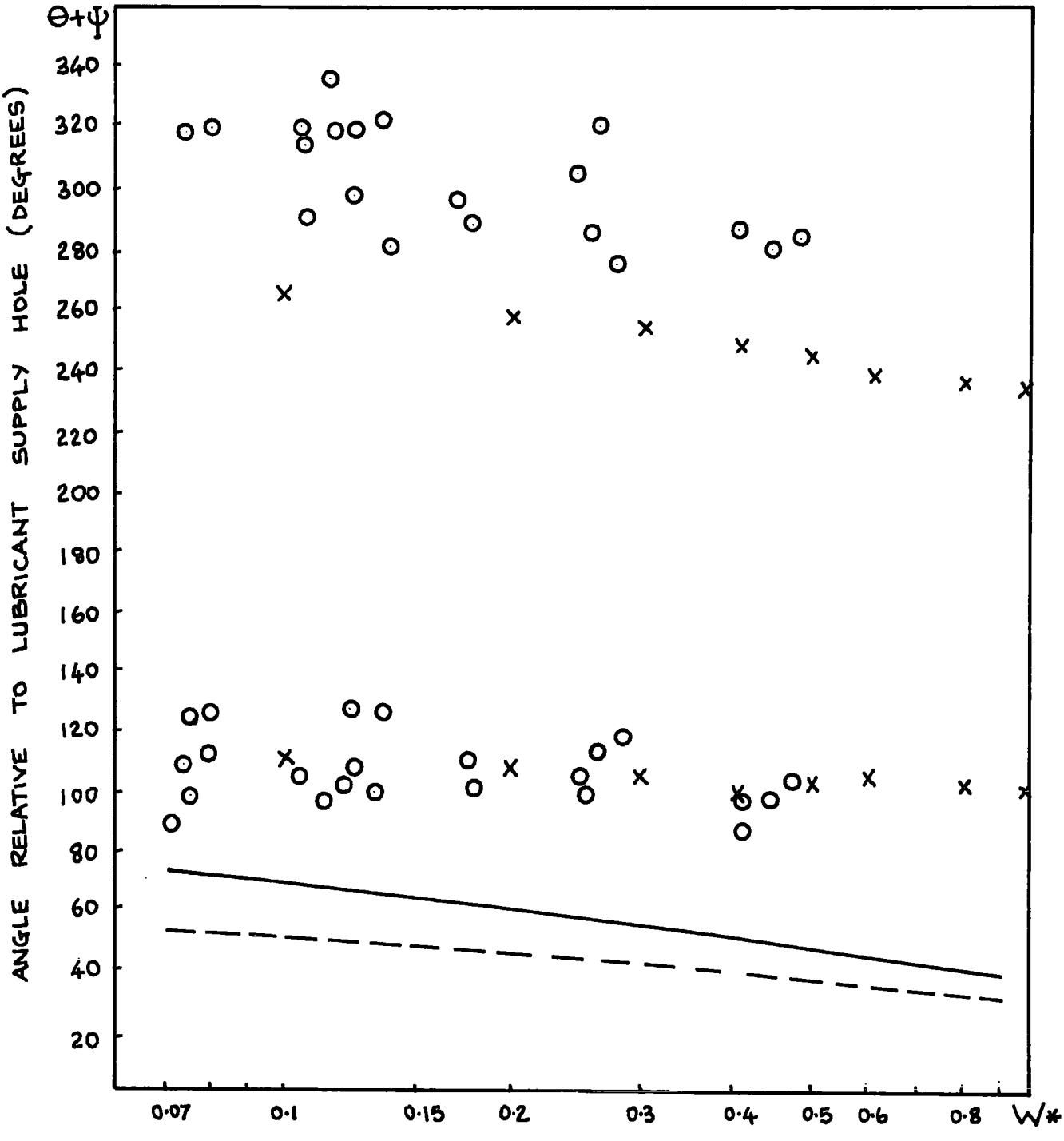

FIG. 36 FILM EXTENT VS. LOAD

O EXPERIMENTAL : COLE AND HUGHES

× THEORETICAL FOR MINIMUM FRICTION

——— } POSITION OF MAX. THICKNESS — $\theta_1 = 0$

– – – } POSITION OF MAX. THICKNESS — MIN. FRICTION

However the film extends farther than predicted. Cole and Hughes suggested that the scatter in the breakdown position could be due to experimental error but they did not offer an explanation of the delay. They recorded flowrates lower than predicted concluding that this was due to the meniscus formed at each side of the bearing. It is possible that this meniscus affected the breakdown of the film. The delay in the start of the film is consistent with the minimum energy dissipation principle, at least for low feed pressures.

Practical bearings are not fed at zero pressure, this would involve the bearing only taking the flow required. A greater flow is used to ensure adequate cooling of the lubricant carried through the loaded region. Most of the additional lubricant leaves near to the supply but the film will be extended. A minimum dissipation condition might still control the formation of the film but a more rigorous analysis would be required.

The effects observed during the development of the test bearing can be explained in terms of the dependence of the friction on film extent. As the speed increased at constant load the friction decreased because the situation approached zero supply pressure. The effect was accentuated by the large clearance ratio and low viscosity used.

In conclusion, the principle of minimum dissipation has been further reinforced and the conditions controlling the formation of lubricating films have been established.

```
>      1        COMPUTER PROGRAMME  SIDE LEAKAGE BEARING IBM LANGUAGE PL/1
>      2         CALCULATES NON D FRICTION FOR BEARING WITH R/L=ALF AT ADVANCING
>      3         FILM START POSITION.FINITE DIFF METHOD USED ON MESH SIZE NX,NY
>      4
>      5
>      6        FDMINF:PROC OPTIONS(MAIN);
>      7               DCL(EX,PI,ALF,RF,ERR,JIM,DTR,DDX,DX,DY,AX,AY,ANG,CANG,SANG,
>      8                   COMP,MC,PMAX,DC,DMAX,WC,WS,W,TR,ATANG,CA,CB,FRIC,INT,A,B,
>      9                   SETW,EX2,W2,STARTEX,Z)FLOAT;
>     10               /* DECLARATION OF PARAMETERS TO BE USED */
>     11               DCL(Q,HO,S,CS,FEDRIC)FLOAT;
>     12               DCL(NX,NY,NYM,I,J,K,XO,L)FIXED BIN;
>     13               DCL FEED FIXED BIN;
>     14               DCL (N,V)FIXED BIN;
>     15               DCL REX FLOAT;
>     16               FEED=0;  /* DEGREES BETWEEN SUPPLY AND LOAD */
>     17               PI=3.1415926;
>     18               DTR=PI/1.8E02;
>     19               ALF=0.5; /* BEARING RADIUS /WIDTH RATIO */
>     20               NX=61;   /* MESH DIMENSION */
>     21               NY=21;   /* MESH DIMENSION */
>     22               NYM=(NY+1)/2;
>     23               DY=1/(NY-1);
>     24               AY=(ALF/DY)**2;
>     25               RF=1E0;  /* RELAX FACTOR FOR ITERATION */
>     26               ERR=1E-05;/* MAX MESH CHANGE FOR CONVERGANCE */
>     27        /*GET INITIAL VAUES FROM DATA LIST */
>     28        WORK:GET LIST(SETW,STARTEX,XO);
>     29               /* EX IS ECC RATIO AND STARTEX ITS INITIAL VALUE */
>     30        BEGIN;
>     31        ON ERROR BEGIN;PUT DATA(L,V,Z,EX,M(I,J),MA(I,J),MB(I,J));END;
>     32               /* DECLARATION OF ARRAYS USED */
>     33               DCL(M(NX,NYM+1),Y(NX),G(NX),H(NX),LM(NX),WI(NX))FLOAT;
>     34               DCL (MA(NX,NYM+1),MB(NX,NYM+1))FLOAT;
>     35               JIM=(NX-1);
```

```
>     36              /* SET INITIAL MESH VALUES */
>     37              DO I=1 TO NX;
>     38                 DO J=1 TO (NYM+1);
>     39                    M(I,J)=0;
>     40                 END;
>     41              END;
>     42              PUT DATA(NX,NY,ALF,ERR,SETW,STARTEX);
>     43              PUT SKIP(8);
>     44              PUT EDIT('IN','OUT','EXTENT','E','LOAD','ATT','FRIC',
>     45              'FEDRIC','Q*','MAXP AT')
>     46              'X(4),A(2),X(5),A(3),X(5),A(6),X(5),A(1),X(6),A(4),X(5),A(3),
>     47              X(6),A(4),X(4),A(6),X(5),A(2),X(4),A(7));
>     48           PUT SKIP(4);
>     49        POINT:
>     50           V=0;
>     51           L=0;EX=STARTEX;
>     52           DDX=(2.7E2-XO)/JIM;
>     53           DX=DDX*DTR;
>     54           AX=(1/DX)**2;
>     55        /* SET MINOR ARRAYS FOR PARTICULAR FILM START ANGLE XO AND ECC RATIO*/
>     56        NEWEX:
>     57           L=L+1;K=0;
>     58           IF L>20 THEN DO;
>     59                        EX=EX2;
>     60                        W=W2;
>     61                        GO TO PROFILE;
>     62                       END;
>     63           DO I=1 TO NX;
>     64              ANG=((DDX*(I-1))+XO)*DTR;
>     65              CANG=COS(ANG);
>     66              SANG=SIN(ANG);
>     67              H(I)=(1E0+(EX*CANG))**1.5;
>     68              Y(I)=-2*(AX+AY)+(0.75E0*((2E0*EX*CANG)+(2*(EX**2)*(CANG**2))
>     69                                -((EX**2)*(SANG**2)))/(H(I)**(4E0/3E0)));
>     70              G(I)=-(EX*SANG)/H(I);
>     71              LM(I)=CANG/H(I);
>     72           END;
```

```
>     73          ITERATE:
>     74          /* LIEBMANN RELAXN WITH ACCD CONVERGENCE */
>     75            V=V+1;
>     76            K=K+1;IF K>30 THEN GO TO LOAD;
>     77            DO N=1 TO 40;
>     78      /* RELAX FOR REST OF MESH */
>     79              DO J=2 TO (NYM-1);
>     80                 DO I=2 TO (NX-1);
>     81                    M(I,J)=M(I,J)-((RF/Y(I))*(((M(I+1,J)+M(I-1,J))*AX)
>     82                                             +((M(I,J+1)+M(I,J-1))*AY)
>     83                                             +(M(I,J)*Y(I))-G(I)));
>     84                 IF M(I,J)<0 THEN M(I,J)=0;
>     85                 IF N=38 THEN DO;
>     86                               MA(I,J)=M(I,J);
>     87                              END;
>     88                 IF N=39 THEN DO;
>     89                               MB(I,J)=M(I,J);
>     90                              END;
>     91              END;
>     92            END;
>     93      /* RELAX FOR MIDDLE OF MESH AND TEST FOR CONVERGENCE */
>     94            COMP=0;
>     95            DO I=2 TO (NX-1);
>     96               J=NYM;
>     97               M(I,J+1)=M(I,J-1);
>     98               MC=M(I,J);
>     99                  M(I,J)=M(I,J)-((RF/Y(I))*(((M(I+1,J)+M(I-1,J))*AX)
>    100                                           +((M(I,J+1)+M(I,J-1))*AY)
>    101                                             +(M(I,J)*Y(I))-G(I)));
>    102               IF M(I,J)<0 THEN M(I,J)=0;
>    103               IF M(I,J)>0 THEN DO;
>    104               TR=(ABS(M(I,J)-MC))/(M(I,J));
>    105               IF TR>COMP THEN COMP=TR;
>    106                              END;
>    107                  IF N=38 THEN DO;
>    108                               MA(I,J)=M(I,J);
>    109                              END;
```

```
>    110                   IF N=39 THEN DO;
>    111                                    MB(I,J)=M(I,J);
>    112                                   END;
>    113             END;
>    114          IF COMP<ERR THEN GO TO LOAD;
>    115          END;
>    116          J=1;
>    117     /*ACCN FOR REST OF MESH */
>    118          REST:J=J+1;IF J<NYM THEN DO;
>    119               I=1;
>    120               US:I=I+1;
>    121               IF I<=NX THEN DO;
>    122               IF M(I,J)=0 THEN GO TO REST;
>    123               IF MB(I,J)=M(I,J) THEN GO TO US;
>    124               Z=((MA(I,J)-MB(I,J))/(MB(I,J)-M(I,J)));
>    125               Z=Z-1E0;
>    126               IF Z=0 THEN Z=1E-02;
>    127               Z=1E0/Z;
>    128               IF Z>1E2 THEN Z=1E2;IF Z<-1E2 THEN Z=-1E2;
>    129               M(I,J)=M(I,J)+(Z*(M(I,J)-MB(I,J)));
>    130                              END;
>    131               GO TO US;
>    132                                    END;
>    133          J=NYM;I=1;
>    134     /* ACCN FOR MIDDLE */
>    135          MID:I=I+1;
>    136               IF M(I,J)>0 THEN DO;
>    137               IF MB(I,J)=M(I,J) THEN GO TO MID;
>    138               Z=((MA(I,J)-MB(I,J))/(MB(I,J)-M(I,J)));
>    139               Z=Z-1E0;
>    140               IF Z=0 THEN Z=1E-02;
>    141               Z=1E0/Z;
>    142               IF Z>1E2 THEN Z=1E2;IF Z<-1E2 THEN Z=-1E2;
>    143               M(I,J)=M(I,J)+(Z*(M(I,J)-MB(I,J)));
>    144               GO TO MID;
>    145                                    END;
>    146     GO TO ITERATE;
```

```
>   147       LOAD:
>   148           /* INTEGRATION TO FIND LOAD */
>   149            DO I=2 TO (NX-1);
>   150               IF M(I,NYM)>0 THEN C=I;
>   151            END;
>   152            C=C+1;
>   153            DO I=1 TO (C-1);
>   154               WI(I)=0;
>   155               DO J=1 BY 2 TO (NYM-2);
>   156                  WI(I)=WI(I)+((DY/3E0)*(M(I,J)+M(I,J+2)+(4*M(I,J+1))));
>   157               END;
>   158            END;
>   159            WC=0;WS=0;
>   160            DO I=1 TO (C-2);
>   161               WS=WS+((DX/2E0)*((G(I)*WI(I))+(G(I+1)*WI(I+1)))/(-EX));
>   162               WC=WC+((DX/2E0)*((LM(I)*WI(I))+(LM(I+1)*WI(I+1))));
>   163            END;
>   164            W=SQRT((WC*WC)+(WS*WS));
>   165            W=W*2E0;
>   166       LOOKLOAD:
>   167       /* LINEAR INTERPOLATION TO GET BETTER EX FROM LOADS AT TWO EX */
>   168               IF ABS(SETW-W)>(SETW*1E-03) THEN DO;
>   169                                                  IF EX=STARTEX THEN DO;
>   170                                                                     EX2=EX;
>   171                                                                     EX=EX2+2E-2;
>   172                                                                     W2=W;
>   173                                                                     GO TO NEWEX;
>   174                                                                     END;
>   175                                                    REX=EX;
>   176                                                 EX=((EX2-EX)/(W2-W))*(SETW-W)+EX;
>   177                                                    EX2=REX;
>   178                                                    W2=W;
>   179                                                    GO TO NEWEX;
>   180                                                    END;
```

```
>    181       PROFILE:PMAX=0;
>    182               DO I=2 TO (NX-1);
>    183                  IF M(I,NYM)/H(I)>PMAX THEN DO;
>    184                                             PMAX=M(I,NYM)/H(I);
>    185                                             NMAX=I;
>    186                                            END;
>    187               END;
>    188            DMAX=(DDX*(NMAX-1))+XO;
>    189            DC=(DDX*(C-1))+XO;
>    190            ATANG=ATAN((WS/WC));
>    191            ATANG=ATANG/DTR;
>    192       FLOW:
>    193            Q=0;CANG=COSD((XO-DDX));
>    194            HO=(1E0+(EX*CANG))**1.5;
>    195            DO J=2 TO (NYM-1);
>    196               Q=Q+((DY/(2E0*DX))*((M(2,J)*(1E0/H(2)+(1E0/HO)))-(DX*DX*G(1)/
>    197                                                                    HO)));
>    198            END;
>    199            DO J=1,NYM;
>    200               Q=Q+((DY/(4E0*DX))*((M(2,J)*(1E0/H(2)+(1E0/HO)))-(DX*DX*G(1)/
>    201                                                                    HO)));
>    202            END;
>    203               Q=Q*((1E0+(EX*COSD(XO)))**3)*2E0;
>    204               Q=(1E0+(EX*COSD(XO)))-(1E0+(EX*COSD(DC)))-Q;
>    205       FRICTION:
>    206               CA=COSD(DC);CB=COSD(XO);CS=COSD(-ATANG+FEED);
>    207               FRIC=6E0*EX*WS;
>    208               A=(EX+CA)/(1+(EX*CA));
>    209               B=(EX+CB)/(1+(EX*CB));
>    210                S=(EX+CS)/(1E0+(EX*CS));
>    211               A=ATAN(SQRT(1E0-A*A),A);
>    212               B=ATAN(SQRT(1E0-B*B),B);
>    213                S=ATAN(SQRT(1E0-S*S),S);
>    214               A=A-PI;
>    215               B=B*SIGN(XO);
#
```

```
>    216              INT=(PI+A-B)+((B+PI-A)-(EX*(SIN(A)+SIN(B)))/(1+(EX*COS(A))));
>    217              INT=INT/((1-EX*EX)**0.5);
>    218              FRIC=FRIC+INT;
>    219                B=PI+PI+B;S=PI+PI-S;
>    220                FEDRIC=Q*(B-S-(EX*(SIN(B)-SIN(S))))/((1E0-(EX*EX))**1.5);
>    221               FEDRIC=FEDRIC+FRIC;
>    222       PRINT:
>    223            PUT EDIT(XO,DC,(DC-XO),EX,W,ATANG,FRIC,FEDRIC,Q,DMAX,L,V)
>    224            (X(3),F(4,0),X(3),F(6,2),X(3),F(6,2),X(3),F(6,4),X(3),
>    225       F(6,4),X(3),F(5,2),X(3),F(6,3),X(3),F(6,3),X(3),F(6,3),X(3),F(6,2),
>    226        X(5),F(3),X(5),F(5));
>    227            PUT SKIP(2);
>    228       ALTIN:
>    229            IF XO<140 THEN DO;
>    230                            XO=XO+10;
>    231                            STARTEX=EX;
>    232                            GO TO POINT;
>    233                           END;
>    234        END;
>    235        PUT PAGE;GO TO WORK;
>    236        END FDMINF;
```

COMPUTER RESULTS FROM SIDE LEAKAGE ANALYSIS

BEARING L/D=1.0 SUPPLY OPPOSITE LOAD
θ1 FILM START ANGLE DEGREES FROM MAX FILM THICKNESS
θ2 FILM BREAKDOWN DEGREES FROM MAX FILM THICKNESS
ECC ECCENTRICITY RATIO
W* NON D LOAD
ATT ATTITUDE ANGLE
F* NON D FRICTION HIGHER VALUE INCLUDES SUPPLY FLOW
Q* NON D SIDE LEAKAGE FLOW

θ1	θ2	ECC	W*	ATT	F*	F*	Q*
-30	210.0	0.2309	0.1000	75.67	6.728	6.971	0.392
-20	212.0	0.2309	0.1000	75.06	6.709	6.990	0.385
-10	209.3	0.2312	0.1000	73.86	6.672	6.988	0.381
0	211.5	0.2328	0.1000	72.02	6.656	6.988	0.364
10	209.3	0.2360	0.1000	69.64	6.627	6.975	0.352
20	211.7	0.2413	0.1000	66.74	6.619	6.965	0.328
30	210.0	0.2491	0.0999	63.42	6.602	6.947	0.311
40	212.5	0.2597	0.0999	59.75	6.607	6.935	0.282
50	211.3	0.2737	0.1000	55.78	6.607	6.922	0.260
60	210.5	0.2917	0.1000	51.59	6.619	6.915	0.236
70	210.0	0.3140	0.1001	47.24	6.646	6.917	0.208
80	206.7	0.3413	0.1000	42.79	6.678	6.931	0.187
90	207.0	0.3746	0.1000	38.29	6.754	6.972	0.154
100	204.8	0.4146	0.1000	33.77	6.853	7.044	0.127
110	203.3	0.4623	0.0999	29.28	7.009	7.169	0.098
120	202.5	0.5185	0.1000	24.86	7.253	7.375	0.066
130	200.0	0.5838	0.1000	20.51	7.613	7.705	0.043
140	196.3	0.6584	0.1000	16.25	8.175	8.247	0.026
150	192.0	0.7420	0.1000	12.10	9.129	9.190	0.015

θ1	θ2	ECC	W*	ATT	F*	6*	Q*
-30	210.0	0.3947	0.1999	65.40	7.402	7.661	0.664
-20	207.2	0.3947	0.2002	64.95	7.342	7.662	0.666
-10	209.3	0.3944	0.2000	64.12	7.318	7.676	0.639
0	207.0	0.3951	0.1999	62.86	7.263	7.655	0.619
10	209.3	0.3974	0.1999	61.14	7.249	7.652	0.576
20	207.5	0.4015	0.1999	59.01	7.211	7.624	0.542
30	210.0	0.4079	0.1999	56.50	7.213	7.613	0.488
40	208.7	0.4168	0.1999	53.65	7.200	7.589	0.445
50	207.7	0.4288	0.1999	50.51	7.202	7.572	0.399
60	207.0	0.4442	0.1999	47.11	7.223	7.568	0.349
70	206.7	0.4634	0.2000	43.51	7.266	7.580	0.299
80	206.7	0.4869	0.2002	39.76	7.339	7.617	0.246
90	204.0	0.5144	0.2000	35.89	7.422	7.672	0.205
100	202.0	0.5473	0.2000	31.95	7.555	7.774	0.163
110	200.7	0.5855	0.1999	27.95	7.757	7.942	0.122
120	200.0	0.6300	0.2000	23.91	8.062	8.208	0.082
130	297.7	0.6807	0.1999	19.89	8.494	8.610	0.052
140	194.2	0.7382	0.2000	15.90	9.150	9.248	0.032
150	192.0	0.8019	0.2000	11.90	10.290	10.356	0.014

θ1	θ2	ECC	W*	ATT	F*	F*	Q*
-30	205.0	0.5030	0.2998	58.44	8.068	8.301	0.862
-20	207.7	0.5030	0.3002	58.08	8.048	8.342	0.841
-10	204.7	0.5025	0.3000	57.50	7.972	8.320	0.824
0	207.0	0.5027	0.2999	56.55	7.951	8.330	0.775
10	205.0	0.5040	0.2999	55.26	7.890	8.296	0.734
20	207.5	0.5068	0.2998	53.62	7.883	8.292	0.668
30	206.0	0.5113	0.2998	51.65	7.845	8.256	0.612
40	204.8	0.5179	0.2997	49.37	7.823	8.224	0.551
50	204.0	0.5273	0.2999	46.78	7.821	8.205	0.487
60	203.5	0.5393	0.2999	43.95	7.839	8.198	0.421
70	203.3	0.5542	0.2998	40.88	7.881	8.209	0.354
80	203.5	0.5729	0.2999	37.61	7.958	8.250	0.288
90	204.0	0.5956	0.3003	34.18	8.078	8.330	0.224
100	202.0	0.6221	0.3000	30.63	8.217	8.438	0.174
110	200.7	0.6534	0.2999	26.98	8.433	8.619	0.127
120	200.0	0.6899	0.2999	23.25	8.762	8.909	0.083
130	197.7	0.7316	0.3000	19.45	9.224	9.342	0.052
140	194.2	0.7790	0.2999	15.62	9.922	10.022	0.032

θ1	θ2	ECC	W*	ATT	F*	F*	Q*
-30	205.0	0.5777	0.3996	53.45	8.758	8.957	0.985
-20	202.3	0.5777	0.4001	53.23	8.672	8.941	0.981
-10	204.7	0.5772	0.4000	52.72	8.652	8.973	0.938
0	202.5	0.5772	0.3998	52.03	8.571	8.936	0.900
10	205.0	0.5780	0.3999	50.96	8.559	8.946	0.831
20	203.3	0.5798	0.3998	49.65	8.497	8.901	0.770
30	206.0	0.5831	0.3997	48.04	8.502	8.900	0.684
40	204.8	0.5880	0.3996	46.13	8.468	8.860	0.611
50	204.0	0.5952	0.3998	43.94	8.456	8.833	0.535
60	203.5	0.6046	0.3998	41.50	8.466	8.819	0.457
70	203.3	0.6166	0.3998	38.83	8.504	8.828	0.381
80	203.5	0.6317	0.3998	35.93	8.577	8.865	0.306
90	201.0	0.6500	0.3998	32.85	8.652	8.915	0.247
100	202.0	0.6722	0.4001	29.60	8.830	9.049	0.180
110	200.7	0.6984	0.3997	26.21	9.046	9.231	0.129
120	197.5	0.7291	0.3998	22.71	9.340	9.503	0.093
130	195.3	0.7648	0.4000	19.10	9.811	9.948	0.060
140	194.2	0.8054	0.3998	15.41	10.576	10.677	0.030

θ1	θ2	ECC	W*	ATT	F*	F*	Q*
-30	205.0	0.6324	0.5000	49.70	9.425	9.584	1.075
-20	202.3	0.6320	0.5001	49.50	9.323	9.564	1.068
-10	204.7	0.6317	0.5001	49.12	9.308	9.604	1.021
0	202.5	0.6315	0.4998	48.52	9.215	9.558	0.977
10	205.0	0.6321	0.4999	47.67	9.206	9.573	0.900
20	203.3	0.6333	0.4998	46.57	9.132	9.519	0.831
30	202.0	0.6356	0.4996	45.22	9.073	9.468	0.753
40	204.8	0.6395	0.4996	43.59	9.092	9.472	0.653
50	204.0	0.6452	0.5000	41.69	9.071	9.438	0.568
60	203.5	0.6527	0.5000	39.55	9.072	9.417	0.482
70	203.3	0.6624	0.5000	37.17	9.101	9.418	0.398
80	200.3	0.6748	0.5000	34.57	9.117	9.414	0.331
90	201.0	0.6901	0.4997	31.74	9.230	9.489	0.254
100	199.2	0.7087	0.4997	28.74	9.356	9.587	0.195
110	198.0	0.7312	0.5000	25.57	9.570	9.769	0.141
120	197.5	0.7577	0.4999	22.24	9.905	10.067	0.092
130	195.3	0.7887	0.5001	18.79	10.377	10.514	0.059
140	194.2	0.8245	0.4999	15.22	11.159	11.258	0.030

#

θ1	θ2	ECC	W*	ATT	F*	F*	Q*
-30	200.0	0.6738	0.6000	46.78	9.953	10.099	1.165
-20	202.3	0.6734	0.6001	46.57	9.946	10.163	1.134
-10	200.0	0.6732	0.6001	46.29	9.841	10.121	1.104
0	202.5	0.6739	0.6000	45.75	9.833	10.155	1.035
10	200.7	0.6733	0.5999	45.05	9.742	10.100	0.971
20	203.3	0.6742	0.5998	44.10	9.743	10.115	0.876
30	202.0	0.6759	0.5995	42.92	9.673	10.055	0.792
40	201.0	0.6789	0.5994	41.51	9.623	10.002	0.701
50	200.3	0.6835	0.6000	39.84	9.596	9.965	0.608
60	200.0	0.6896	0.6000	37.93	9.591	9.940	0.516
70	200.0	0.6976	0.6000	35.78	9.614	9.937	0.425
80	200.3	0.7080	0.6000	33.39	9.673	9.965	0.339
90	201.0	0.7211	0.6000	30.80	9.780	10.035	0.258
100	199.2	0.7371	0.5997	28.00	9.896	10.124	0.197
110	198.0	0.7564	0.5998	25.01	10.099	10.296	0.141
120	197.5	0.7797	0.5990	21.84	10.431	10.593	0.092
130	195.3	0.8071	0.5996	18.52	10.898	11.034	0.058

θ1	θ2	ECC	W*	ATT	F*	F*	Q*
-20	202.3	0.7326	0.8007	42.19	11.117	11.298	1.228
-10	200.0	0.7321	0.8002	41.96	10.989	11.234	1.193
0	198.0	0.7321	0.8001	41.62	10.879	11.176	1.137
10	200.7	0.7321	0.8003	41.02	10.885	11.214	1.044
20	199.2	0.7326	0.7999	40.32	10.789	11.144	0.958
30	202.0	0.7337	0.7995	39.38	10.804	11.164	0.845
40	201.0	0.7356	0.7993	38.26	10.736	11.098	0.745
50	200.3	0.7387	0.7997	36.90	10.692	11.045	0.643
60	200.0	0.7430	0.8000	35.32	10.670	11.006	0.541
70	200.0	0.7488	0.8000	33.53	10.677	10.989	0.442
80	200.3	0.7564	0.8000	31.50	10.720	11.004	0.349
90	198.0	0.7661	0.8000	29.24	10.743	11.004	0.277
100	199.2	0.7783	0.7999	26.76	10.900	11.123	0.198
110	198.0	0.7934	0.8000	24.07	11.084	11.277	0.140
120	195.0	0.8119	0.7996	21.17	11.333	11.509	0.100

θ1	θ2	ECC	W*	ATT	F*	F*	Q*
0	198.0	0.7722	1.0001	38.53	11.922	12.196	1.192
10	200.7	0.7722	0.9996	38.09	11.939	12.248	1.094
20	199.2	0.7725	0.9999	37.49	11.831	12.167	1.001
30	198.0	0.7732	0.9995	36.74	11.737	12.088	0.899
40	197.2	0.7746	0.9991	35.82	11.662	12.017	0.790
50	196.7	0.7769	1.0000	34.68	11.612	11.962	0.680
60	200.0	0.7800	0.9999	33.31	11.674	12.001	0.556
70	196.7	0.7843	1.0000	31.78	11.577	11.891	0.467
80	197.2	0.7900	1.0000	29.99	11.608	11.895	0.369
90	198.0	0.7976	0.9999	27.98	11.688	11.944	0.279
100	196.3	0.8073	0.9997	25.75	11.752	11.983	0.211
110	195.3	0.8195	0.9999	23.29	11.913	12.117	0.150
120	195.0	0.8347	0.9999	20.59	12.209	12.382	0.098
130	193.0	0.8534	1.0000	17.67	12.638	12.789	0.063

APPENDIX 2

TABULATED TEST RESULTS

All of the test results and calculated non-dimensionals plotted in the text are given below. The variation of the viscosity of water with temperature was obtained from Perry (1963)

N	speed (r/s)
W	load (Newtons)
ϕ	outlet temp. (degrees centigrade)
PS	Supply pressure $(N/m^2) \times 10^{-5}$
$\dot{M}$	flowrate (Kg/S)
Re	Reynolds number = Uc/ν
1/S	Inverse of the Sommerfeld number = $NR^2\eta/Pc^2$
F	bearing friction (Newtons)
FC	reduced friction coefficient = $F/w \cdot R/C$
T^*	non-dimensional torque = T/N^2D^4L

Superscripts ' friction corrected for bearing imbalance and defects of loading system

" friction with angular momentum contribution subtracted

The letter at the end of each test number denotes the direction of rotation. 'U' direction corresponds to an extension of the torque measuring ring. The number after this denotes the concentration of Polyox WSR 301.

TEST 01U 0 PPM

N	W	Ø	PS	MX10⁴	RE	1/S	F	T*X10⁴
25	910	24	0.4	200	664	.087	0.94	94
29	910	24			776	.101	1.39	103
33	910	25	0.3	200	908	.113	1.88	106
38	910	25	0.4	200	1022	.127	2.44	109
42	910	26			1135	.141	3.01	109
46	910	26			1275	.152	3.83	115
50	910	27	0.6	210	1391	.165	4.63	116
54	910	27	0.6	217	1540	.175	5.38	115
58	910	28	0.8	217	1661	.189	6.21	114
63	910	29	1.0	224	1816	.198	7.60	122
66	910	30	1.3	250	1981	.206	9.78	138
71	910	31	1.4	224	2154	.214	12.15	152
75	910	31	1.5	224	2325	.225	14.67	164
79	910	32	1.6	224	2454	.235	17.11	172
83	910	32	1.7	220	2636	.242	19.37	175
88	910	34	1.8	217	2884	.244	20.87	171

TEST 02U 0 PPM

N	W	Ø	PS	MX10⁴	RE	1/S	F	T*X10⁴
25	910	20	1.0	342	606	.095	1.58	158
29	910	21	1.1	350	723	.108	2.03	150
33	910	21	1.1	350	827	.124	2.44	138
42	910	22	1.2	350	1057	.151	3.98	144
46	910	22	1.3	350	1162	.166	4.81	144
50	910	23	1.4	350	1298	.177	5.72	144
54	910	23	1.5	350	1406	.192	6.51	139
58	910	24	1.5	340	1551	.202	7.45	137
63	910	25	1.6	340	1703	.211	8.54	137
67	910	26	1.8	334	1855	.220	9.85	139
75	910	28	2.0	317	2179	.237	13.62	152
83	910	29	2.4	300	2476	.258	19.07	172
92	910	31	2.5	280	2841	.272	23.77	177

TEST 03U 0 PPM

N	W	Ø	PS	MX10⁴	RE	1/S	F	T*X10⁴
25	910	18	1.5	467	575	.099	1.92	193
29	910	18	1.6	460	671	.117	2.44	181
33	910	18	1.6	455	767	.133	2.94	166
38	910	18	1.7	458	863	.149	3.57	160
42	910	19	1.8	434	984	.162	4.29	155
46	910	20	1.9	430	1111	.174	5.15	154
50	910	20	2.0	424	1212	.189	6.06	152
54	910	21	2.0	418	1343	.201	7.03	151
58	910	21	2.1	410	1446	.216	8.01	148
67	910	22	2.6	350	1691	.242	10.64	150

TEST 04U 0 PPM

N	W	Ø	PS	RE	1/S	F	T*X10⁴
25	910	18	2.0	575	.099	2.37	238
29	910	18	2.0	671	.117	2.78	206
33	910	19	2.0	787	.130	3.27	185
38	910	19	2.0	886	.146	4.02	179
42	910	20	2.0	1010	.158	4.18	174
46	910	23	2.0	1190	.162	5.56	166
50	910	24	2.0	1329	.173	6.43	162
58	910	24	2.0	1555	.202	8.27	152
67	910	27	2.0	1895	.216	11.96	169
75	910	28	2.0	2179	.237	17.49	195

TEST 05U 0 PPM

N	W	∅	PS	RE	1/S	F	T*X10^4
25	1120	24	2.0	664	.070	1.71	172
29	1120	24	2.0	775	.082	2.24	165
33	1120	25	2.0	908	.091	2.77	157
38	1120	25	2.0	1022	.103	3.34	149
42	1120	26	2.0	1159	.112	3.99	144
50	1120	26	2.0	1391	.134	5.62	141
58	1120	27	2.0	1658	.153	7.52	139
67	1120	28	2.0	1937	.172	9.31	132
75	1120	30	2.0	2280	.184	14.62	163
83	1120	31	2.0	2584	.201	19.75	179
92	1120	33	2.0	2959	.212	24.30	182

TEST 06U 0 PPM

N	W	∅	PS	RE	1/S	F	T*X10^4
41	1433	20	2.0	1010	.100	3.05	110
50	1433	20	2.0	1212	.120	4.25	107
58	1433	21	2.0	1446	.137	6.32	117
66	1433	22	2.0	1691	.153	8.16	115
75	1433	24	2.0	1994	.165	9.97	111
83	1433	26	2.0	2320	.175	13.73	124
92	1433	28	2.0	2666	.184	17.97	134
100	1433	31	2.0	3100	.188	22.08	139
108	1433	34	2.0	3570	.192	24.82	133

TEST 07U 0 PPM

N	W	ø	PS	$\dot{M}X10^4$	RE	1/S	F	$T*X10^4$	F′	FC′	$T'*X10^4$	F″	FC″	$T''*X10^4$
50	1224	25	2.0		1363	.125	5.24	132	7.60	4.14	191			
58	1433	25	2.0		1623	.122	6.50	120	9.40	4.37	173			
67	1643	26	2.0	512	1855	.122	7.79	110	11.23	4.56	159	10.14	4.12	143
75	1852	27	2.0		2132	.119	9.23	103	13.22	4.76	148			
83	1957	28	2.0	466	2422	.123	10.64	96	14.90	5.08	135	13.66	4.65	124
92	2166	28	2.0	450	2664	.122	13.48	101	18.29	5.63	137	16.97	5.22	127
100	2271	29	2.0	411	2972	.124	16.71	105	21.80	6.40	137	20.48	6.01	129
108	2480	31	2.0	395	3359	.118	19.75	106	25.37	6.82	136	24.01	6.45	128
117	2690	32	2.0		3690	.115	22.79	105	28.96	7.18	134			
133	2899	34	2.0	341	4394	.117	28.30	100	35.01	8.05	124	33.56	7.72	119

TEST 08U 0 PPM

N	W	ø	PS	$\dot{M}X10^4$	RE	1/S	F	$T*X10^4$	F′	FC′	$T'*X10^4$	F″	FC″	$T''*X10^4$
25	596	15	2.0		533	.165	2.73	275	3.46	3.87	348			
29	701	16	2.0	520	638	.159	3.53	261	4.53	4.31	334	4.04	3.85	299
33	805	16	2.0	528	730	.158	3.99	225	5.26	4.35	297	4.70	3.89	265
38	910	16	2.0	528	839	.161	4.41	188	5.95	4.36	254	5.30	3.88	227
43	1015	17	2.0	524	973	.159	4.94	165	6.75	4.44	226	6.03	3.96	202
50	1224	17	2.0	524	1123	.152	5.89	148	8.25	4.49	207	7.41	4.04	186
58	1433	17	2.0	505	1310	.152	6.91	128	9.81	4.56	181	8.88	4.13	164
67	1643	18	2.0	489	1534	.148	8.51	120	11.95	4.85	169	10.91	4.43	154
75	1852	18	2.0	481	1726	.147	9.69	108	13.67	4.92	153	12.52	4.51	140
83	1957	19	2.0	450	1968	.151	11.39	103	15.66	5.33	142	14.46	4.93	131
92	2166	20	2.0	442	2223	.146	13.60	103	18.41	5.66	138	17.11	5.27	128
100	2271	21	2.0	411	2480	.149	15.88	100	20.96	6.15	132	19.64	5.77	123

TEST 09U 0 PPM

N	W	ø	PS	ṀX10⁴	RE	1/S	F	T*X10⁴	F′	FC′	T′*X10⁴	F″	FC″	T″*X10⁴
92	2166	25	2.0	458	2498	.130	12.91	97	17.72	5.45	132	16.38	5.04	122
100	2271	27	2.0	434	2843	.130	16.14	101	21.22	6.23	133	19.84	5.82	125
108	2480	28	2.0	411	3148	.126	19.37	104	24.99	6.72	134	23.57	6.34	126
117	2690	30	2.0	380	3547	.119	22.11	102	28.27	7.01	130	26.86	6.66	124
133	3004	33	2.0	356	4304	.115	28.87	102	35.85	7.96	127	34.33	7.62	121
150	3318	37	2.0	317	5241	.108	32.66	91	40.47	8.13	113	38.95	7.83	109

TEST 10D 0 PPM

N	W	ø	PS	ṀX10⁴	RE	1/S	F	T*X10⁴	F′	FC′	T′*X10⁴	F″	FC″	T″*X10⁴
25	596	15	2.0		533	.165	4.68	470	3.96	4.43	398			
29	701	15	2.0	489	622	.163	5.37	397	4.37	4.16	323	3.92	3.73	289
33	805	16	2.0	489	730	.158	6.10	345	4.83	4.00	273	4.31	3.57	244
38	910	16	2.0	489	839	.161	7.17	307	5.63	4.13	241	5.03	3.69	215
43	1015	16	2.0	489	949	.163	9.09	304	7.28	4.78	243	6.60	4.34	221
50	1224	17	2.0	485	1123	.152	10.55	265	8.19	4.46	206	7.42	4.04	186
58	1433	17	2.0	473	1310	.152	12.85	237	9.95	4.62	184	9.07	4.22	167
67	1643	18	2.0	454	1534	.148	14.96	211	11.51	4.67	163	10.55	4.28	149
75	1852	18	2.0	438	1726	.147	17.26	193	13.27	4.78	148	12.22	4.40	136
83	1957	19	2.0	411	1968	.151	20.02	181	15.76	5.37	143	14.66	4.99	133
92	2166	20	2.0	395	2223	.146	23.01	172	18.21	5.60	136	17.05	5.25	127
100	2271	21	2.0	372	2480	.149	26.85	169	21.77	6.39	137	20.58	6.04	129

TEST 11D 0 PPM

N	W	ø	PS	$\dot{M}X10^4$	RE	1/S	F	T^*X10^4	F′	FC′	T'^*X10^4	F″	FC″	T''^*X10^4
92	2166	22	2.0	395	2325	.140	22.82	171	18.02	5.54	135	16.86	5.19	126
100	2271	25	2.0	372	2725	.135	26.47	166	21.39	6.28	134	20.20	5.93	127
108	2480	26	2.0	364	3015	.131	30.30	162	24.68	6.63	132	23.42	6.29	125
117	2690	28	2.0	333	3390	.125	34.52	159	28.35	7.03	131	27.11	6.72	125
133	3004	32	2.0	294	4217	.117	41.81	148	34.82	7.73	123	33.57	7.45	119

TEST 12D 0 PPM

N	W	ø	PS	$\dot{M}X10^4$	RE	1/S	F	T^*X10^4	F′	FC′	T'^*X10^4	F″	FC″	T''^*X10^4
25	596	17	2.0	497	562	.156	5.73	515	4.40	4.93	443	4.01	4.48	403
29	701	18	2.0	497	671	.151	5.60	435	4.89	4.65	361	4.43	2.21	327
33	805	18	2.0	497	767	.151	5.34	365	5.19	4.29	293	4.66	3.86	263
38	910	18	2.0	489	882	.153	5.70	333	6.25	4.58	267	5.65	4.14	241
43	1015	18	2.0		997	.155	5.61	286	6.73	4.42	225			
50	1224	18	2.0	481	1151	.149	5.83	269	8.35	4.55	210	7.59	4.13	191
58	1433	19	2.0	473	1378	.144	5.86	233	9.71	4.52	179	8.83	4.11	163
67	1643	19	2.0	466	1574	.144	6.16	215	11.75	4.77	166	10.76	4.36	152

TEST 13U 50 PPM

N	W	ø	PS	$\dot{M}X10^4$	RE	1/S	F	T^*X10^4	F′	FC′	T'^*X10^4	F″	FC″	T''^*X10^4
25	596	17	2.0	512	562	.156	2.36	237	3.08	3.45	309	2.67	2.99	268
29	701	17	2.0	485	655	.155	2.85	210	3.85	3.66	284	3.39	3.23	251
33	805	17	2.0	485	749	.154	3.30	187	4.57	3.79	259	4.06	3.36	229
38	910	17	2.0	485	861	.157	3.72	159	5.26	3.86	225	4.67	3.42	200
43	1015	17	2.0	485	973	.159	4.33	145	6.14	4.04	205	5.47	3.60	183
50	1224	17	2.0	492	1123	.152	4.71	118	7.07	3.85	178	6.28	3.42	158
58	1433	17	2.0	502	1310	.152	5.32	98	8.22	3.82	152	7.28	3.39	134
67	1643	17	2.0	506	1497	.151	5.96	84	9.41	3.82	133	8.33	3.38	118
75	1852	18	2.0	509	1726	.147	6.65	74	10.64	3.83	119	9.42	3.39	105
83	1957	18	2.0	502	1918	.155	7.41	67	11.67	3.98	106	10.33	3.52	93
92	2166	19	2.0	499	2165	.150	8.09	60	12.90	3.97	96	11.44	3.52	86

TEST 14U 50 PPM

N	W	Ø	PS	$\dot{M}X10^4$	RE	1/S	F	T^*X10^4	F′	FC′	T'^*X10^4	F″	FC″	T''^*X10^4
92	2166	20	2.0	519	2223	.146	7.60	57	12.40	3.82	93	10.88	3.35	81
100	2271	20	2.0	506	2425	.152	9.00	57	14.08	4.13	88	12.47	3.66	78
108	2480	21	2.0	499	2686	.147	9.69	52	15.31	4.12	82	13.58	3.65	73
117	2690	12	2.0	478	2959	.143	10.56	49	16.73	4.15	77	14.95	3.70	69
133	3004	23	2.0	465	3462	.143	13.10	46	20.09	4.46	71	18.11	4.02	64
150	3318	25	2.0	444	4088	.139	15.57	43	23.37	4.70	65	21.25	4.27	59

TEST 15D 50 PPM

N	W	Ø	PS	$\dot{M}X10^4$	RE	1/S	F	T^*X10^4	F′	FC′	T'^*X10^4	F″	FC″	T''^*X10^4
25	596	17	2.0	444	562	.156	4.03	405	3.30	3.69	332	2.95	3.30	296
29	701	16	2.0	430	638	.159	4.94	365	3.94	3.75	291	3.54	3.37	261
33	805	16	2.0	437	730	.158	5.89	333	4.62	3.82	261	4.15	3.44	235
38	910	16	2.0	444	839	.161	6.76	298	5.22	3.82	223	4.68	3.43	200
43	1015	17	2.0	430	973	.159	7.82	262	6.01	3.95	201	5.42	3.56	181
50	1224	17	2.0	458	1123	.152	9.42	237	7.06	3.85	177	6.33	3.45	159
58	1443	17	2.0	448	1310	.152	11.20	207	8.30	3.86	153	7.47	3.47	138
67	1643	18	2.0	458	1534	.148	12.91	183	9.47	3.84	134	8.49	3.45	120
75	1852	18	2.0	465	1726	.147	14.51	162	10.52	3.79	117	9.41	3.39	105
83	1957	19	2.0	465	1968	.151	16.03	145	11.77	4.01	106	10.53	3.59	95
92	2166	19	2.0	465	2165	.150	17.66	132	12.85	3.96	96	11.49	3.54	86
100	2271	20	2.0	451	2425	.152	19.18	120	14.10	4.14	89	12.66	3.72	30

#

TEST 16D 50 PPM

N	W	ø	PS	MX10⁴	RE	1/S	F	T*X10⁴	F′	FC′	T′*X10⁴	F″	FC″	T″*X10⁴
92	2166	23	2.0	485	2380	.136	17.85	133	13.04	4.01	98	11.62	3.58	87
100	2271	23	2.0	478	2597	.142	19.37	122	14.29	4.20	90	12.76	3.75	80
108	2480	24	2.0	478	2881	.137	21.27	114	15.65	4.21	84	13.99	3.76	75
117	2690	24	2.0	471	3103	.136	22.79	105	16.62	4.12	77	14.86	3.68	69
133	3004	26	2.0	437	3710	.133	28.49	101	21.50	4.77	76	19.64	4.36	69

TEST 17U 0 PPM

N	W	ø	PS	MX10⁴	RE	1/S	F	T*X10⁴	F′	FC′	T′*X10⁴	F″	FC″	T″*X10⁴
50	1224	18	2.0	536	1151	.149	5.14	129	7.50	4.08	188	6.64	3.62	167
58	1433	19	2.0	528	1378	.144	6.60	122	9.50	4.42	175	8.52	3.96	157
67	1643	21	2.0	512	1653	.137	8.36	118	11.81	4.79	167	10.72	4.35	151
75	1852	22	2.0	501	1903	.134	9.78	109	13.77	4.96	154	12.57	4.53	140
83	1952	24	2.0	473	2216	.134	12.27	111	16.54	5.63	150	15.28	5.21	138
92	2166	25	2.0	450	2488	.130	14.96	112	19.77	6.08	148	18.45	5.68	138
100	2271	27	2.0	419	2843	.130	17.84	112	22.92	6.73	144	21.58	6.33	136
108	2480	30	2.0		3294	.120	20.64	110	26.26	7.06	141			
117	2585	33	2.0	395	3766	.117	22.25	103	28.14	7.26	130	24.89	6.69	133
133	2795	36	2.0	333	4572	.116	28.58	101	35.02	8.35	124	33.60	8.02	119

TEST 18U 0 PPM

N	W	ø	PS	MX10⁴	RE	1/S	F	T*X10⁴	F′	FC′	T′*X10⁴	F″	FC″	T″*X10⁴
50	1224	15	2.0	528	1066	.160	5.57	140	7.92	4.32	199	7.08	3.86	178
58	1433	15	2.0	505	1244	.160	6.58	122	9.48	4.41	175	8.55	3.97	158
67	1643	16	2.0	489	1459	.155	7.90	112	11.35	4.60	160	10.30	4.18	146
75	1852	17	2.0	481	1685	.151	9.10	102	13.09	4.71	146	11.94	4.30	133
83	1957	17	2.0	458	1872	.159	10.91	99	15.17	5.17	137	13.95	4.75	126
92	2166	18	2.0	442	2110	.154	12.79	96	17.60	5.42	132	16.30	5.02	122
108	2480	18	2.0	395	2627	.151	19.56	105	25.18	6.77	135	23.82	6.40	127
117	2585	20	2.0	372	2959	.149	23.24	107	29.14	7.52	134	27.76	7.16	128
133	3005	25	2.0	341	3634	.136	29.34	104	36.32	8.06	128	34.87	7.74	123

TEST 19U 0 PPM

N	W	ø	PS	MX10⁴	RE	1/S	F	T*X10⁴	F′	FC′	T′*X10⁴	F″	FC″	T″*X10⁴
50	1224	15	2.0	528	1066	.160	5.32	134	7.68	4.18	193	6.83	3.72	172
58	1433	15	2.0	497	1244	.160	6.15	114	9.06	4.21	167	8.13	3.78	150
67	1643	16	2.0	481	1459	.155	8.05	114	11.50	4.67	163	10.47	4.25	148
75	1852	17	2.0	466	1685	.151	9.50	106	13.48	4.85	151	12.37	4.45	138
83	1957	18	2.0	450	1918	.155	10.82	98	15.09	5.14	136	13.89	4.73	126
92	2166	18	2.0	427	2110	.154	11.77	88	16.58	5.10	124	15.33	4.72	115
100	2271	20	2.0	395	2425	.152	13.29	84	18.37	5.39	115	17.11	5.02	107
108	2480	21	2.0	388	2686	.147	18.99	102	24.61	6.62	132	23.27	6.26	125
117	2690	23	2.0	349	3029	.140	22.03	102	28.20	6.99	130	26.89	6.67	124
133	3004	26	2.0	333	3710	.133	26.97	95	33.95	7.54	120	32.53	7.22	115

TEST 20U 214 PPM

N	W	∅	PS	RE	1/S	F	T*X10⁴	F′	FC′	T′*X10⁴
50	1224	20	2.0	1212	.141	4.48	113	6.84	3.73	172
58	1433	20	2.0	1415	.140	5.47	101	8.37	3.89	155
67	1643	20	2.0	1617	.140	5.89	83	9.33	3.79	132
75	1852	20	2.0	1819	.140	6.99	78	10.98	3.85	123
83	1957	21	2.0	2066	.144	7.75	70	12.01	4.09	109
92	2166	22	2.0	2325	.140	8.55	64	13.35	4.11	100
100	2271	22	2.0	2537	.145	9.69	61	14.77	4.33	93
108	2480	23	2.0	2813	.141	10.33	55	15.96	4.29	85
117	2585	24	2.0	3103	.142	11.20	52	17.10	4.41	79
133	2795	26	2.0	3710	.143	14.43	51	20.87	4.98	74

TEST 21U 121 PPM

N	W	∅	PS	RE	1/S	F	T*X10⁴	F′	FC′	T′*X10⁴
50	1224	18	2.0	1151	.149	4.75	119	7.11	3.87	179
58	1433	18	2.0	1343	.148	5477	107	8.68	4.04	160
67	1643	18	2.0	1534	.148	6434	90	9.79	3.97	138
75	1852	18	2.0	1726	.147	7403	78	11.02	3.97	123
83	1957	18	2.0	1918	.155	8405	73	12.32	4.20	111
92	2166	19	2.0	2165	.150	8474	65	13.54	4.17	101
100	2271	19	2.0	2362	.156	9480	62	14.88	4.37	93
108	2480	21	2.0	2686	.147	10426	55	15.88	4.27	85
117	2585	21	2.0	2893	.152	11432	52	17.22	4.44	79
133	3004	23	2.0	3462	.143	13410	46	20.09	4.46	71

TEST 22U 63 PPM

N	W	ø	PS	RE	1/S	F	T*X10^4	F′	FC′	T′*X10^4
50	1224	17	2.0	1123	.152	4.75	119	7.11	3.87	179
58	1433	17	2.0	1310	.152	5.58	103	8.49	3.95	157
67	1643	17	2.0	1497	.151	6.38	90	9.83	3,99	139
75	1852	17	2.0	1685	.151	7.10	79	11.09	3.99	124
83	1957	17	2.0	1872	.159	8.39	76	12.66	4.31	114
92	2166	17	2.0	2059	.158	8.74	65	13.54	4.17	101
100	2271	18	2.0	2301	.160	9.61	60	14.69	4.31	92
108	2480	19	2.0	2558	.155	9.38	50	15.01	4.03	80
117	2690	20	2.0	2829	.150	9.80	45	15.97	3.97	74
133	3004	21	2.0	3306	.150	11.39	40	18.38	4.08	65

TEST 23U 28 PPM

N	W	ø	PS	RE	1/S	F	T*X10^4	F′	FC′	T′*X10^4
50	1224	16	2.0	1094	.156	5.01	126	7.37	4.01	185
58	1433	16	2.0	1277	.156	5.77	107	8.68	4.04	160
67	1643	16	2.0	1459	.155	6.53	92	9.98	4.05	141
75	1852	16	2.0	1642	.155	7.14	80	11.13	4.01	124
83	1957	16	2.0	1824	.163	8.09	73	12.35	4.21	112
92	2166	17	2.0	2059	.158	8.81	66	13.62	4.19	102
100	2271	17	2.0	2246	.164	9.80	62	14.88	4.37	93
108	2480	18	2.0	2493	.159	10.75	58	16.37	4.40	88
117	2690	19	2.0	2755	.154	10.64	49	16.80	4.17	78
133	3004	21	2.0	3306	.150	13.29	47	20.28	4.50	72

#

TEST 24U 15.7PPM

N	W	ø	PS	RE	1/S	F	T*X10⁴	F′	FC′	T′*X10⁴
50	1224	20	2.0	1212	.141	4.18	105	6.54	3.56	164
58	1433	20	2.0	1415	.140	5.20	96	8.11	3.77	150
67	1643	20	2.0	1617	.140	6.08	86	9.52	3.87	135
75	1852	21	2.0	1860	.137	6.53	73	10.52	3.79	118
83	1957	21	2.0	2066	.144	7.52	68	11.78	4.01	107
92	2166	22	2.0	2325	.140	8.13	61	12.94	3.98	97
100	2271	22	2.0	2537	.145	9.31	58	14.39	4.22	90
108	2480	23	2.0	2813	.141	10.48	56	16.11	4.33	86
117	2690	24	2.0	3103	.136	11.01	51	17.18	4.26	79
133	3004	26	2.0	3710	.133	15.19	54	22.18	4.92	78

TEST 25U 5.1 PPM

N	W	ø	PS	RE	1/S	F	T*X10⁴	F′	FC′	T′*X10⁴
50	1224	26	2.0	1391	.123	4.18	105	6.54	3.56	164
58	1433	26	2.0	1623	.122	4.86	90	7.76	3.61	143
67	1643	27	2.0	1895	.119	5.51	78	8.95	3.63	127
75	1852	27	2.0	2132	.119	6.53	73	10.52	3.79	118
83	1957	28	2.0	2422	.123	7.79	70	12.05	4.11	109
92	2166	28	2.0	2664	.122	9.12	68	13.92	4.29	104
100	2271	29	2.0	2972	.124	10.82	68	15.90	4.67	100
108	2480	30	2.0	3294	.120	13.10	70	18.73	5.03	100
117	2690	32	2.0	3690	.115	16.33	75	22.50	5.58	104
133	3004	34	2.0	4394	.113	23.09	82	30.08	6.68	106

APPENDIX 3

METHOD OF MIXING POLYMER SOLUTIONS

As has been noted previously the method of mixing can greatly affect the final experimental results. Several methods are suggested by Union Carbide for Polyox WSR301; the most effective was found to be that based on the insolubility of the polymer in certain liquids. The powder cannot simply be stirred into water because coagulations form stopping complete dissolving. The method used throughout the project is given below.

Mix about 10 g of polymer (weighed exactly) into about 50 g of anhydrous methyl alcohol which has been cooled to $0^{\circ}C$. The polymer will not dissolve at this temperature. The mixture is stirred up to separate all the particles and then tipped slowly into about 6 kg of tap water which is being stirred at 600 r.p.m. Wash any remaining sludge into the water with a little more alcohol. Keep the stirrer at this speed for 2 or 3 minutes and then at 200 r.p.m. for 15 minutes. This process produces a concentrated mixture at about 1600 ppm. When required an amount calculated to give the final concentration is weighed. This is poured into a measured amount of water and stirred by hand for a short time. The final solution is then left overnight before being stirred again and used for the experiment.

APPENDIX 4

TEST PROCEDURE

The procedure recorded below was followed for all the experimental tests.

1. Allow electronic instruments to reach thermal equilibrium.
2. Set zero for load and torque measurements.
3. Check calibration of torque ring with weight (117 g).
4. Start supplies to hydrostatic bearing and slave bearings.
5. Start main drive motor.
6. Increase ram load to take weight of test bearing and the hydrostatic bearing.
7. Supply lubricant at low flowrate to test bearing.
8. Start shaft rotating at about 10 r/s.
9. Connect friction measuring ring to torque arm.
10. Adjust bearing load, shaft speed and supply pressure as required.
11. Record load, speed, friction, supply pressure and flowrate, and lubricant outlet temperature.
12. Adjust machine and take readings as required.
13. Stop machine when at load speed with ram carrying bearing weight only.
14. Retest friction zero and calibration.

The friction measuring device was disconnected and re-zeroed at all scale changes required. Very little time was necessary for the lubricant outlet temperature to reach equlibrium because of small rise in temperature.

The weights of the test bearing and the hydrostatic bearing were subtracted from the load measurement to give the true upward load. The valve in the loading system held the ram at constant position and so adjustment was required to provide a constant load as the eccentricity changed with speed.

At the end of each day, a 2% solution of sodium nitrite in tap water was fed through the bearing with the shaft rotating. This was extremely effective in controlling rusting of the steel shaft and drainage system.

REFERENCES

CAMERON, A. 1966. Principles of lubrication, Longmans, p.425.

CANHAM, H.J.S. 1970. R.I.N.A. report. Boundary additives to reduce ship resistance.

CASTLE, P. and MOBBS, F.R. 1967. Proc. I.M.S. Hydrodynamic stability of the flow between eccentric cylinders.

CASTLE, MOBBS and MARKHO. 1970. A.S.M.E. 70-LUB-13. Visual observations and torque measurements in the Taylor vortex regime between eccentric cylinders.

CHRISTOPHERSON, D.G. 1957. The Engineer Jan.18, p.100. Boundary conditions in lubricating films.

CHRISTOPHERSON, D.G. and DOWSON, D. 1959. Proc. Roy. Soc., A, 251. An example of minimum energy dissipation in viscous flow.

CHRISTOPHERSON, D.G. and NAYLOR, H. 1955. Proc. I.M.E., vol. 169. The promotion of fluid lubrication in wire drawing.

COLE, J.A. and HUGHES, C.J. 1956. Proc. I.M.E., vol. 170. Oil flow and film extent in complete journal bearings.

COLE, J.A. 1957. Proc. Conf. Lubrication and Wear, I.M.E. Experiments on the flow in rotating annular clearances.

ELATA, H. and RUBIN, C. 1966. Phys. Fluids, vol.9, No.10. Stability of Couette flow of dilute polymer solutions.

GADD, G.E. 1965. NATURE, MAY 1. Turbulence damping and drag reduction produced by certain additives in water.

GADD, G.E. 1966. NATURE, JUL 9. Effects of long chain molecule additives in water on vortex sheets.

GADD, G.E. 1966. NATURE, NOV 26. Reduction of turbulent friction in liquids by dissolved additives.

GADD, G.E. 1966. NATURE, DEC 17. Differences in normal stress in aqueous solutions of turbulent drag reducing additives.

GADD, G.E. and BRENNEN, C. 1967. NATURE, SEP 23. Ageing and degradation in dilute polymer solutions.

GILES, W.B. and PETTIT, W.T. 1967. NATURE, NOV 24. Stability of dilute viscoelastic flows.

GOREN, Y. and NORBURY, J.F. 1967. A.S.M.E. 67-WA/FE-3. Turbulent flow of dilute aqueous polymer solutions.

HUGGINS, N.J. 1966. Proc. I.M.E., vol. 181. Tests on a 24 in. diameter journal bearing: transition from laminar to turbulent flow.

LUMLEY, J.L. 1967. APP MECH REV, 20, No.12. The Toms phenomenon.

MERRIL, E. et al. 1966. TRANS SOC RHEO. Study of turbulent flow of dilute polymer solutions in Covette viscometer.

NEAL, P.B. 1967. Proc. I.M.E., vol. 182. Basic principles of bearing testing machine design.

OSBOURNE, M.R. 1966. Chap. 18, Principles of lubrication, Cameron. Computation of Reynolds equation.

PERRY. 1963. PERRYS CHEM ENG HANDBOOK, McGRAW-HILL.

RAIMONDI, A.A. and BOYD, J. 1957. ASME, Lub Eng, Jan vol.13. The analysis of orifice and capillary compensated hydrostatic journal bearings.

REYNOLDS, O. 1886. Phil. Trans. Roy. Soc., 177.

ROSEN and CORNFORD. 1971. NATURE, 234, NOV 5. Fluid friction of fish slimes.

SMITH, M.I. and FULLER, D.D. 1956. Trans. A.S.M.E., 78. Journal bearing operation at super-laminar speeds.

SQUIRE, W. et al. 1967. NATURE, MAR 11. Mechanism of turbulent friction reduction in pipes by dissolved additives.

TAYLOR, G.I. 1923. Phil. Trans. Roy. Soc., 223. Hydrodynamic stability of the flow between concentric rotating cylinders.

TAYLOR, G.I. 1936. Proc. Roy. Soc., 157. Fluid friction between rotating cylinders.

TOMS, B.A. 1948. Proc. Inter. Rheo. Congress (Holland). Some observations on the flow of linear polymer solutions through straight tubes at large Reynolds numbers.

VIRK, P.S. et al. 1967. J. Fluid Mech., vol.30, pt.2. The Toms phenomenon: turbulent flow of dilute polymer solutions.

VIRK, P.S. 1971. J. Fluid Mech., vol.45, pt.2. Drag reduction in rough pipes.

WELLS, C.S. and SPANGLER, J.G. 1967. Phys Fluids, 19.

WILCOCK, D.F. 1950. Trans. ASME, 72. Turbulence in high speed journal bearings.